Final Report

IMPACTS OF THE PROPOSED ALTON COAL PROJECT ON THE NIGHT SKY NEAR BRYCE CANYON NATIONAL PARK

SYSAPP-88/194

6 March 1989

Prepared for

Don Henderson
National Park Service
P.O. Box 25287
Denver, Colorado 80225

Contract CX-0001-4-0055

Prepared by

E. L. Carr
H. Hogo
M. A. Yocke
G. W. Lundberg
B. D. Miller

Systems Applications, Inc.
101 Lucas Valley Road
San Rafael, CA 94903

Final Report

IMPACTS OF THE PROPOSED ALTON COAL PROJECT ON THE NIGHT SKY NEAR BRYCE CANYON NATIONAL PARK

SYSAPP-88/194

6 March 1989

Prepared for

Don Henderson
National Park Service
P.O. Box 25287
Denver, Colorado 80225

Contract CX-0001-4-0055

Prepared by

E. L. Carr
H. Hogo
M. A. Yocke
G. W. Lundberg
B. D. Miller

Systems Applications, Inc.
101 Lucas Valley Road
San Rafael, CA 94903

D0070 87131r5

CONTENTS

List of Exhibits..... iii

List of Tables..... vi

1 POTENTIAL EFFECTS OF NIGHT LIGHTING ON BRYCE CANYON NATIONAL PARK..... 1

2 TECHNICAL APPROACH..... 4

Night Sky Glow Model..... 4

Primary Scattering..... 4
Multiple Scattering..... 6

3 RESULTS AND DISCUSSION..... 8

Testing and Evaluation of the Night Sky Glow Model..... 8

Application of the Night Sky Glow Model..... 12

Predicted Sky Glow from the Alton Coal Project..... 15
Perceptibility of Predicted Sky Glow..... 15
Comparison of Night Glow Caused by Artificial and Natural Light Sources..... 39
Obscuration of Starlight by Night Glow Caused by the Alton Coal Project..... 42

4 SUMMARY AND CONCLUSIONS..... 46

Summary of Results..... 46

Conclusions..... 47

References..... R-1

Appendix A: TECHNICAL DESCRIPTION OF THE NIGHT SKY GLOW MODEL

Appendix B: NIGHT SKY GLOW MODEL LISTING AND SAMPLE INPUT

Appendix C: GLOSSARY

7131r3 1

EXHIBITS

1-1 Sites shown for Alton Coal Project are the closest mining locations occurring in years 21-22..... 2

2-1 Relationship of light source and observer for a discrete spherical sky grid element..... 5

2-2 Schematic diagram of numerical sky glow modeling framework..... 7

3-1 Viewing points within Bryce Canyon National Park..... 9

3-2 Percentage of nighttime observations for which visual range exceeded an indicated value as a function of time of night at Bald Knoll, Utah, 1978-1980..... 14

3-3 Layout of the proposed Alton Coal Industrial Area..... 16

3-4a Spectral output of a high pressure sodium lamp..... 22

3-4b Spectral output of a halogen lamp..... 22

3-5 Spatial distribution of sky brightness (10^{-3} lm/m^2/sr) caused by the "uncontrolled" Alton Coal Project as seen from Yovimpa Point (assumed visual range is 30 km)..... 23

3-6 Spatial distribution of sky brightness (10^{-3} lm/m^2/sr) caused by the "uncontrolled" Alton Coal Project from Yovimpa Point (background visual range within each layer is 0-1 km--70 km; 1-3 km--100 km; 3-7 km--400 km; 7-20 km--1000 km)..... 24

3-7 Spatial distribution of sky brightness (10^{-3} lm/m^2/sr) caused by the "uncontrolled" Alton Coal Project as seen from Yovimpa Point (assumed visual range is 391 km)..... 25

3-8 Spatial distribution of sky brightness (10^{-3} lm/m^2/sr) caused by the "uncontrolled" Alton Coal Project as seen from View Point (assumed visual range is 30 km)..... 26

3-9 Spatial distribution of sky brightness (10^{-3} lm/m^2/sr) caused by the "uncontrolled" Alton Coal Project as seen from View Point (background visual range within each layer is 0-1 km--70 km; 1-3 km--100 km; 3-7 km--400 km; 7-20 km--1000 km)..... 27

3-10 Spatial distribution of sky brightness (10^{-3} lm/m^2/sr) caused by the "uncontrolled" Alton Coal Project as seen from View Point (assumed visual range is 391 km)..... 28

3-11 Spatial distribution of sky brightness (10^{-3} lm/m^2/sr) caused by the "uncontrolled" Alton Coal Project as seen from Bryce Point (assumed visual range is 30 km)..... 29

3-12 Spatial distribution of sky brightness (10^{-3} lm/m^2/sr) caused by the "uncontrolled" Alton Coal Project as seen from Bryce Point (background visual range within each layer is 0-1 km--70 km; 1-3 km--100 km; 3-7 km--400 km; 7-20 km--1000 km)..... 30

3-13 Spatial distribution of sky brightness (10^{-3} lm/m^2/sr) caused by the "uncontrolled" Alton Coal Project as seen from Bryce Point (assumed visual range is 391 km)..... 31

3-14 Spatial distribution of sky brightness (10^{-3} lm/m^2/sr) caused by the Alton Coal Project "preliminary design" case as seen from Yovimpa Point (background visual range within each layer is 0-1 km--70 km; 1-3 km--100 km; 3-7 km--400 km; 7-20 km--1000 km)..... 32

3-15 Spatial distribution of sky brightness (10^{-3} lm/m^2/sr) caused by the Alton Coal Project "preliminary design" case as seen from View Point (background visual range within each layer is 0-1 km--70 km; 1-3 km--100 km; 3-7 km--400 km; 7-20 km--1000 km)..... 33

3-16 Spatial distribution of sky brightness (10^{-3} lm/m^2/sr) caused by the Alton Coal Project "preliminary design" case as seen from Bryce Point (background visual range within each layer is 0-1 km--70 km; 1-3 km--100 km; 3-7 km--400 km; 7-20 km--1000 km)..... 34

3-17 The darkness adaptation function of a light-adapted subject..... 36

3-18 Contours of constant luminosity measured for a range of background luminances..... 36

3-19 Illuminance threshold as a function of field luminance..... 37

3-20 Apparent glow dome intensity as a function of distance from light source..... 38

3-21 Spatial distribution of sky brightness (10^{-3} lm/m^2/sr) caused by a full moon at the zenith as seen from Bryce Canyon National Park..... 40

3-22 Spatial distribution of sky brightness (10^{-3} lm/m^2/sr) caused by Tropic, Utah as seen from Bryce Point based on street lighting inventory only (background visual range within each layer is 0-1 km--70 km; 1-3 km--100 km; 3-7 km--400 km; 7-20 km--1000 km)..... 41

3-23 Spatial distribution of sky brightness (10^{-3} lm/m^2/sr) caused by Tropic, Utah as seen from Bryce Point based on Walker's relationship between population and luminosity (background visual range within each layer is 0-1 km--70 km; 1-3 km--100 km; 3-7 km--400 km; 7-20 km--1000 km)..... 43

TABLES

3-1 Viewing site locations within Bryce Canyon National Park..... 10

3-2 Comparison between predicted and measured sky brightness for various visual ranges at Salinas, California..... 11

3-3 Vertical structure profile of scattering coefficients for the typical adverse effects scenario at Bryce Canyon National Park..... 13

3-4a Mining equipment lighting list..... 17

3-4b Lighting emissions from mining equipment locations for years 21-22..... 18

3-4c Alton mining industrial site light distribution..... 20

3-5 Stellar magnitude of selected stars and planets..... 44

3-6 Number of stars visible by magnitude for the entire celestial sphere..... 44

87131r3 1

1 POTENTIAL EFFECTS OF NIGHT LIGHTING ON BRYCE CANYON NATIONAL PARK

BHP-Utah International (UII) proposes to develop the Alton Coal Project located southwest of Bryce Canyon (see Exhibit 1-1). Coal will be recovered through surface mining techniques.

The National Park Service, as manager of Bryce Canyon National Park, expressed concern that the effects of lighting at the Alton Coal Project might affect visitor enjoyment of the night sky (i.e., stars, constellations, etc.) at Bryce Canyon National Park. In order to estimate the possible effects, Systems Applications Inc. was retained by the National Park Service and BHP-Utah International to study the potential effects of night lighting from the proposed coal project on Bryce Canyon National Park. In this study night sky glow resulting from nighttime operation of the proposed mine was calculated, and the potential for human perception of these effects was estimated. The study involved the following steps:

Enhancement of a mathematical model of atmospheric optics to predict the nighttime sky-glow effects of the proposed mining operation.

Verification of the model's prediction performance to the extent possible with existing data.

Application of the model to the area surrounding the proposed Alton Coal Project, calculating results from three viewpoints within the park for two lighting scenarios and three meteorological conditions at the Alton Coal Project.

Estimation of the potential for human perception of the calculated night sky glow and the potential of the night sky glow to obscure starlight.

Application of the graphic program to several vistas within the park.

Providing national park personnel with the enhanced computer model and supporting documentation.

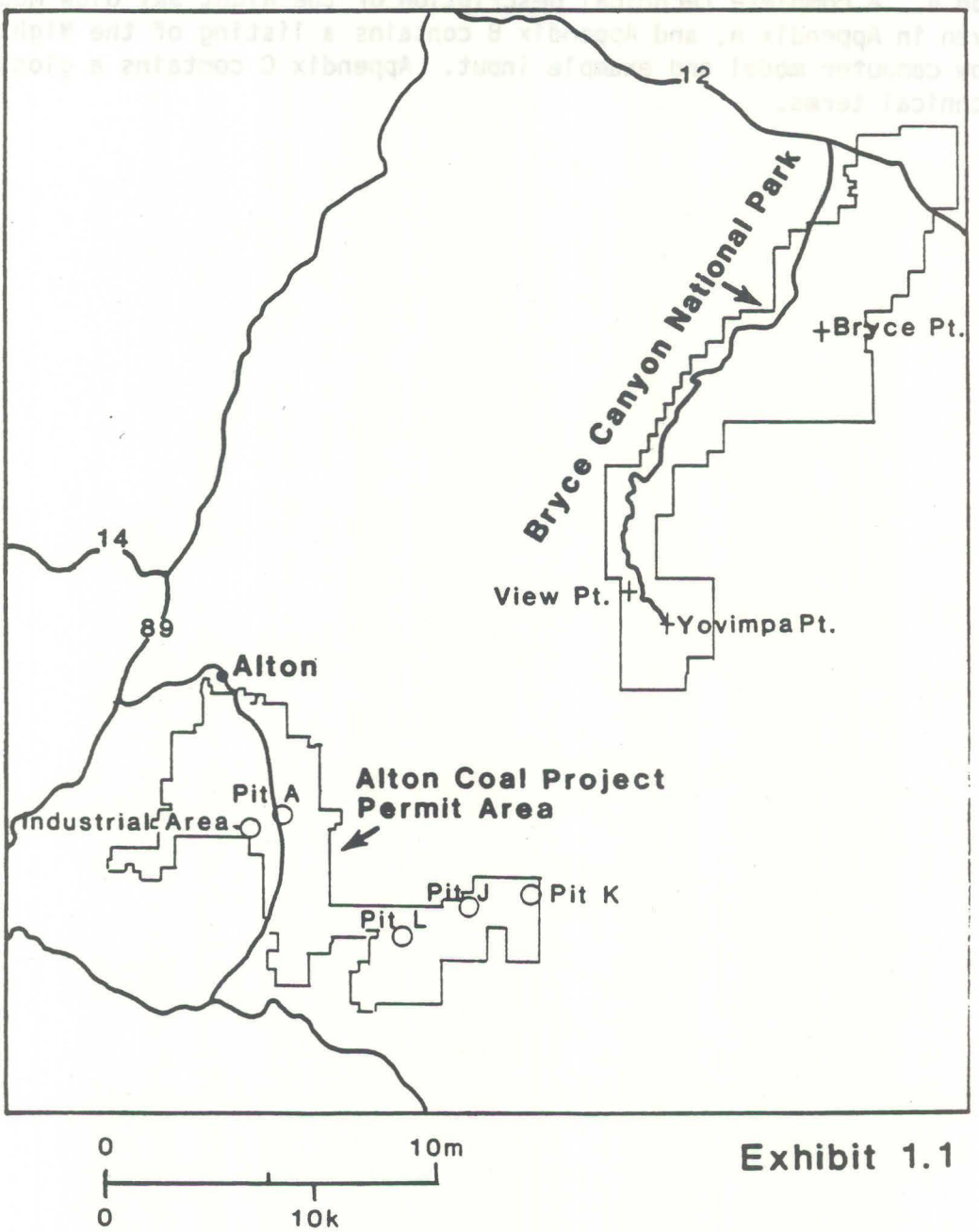


EXHIBIT 1-1. Sites shown for Alton Coal Project are the closest mining locations occurring in years 21-22.

This report documents the results of our study. Section 2 contains a brief description of the technical approach employed in the study. The results are presented in Section 3, and conclusions are provided in Section 4. A complete technical description of the Night Sky Glow Model is given in Appendix A, and Appendix B contains a listing of the Night Sky Glow computer model and example input. Appendix C contains a glossary of technical terms.



2 TECHNICAL APPROACH

The computer program written for this study is a numerical model of atmospheric optics for prediction of night sky glow. This model predicts the luminosity of the night sky and has been applied to estimating effects of nighttime operations at the proposed Alton Coal Project. The program is described in general in this chapter. A complete technical description of the numerical Night Sky Glow Model is given in Appendix A.

NIGHT SKY GLOW MODEL

The Night Sky Glow Model was designed to predict the luminosity of scattered light in the night sky due to the lighting of facilities. Such a model must be capable of predicting the glow in any portion of the sky under various atmospheric conditions and must be flexible enough to address any combination of facility sites and viewing points. Because of the complexity of the equations that describe radiation transfer in the atmosphere and the large number of calculations that are required, a numerical (computer) modeling approach was adopted (Yocke et al., 1985).

Primary Scattering

The hemisphere of the sky viewed from a single point on the earth's surface is divided into a number of discrete angles. For this model we selected 10 degrees as the size of each angle; this represents a compromise between precision and cost of the calculations. Each angle is divided into a number of elements, the selection of which also represents a compromise between the cost and precision of the predictions; we selected 1000 meters as the length of each element. However, both the size of the angle and the length of each element may be specified by the user at program run time. By partitioning the sky in this fashion, we have in effect created a spherical grid encompassing the visible portion of the sky. The model uses this grid as a framework for its calculation procedures. Exhibit 2-1 illustrates the relationship of the light source to the observer.

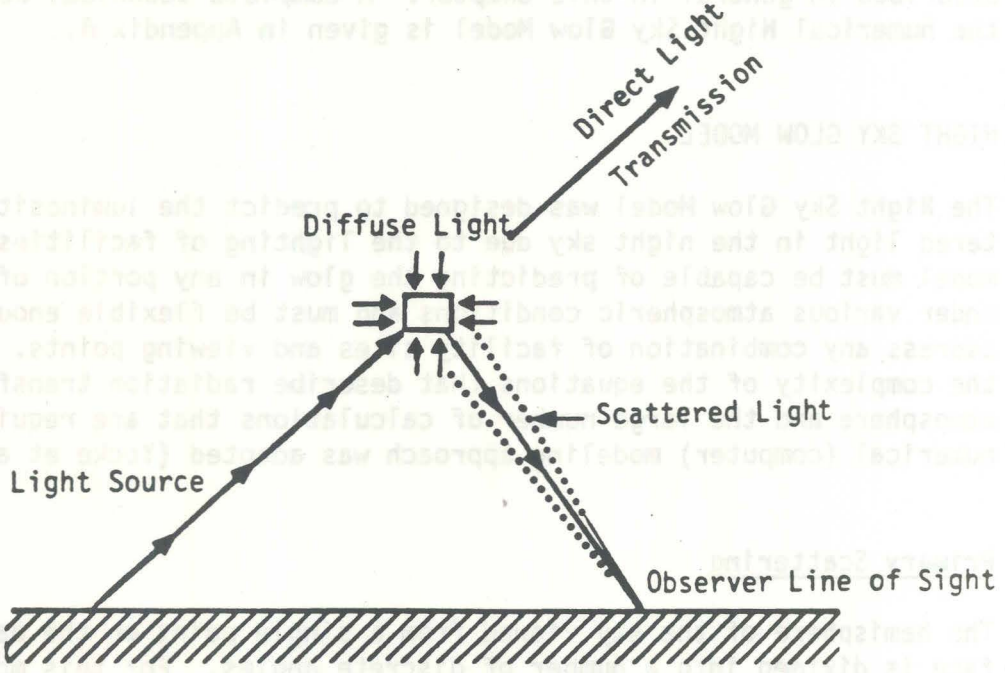


EXHIBIT 2-1. Relationship of light source and observer for a discrete spherical sky grid element.

For each grid element, the model performs a series of calculations for each of a number of wavelength intervals that encompass the visible light spectrum. For a given wavelength interval and light source, the model calculates the light intensity attenuation (due to absorption and scattering by atmospheric gases and particles) and the fraction of the attenuated light in the wavelength interval that is scattered toward the observer by gases and particles within the grid element. This sequence of calculations is repeated for every combination of spherical grid element, wavelength segment, and light source. By following these calculation procedures, the model in effect is numerically integrating the atmospheric radiation transfer equation for primary scattering events. The result is a field of sky luminosity predictions for the entire visible spectrum in all viewing directions (Exhibit 2-2 illustrates the modeling framework).

To treat an extended area light source, as would exist in the Alton Coal Project, the source is divided into a number of smaller area sources. A square grid is laid over the source area, and a light source intensity is assigned to each grid. The model then treats each of the smaller area sources as a point source. The calculation procedure described above is carried out for each combination of sky grid element and light source grid element.

Multiple Scattering

In the atmosphere several scattering events may occur before a particular photon reaches the observer's eye. These multiple scattering events become more important in situations with high surface reflectivity or high atmospheric aerosol concentrations. In principle, the treatment of multiple scattering events is a simple extension of the treatment of primary scattering described above. In practice, however, detailed multiple scattering calculations are extremely expensive because of the huge numbers of scattering events that must be simulated. For this study it was determined that detailed calculation of multiple scattering could not be undertaken. However, a simplified treatment of multiple scattering was devised and implemented within the Sky Glow Model.

In our treatment of multiple scattering, we calculate an approximate value of the ratio (total scattered light)/(primary scattered light). The calculation incorporates the probability of forward and backward scattering and the atmospheric aerosol concentration (or visual range, which is dependent on aerosol concentration) parameters. Hence, the model first calculates the sky luminosity due to primary scattering using the procedures described earlier, and then applies a multiple scattering algorithm to calculate the luminosity due to both primary and multiple scattering. The output of the model is provided in graphic form.

For a complete technical description of the Night Sky Glow Model developed in this study, the reader is referred to Appendix A.

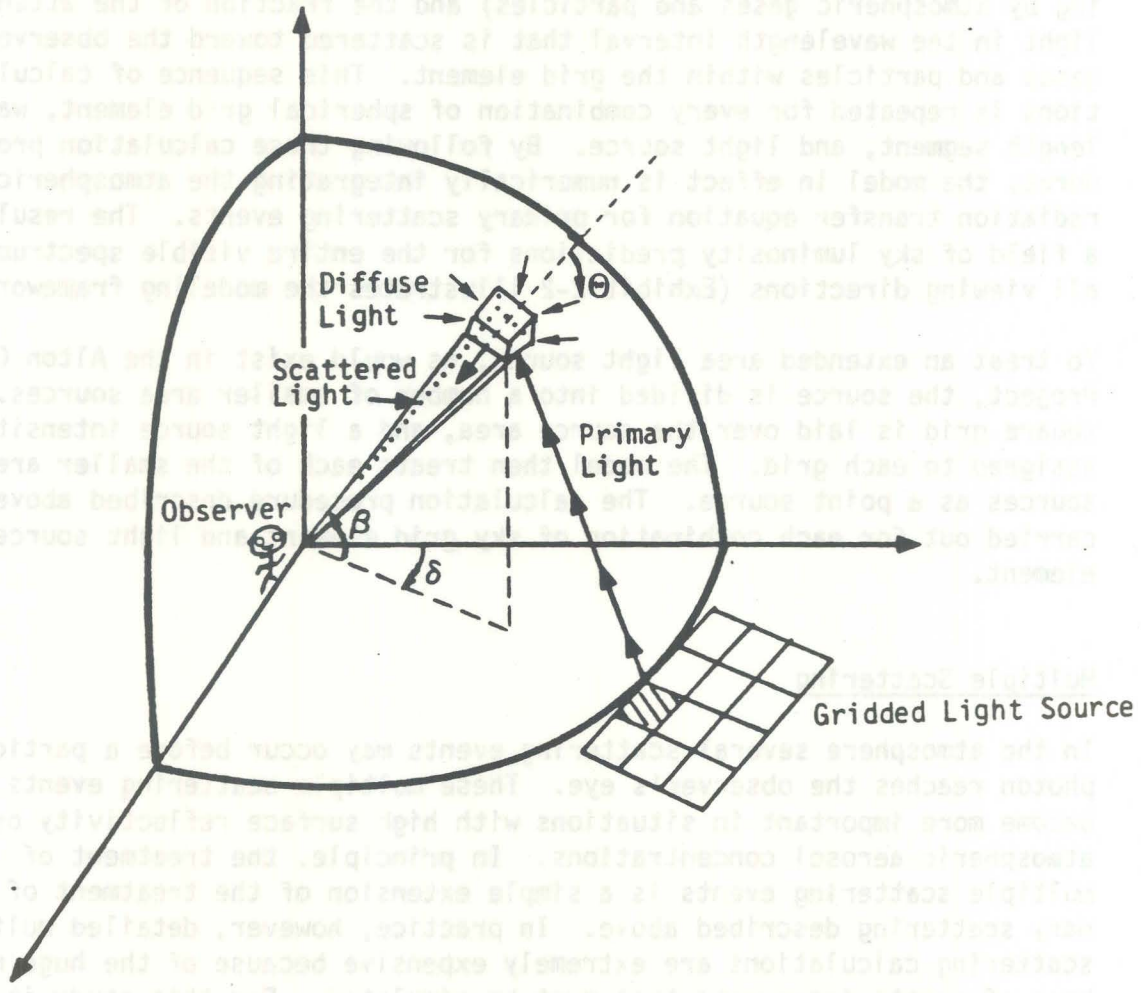


EXHIBIT 2-2. Schematic diagram of numerical sky glow modeling framework.

3 RESULTS AND DISCUSSION

The models described in the previous section were applied to three viewing sites within the Bryce Canyon National Park for a scenario typifying years 21 through 25 of the 35-year mine plan. These years of mining represent full production and include mining at the closest geographic distance to Bryce Canyon National Park. The viewing sites, in order of increasing distance from the Industrial Area, are Yovimpa Point (approximately 22 kilometers from industrial site), View Point (approximately 23 kilometers from industrial site), and Bryce Point (approximately 40 kilometers from industrial site) (Exhibit 3-1 and Table 3-1). In this section we discuss the results of those model runs, as well as the results of testing and evaluation of the Night Sky Glow Model.

TESTING AND EVALUATION OF THE NIGHT SKY GLOW MODEL

To test whether the Night Sky Glow Model operates correctly and generates reasonable predictions of night sky luminosities (i.e., glow), it is necessary to evaluate the performance of the model against field measurements of night sky glow. Although considerable data have been collected at a number of astronomical observatories concerned with "light pollution," very few of these studies were usable for purposes of our study. Most of these studies were concerned with the night glow resulting from large urban areas rather than the glow due to smaller sources (i.e., of a size comparable to the proposed Alton Coal Project). Furthermore, most of the observatory sites studied in these measurement programs were considerably farther from urban light sources than the Bryce Canyon National Park is from the proposed coal project. In principle, the Night Sky Glow Model is capable of treating these situations, but no inventories of existing light sources were made in these measurement studies, and construction of such an inventory is beyond the scope of our study. Even if a light source inventory were available, evaluation of the model using data from these large urban area studies leaves open the question of the model's performance over shorter distances and with smaller sources.

The only data we found acceptable for our study were collected by the Lick Observatory of the University of California. In that study, Walker (1977)

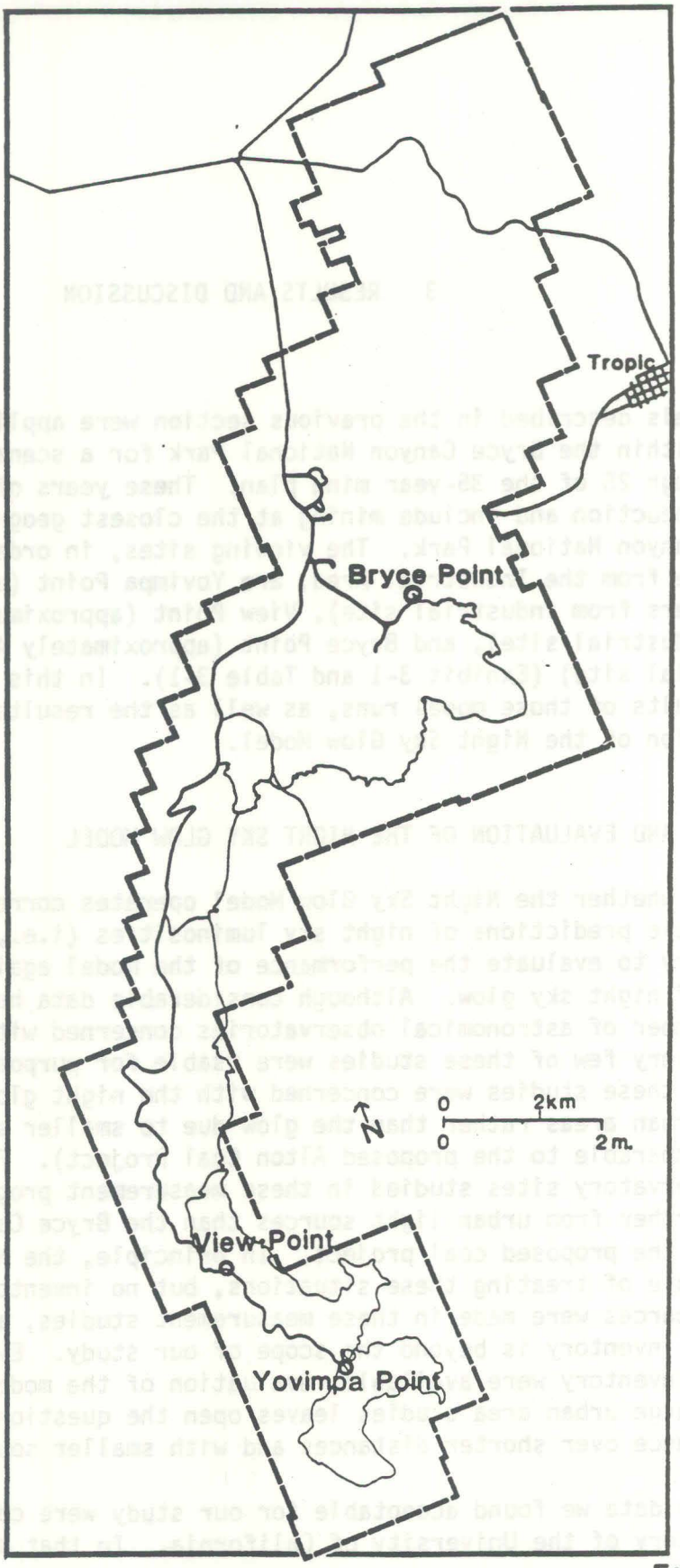


Exhibit 3.1

87131r3

EXHIBIT 3-1. Viewing points within Bryce Canyon National Park.

TABLE 3-1. Viewing site locations within Bryce Canyon National Park.

Location	Latitude (degrees)	Longitude (degrees)	Elevation (meters)	Distance* (km)
Yovimpa Point	37.4728	112.2394	2774	22
View Point	37.4993	112.2540	2743	23
Bryce Point	37.5161	112.1553	2528	40

* Distance from viewing point to Industrial Area.

used a sensitive telephotometer to measure sky brightness values at various distances from several cities in California. One of the cities, Salinas, is fairly isolated (i.e., surrounded by large unpopulated and unlit areas) and is relatively compact compared to most cities studied. Its situation is thus more similar to that of the Bryce Canyon-Alton Coal Project area. Nevertheless, only a limited amount of the sky brightness data for Salinas was usable--a fixed 45-degree elevation angle above six viewing locations between 8 and 32 kilometers from the city. These data are summarized in Table 3-2. The values given in this table are a ratio of relative brightness, R_b, defined as the visible brightness measured at 45 degrees of elevation toward the city minus the visible brightness measured at 45 degrees of elevation away from the city divided by the background visible brightness. Walker's study also provided estimates of the total lumen output by Salinas.

TABLE 3-2. Comparison between predicted and measured sky brightness for various visual ranges at Salinas, California.

Distance (km)	Measured Values	Predicted Values Based on Background Visual Range		
		30 km	50 km	70 km
8.0	2.41	4.13	3.17	2.14
10.5	1.91	3.81	2.82	1.94
14.2	1.23	0.97	1.02	0.80
18.7	0.68	0.36	0.47	0.41
24.5	0.27	0.12	0.20	0.19
32.2	0.09	0.03	0.07	0.08

For input to the model, we assumed a uniform spatial distribution over the limits of greater Salinas and the total light output of Salinas (42.31×10^6 lumens) estimated by Walker (1977). The geographic limits of greater Salinas were determined by examination of USGS and NOAA maps that include an indication of the lighting in populated areas (approximately 32 km^2). We also assumed an average surface reflectivity of 15 percent, which is probably representative of the Salinas area (Krinov, 1953; Penndorf, 1956; and Earing and Smith, 1966). Background sky glow (due to starlight and airglow) was assumed to be 1.9×10^{-4} lumens per square meter per steradian ($lm/m^2/sr$) (Walker, 1970, 1973).

Comparison of observed and predicted brightness ratios provides some encouragement that the model predicts luminosities that are approximately

correct. The tendency of the model to overpredict sky brightness at a location that is close to the source is probably attributable to a combination of uncertainty about the actual light source distribution and the particle distribution on the day the data were collected. The sensitivity test shows a strong response of the brightness ratio to changes in the visual range. However, the average slope between the distance D = 8 km and D = 32 km that represents the best fit to the observations for the 50-kilometer visual range is -2.3. This result agrees well with Walker's observation that the data seem to follow a $R_b \propto D^{-2.5}$ law. Given the uncertainty in the light source data as well as other input to the model, we conclude that the model performance is acceptable and that the model is appropriate for application to the Bryce Canyon area. However, this evaluation of the Night Sky Glow Model is by no means comprehensive. The values provide ratios only, not absolute values; thus further comparison with observed measurements is needed. A more thorough evaluation of the model is required if great confidence is to be placed in its predictions.

APPLICATION OF THE NIGHT SKY GLOW MODEL

The model was applied to three atmospheric visual ranges--30 and 391 kilometers, and a case with varying visual ranges as a function of height, for each combination of viewing point and the years in which the mining operations are closest to Bryce Canyon National Park. The lower visual range (30 km) represents an extreme case of highest aerosol concentration. The higher visual range (391 km) is representative of visibility associated with absorption and scattering by low concentration of aerosols (Rayleigh scattering.) The third case represents a typical aerosol profile of the atmosphere. In all three cases, two particle size distribution shapes were assumed, one for fine particles and one for coarse particles. A fine particle size distribution having a geometric mean diameter of 0.125 μm and a geometric standard deviation of 1.6 was assumed along with coarse particle size distribution with a mean of 3.0 μm and standard deviation of 2.2 (Johnson et al., 1980). The number of particles described by each of these distributions was calculated from the assumed visual range (Johnson et al., 1980). In all three cases a uniform spatial aerosol concentration distribution was assumed within each model layer. Fugitive dust emissions were not explicitly addressed because fewer than 10 percent of the emissions from fugitive dust are in the fine particle mode (EPA, 1981) and should not produce a significant change in the scattering of light. This scattering, which is due mainly to suspended fine particulates at high altitudes, is represented in the distribution described. Furthermore, since fugitive dust is confined to a thin layer at the bottom of the atmosphere, any increase in the amount of dust in this thin layer would result in an increased amount of light

scattered before reaching the higher layers of the atmosphere, which are the layers most responsible for the glow dome visible from view points within Bryce Canyon National Park.

To simulate a more realistic atmosphere, whose aerosol distributions are a function of altitude, we examined data collected in the southwestern United States. UII has collected surface visual range data for the three year period, 1978-1980, at the Bald Knoll site from nephelometer observations (Exhibit 3-2). These data show that approximately 80 percent of the time the visual range exceeds 70 km. Thus, we used the 70 km visual range in the surface layer for the more realistic case. Since very little data exist for nighttime vertical aerosol distributions, we made the assumption that daytime conditions occur at night (Latimer et al., 1978). During the VISTTA study, Herring et al. (1981) found that visual range generally increased with increasing height. On the most polluted sampling day, the visual range changed from 70 km at the surface, to 90 km at 1 km, 100 km at 2 km, and 110 km at 3 km. These values plus the UII surface visual range values, together with values suggested by the Handbook of Optics (1978) for hazy conditions above 3 km, were used to develop a vertical structure profile for scattering coefficients averaged over the visible wavelengths as shown in Table 3-3.

TABLE 3-3. Vertical structure profile of scattering coefficients for typical adverse effects scenario at Bryce Canyon National Park.

Height (km)	Scattering Coefficient (km^{-1})	Visual Range (km)
0-1	6×10^{-2}	70
1-3	4×10^{-2}	100
3-7	9×10^{-3}	400
7-20	4×10^{-3}	1000

In each model run a natural background sky brightness of 1.9×10^{-4} $lm/m^2/sr$ was assumed. This brightness level is representative of a moonless, clear night sky (Walker, 1970, 1973). The background value is simply added to the incremental luminosities predicted by the model and does not affect the predicted incremental sky-glow impacts. In estimating the potential for obscuration of visible stars, absolute sky-glow levels only are of concern, and for this case 1.9×10^{-4} $lm/m^2/sr$ is the most

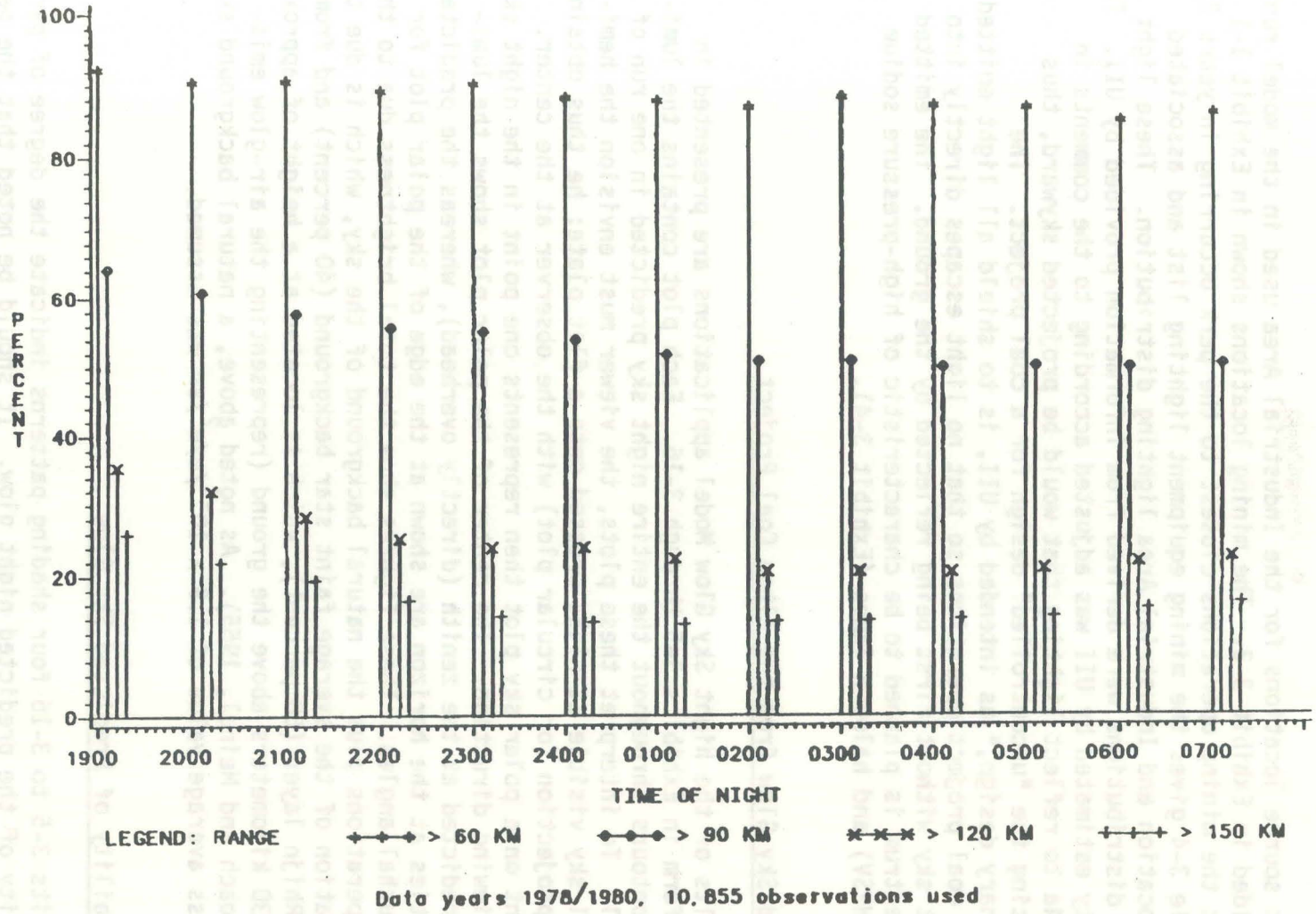


EXHIBIT 3-2. Percentage of nighttime observations for which visual range exceeded an indicated value as a function of time of night at Bald Knoll, Utah, 1978-1980.

appropriate background value because the greatest number of stars are visible on moonless, clear nights.

The light source locations for the Industrial Area used in the model runs are provided in Exhibit 3-3. The mining locations shown in Exhibit 1-1 represent the mining operations closest to the park occurring in years 21-22. Table 3-4 gives the mining equipment lighting list and associated mining location and Industrial Area lighting distribution. These light emission distributions were derived from information provided by UII. The luminosity estimated by UII was adjusted according to the comments in Table 3-4a to reflect lighting that would be projected skyward, thus representing the "uncontrolled" design for a coal project. The "preliminary design," as intended by UII, is to shield all light emitted from the coal project operations so that no light escapes directly into the night sky without first being reflected by the ground. The emitted light spectrum is planned to be characteristic of high-pressure sodium lights (HPSV) and halogen lamps (Exhibit 3-4).

Predicted Sky Glow from the Alton Coal Project

The results of the Night Sky Glow Model applications are presented in graphic form in Exhibits 3-5 through 3-16. Each plot contains the luminosity contours throughout the entire night sky predicted in one run of the model. To interpret these plots, the viewer must envision the hemispherical sky visible at night pressed onto a flat plate; he thus obtains a polar projection (or circular plot) with the observer at the center. Each point on a polar sky plot then represents one point in the night sky, or one viewing direction. The center of the polar plot shows the luminosity predicted at the zenith (directly overhead), whereas the predicted luminosities at the horizon are shown at the edge of the polar plot for all azimuthal angles. These figures show the total brightness due to the mining operations plus the natural background of the sky, which is due to a combination of the average faint star background (40 percent) and from the van Rhijn layer (60 percent), which is located at a height of approximately 130 kilometers above the ground (representing the air-glow emission) (Roach and Meinel, 1955). As noted above, a natural background sky brightness average value of 1.9×10^{-4} /m/m^2/sr was assumed.

Perceptibility of Predicted Sky Glow

In Exhibits 3-5 to 3-16 four shading patterns indicate the degree of perceptibility of the predicted night glow. It should be noted that the perceived brightnesses of the shading patterns do not illustrate for the

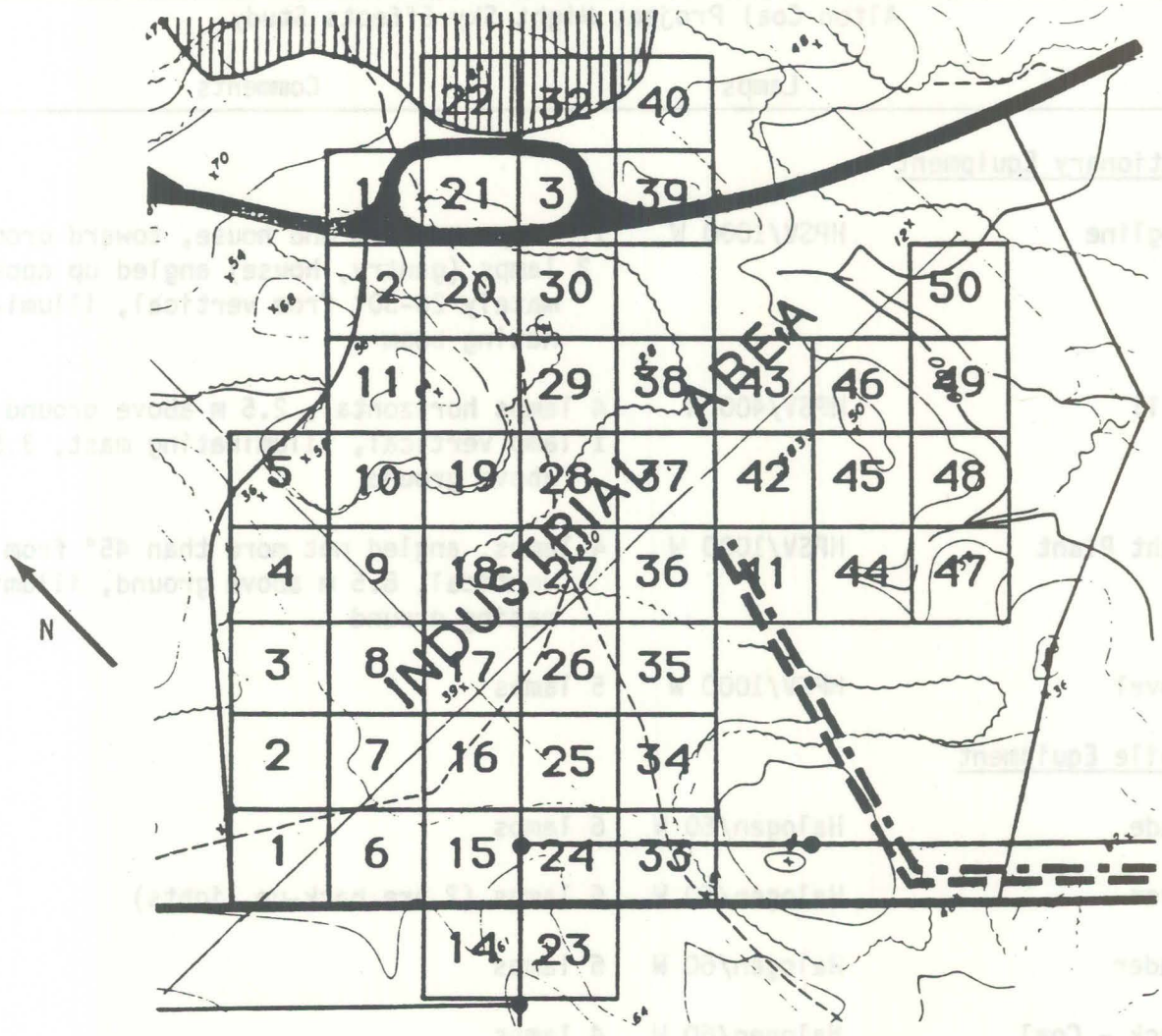


EXHIBIT 3-3. Layout of proposed Alton Coal industrial area. Numbers refer to locations given in Table 3-5c. Grids are 100 m by 100 m.

TABLE 3-4a. Mining equipment lighting list.

Alton Coal Project Night Sky Effects Study		
	Lamps	Comments
Stationary Equipment		
Dragline	HPSV/1000 W	17 lamps on boom and house, toward ground 2 lamps (gantry, house) angled up approximately 20-30° from vertical, illuminating boom
Drill	HPSV/400 W	4 lamps horizontal, 2.5 m above ground 1 lamp vertical, illuminating mast, 3.5 m above ground
Light Plant	HPSV/1000 W	4 lamps, angled not more than 45° from vertical, 8.5 m above ground, illuminating ground
Shovel	HPSV/1000 W	5 lamps
Mobile Equipment		
Blade	Halogen/60 W	6 lamps
Dozer	Halogen/60 W	6 lamps (2 are back-up lights)
Loader	Halogen/60 W	6 lamps
Truck - Coal	Halogen/60 W	4 lamps
Rock	Halogen/60 W	8 lamps
Water	Halogen/60 W	4 lamps

* All are head lamps (or, for dozer, back-up lamps).

TABLE 3-4b. Lighting emissions from mining equipment locations for years 21-22. (Cells are 100 m x 100 m.)

Area Name	Latitude	Longitude	Decimal Latitude	Decimal Longitude	Mining Equipment	Total Luminosity (lumens)	Elevation (meters)	Light Source*
PIT K	37 21 1.5	112 18 54.8	37.3504	112.3152	Drill	712,800‡	2057	1
	37 21 1.6	112 18 46.6	37.3504	112.3129	Dozer	13,800	2057	2
	37 21 1.6	112 18 42.6	37.3504	112.3118	Shovel, coal truck	403,000; 9,200	2057	1,2
	37 21 1.7	112 18 38.5	37.3505	112.3107	Light plant, loader	743,977‡‡‡; 13,800	2057	1,2
	37 20 58.3	112 18 50.6	37.3495	112.3141	Rock truck	18,400	2057	2
	37 20 58.4	112 18 38.5	37.3496	112.3107	Coal truck	9,200	2057	2
	37 20 58.5	112 18 34.4	37.3496	112.3096	Coal truck	9,200	2057	2
	37 20 55.1	112 18 50.6	37.3486	112.3141	Rock truck	18,400	2057	2
	37 20 51.9	112 18 46.5	37.3477	112.3129	Rock truck	18,400	2057	2
	37 20 51.9	112 18 42.4	37.3477	112.3118	Blade	13,800	2057	2
	37 20 48.6	112 18 46.4	37.3468	112.3129	Light plant, dozer	743,977‡‡‡; 13,800	2057	1,2
	37 20 48.7	112 18 42.3	37.3469	112.3117	Light plant, rock truck	743,977‡‡‡; 18,400	2057	1,2
	37 20 48.7	112 18 34.2	37.3469	112.3095	Coal truck	9,200	2057	2
	37 20 45.3	112 18 54.5	37.3459	112.3151	Water truck, coal truck	9,200 and 9,200	2057	2
PIT L	37 19 51.1	112 23 11.4	37.3309	112.3865	Drill	712,800‡	2012	1
	37 19 51.3	112 23 3.2	37.3309	112.3842	Shovel, coal truck, dozer	403,000; 23,000	2012	1,2
	37 19 47.9	112 23 7.2	37.3300	112.3853	Coal truck	9,200	2012	2
	37 19 41.4	112 23 3.0	37.3282	112.3842	Coal truck	9,200	2012	2

continued

TABLE 3-4b. (concluded)

Area	Name	Latitude	Longitude	Decimal Latitude	Decimal Longitude	Mining Equipment	Total Luminosity (lumens)	Elevation (meters)	Light Source*
PIT	L	37 19 41.5	112 22 59.0	37.3282	112.3831	Blade	13,800	2012	2
continued		37 19 38.2	112 23 3.0	37.3273	112.3842	Light plant, dozer	743,977‡‡‡; 13,800	2012	1,2
		37 19 38.2	112 22 58.9	37.3273	112.3830	Light plant, coal truck	743,977‡‡‡; 9,200	2012	1,2
		37 19 34.9	112 23 11.1	37.3264	112.3864	Water truck	9,200	2012	2
PIT	J	37 20 34.0	112 20 58.4	37.3428	112.3496	Drill	712,800‡	2005	1
		37 20 34.1	112 20 46.2	37.3428	112.3462	Rock truck	18,400	2005	2
		37 20 34.2	112 20 42.2	37.3428	112.3451	Dozer	13,800	2005	2
		37 20 34.2	112 20 38.1	37.3428	112.3439	Dragline	1,063,140‡‡	2005	1
PIT	A	37 23 9.7	112 26 58.2	37.3860	112.4495	Drill	712,800‡	2072	1
		37 23 0.0	112 26 58.1	37.3833	112.4495	Dozer	13,800	2072	2
		37 22 56.7	112 26 58.0	37.3824	112.4494	Dragline	1,063,140‡‡	2072	1

* 1 = High pressure sodium lamps (HPSV).
2 = Halogen head lamps.

‡ For "preliminary design" 162,000 lumens.

‡‡ For "preliminary design" 787,000 lumens.

‡‡‡ For "preliminary design" 323,000 lumens.

TABLE 3-4c. Alton mining industrial site light distribution (100 x 100 meter squares).

	Center Location		Elevation	Luminosity
	Latitude	Longitude	(m)	(lumens)
1.	37.376862	112.46912	2082	49,340
2.	37.377485	112.46863	2082	66,820
3.	37.378108	112.46813	2082	23,030
4.	37.378731	112.46763	2082	40,990
5.	37.379354	112.46714	2082	24,860
6.	37.376239	112.46863	2082	42,720
7.	37.376862	112.46813	2082	44,340
8.	37.377485	112.46763	2082	84,120
9.	37.378108	112.46714	2082	32,440
10.	37.378731	112.46664	2082	37,240
11.	37.379354	112.46614	2082	11,800
12.	37.379977	112.46565	2082	4,800
13.	37.380600	112.46515	2082	15,320
14.	37.374933	112.46863	2082	3,240
15.	37.375616	112.46813	2082	39,040
16.	37.376239	112.46763	2082	37,280
17.	37.376862	112.46714	2082	31,440
18.	37.377485	112.46664	2082	74,640
19.	37.378108	112.46614	2082	16,920
20.	37.379354	112.46515	2082	1,400
21.	37.379977	112.46465	2082	111,760
22.	37.380600	112.46416	2082	22,680
23.	37.374370	112.46813	2082	6,480
24.	37.374933	112.46763	2082	59,920
25.	37.375616	112.46714	2082	51,680
26.	37.376239	112.46664	2082	419,760
27.	37.376862	112.46614	2082	538,840

continued

TABLE 3-4c. (concluded)

	Center Location		Elevation	Luminosity
	Latitude	Longitude	(m)	(lumens)
28.	37.377485	112.46565	2082	74,520
29.	37.378108	112.46515	2082	57,560
30.	37.378731	112.46465	2082	69,760
31.	37.379354	112.46416	2082	30,024
32.	37.379977	112.46366	2082	32,400
33.	37.37437	112.46714	2082	9,240
34.	37.374933	112.46664	2082	9,760
35.	37.375616	112.46614	2082	8,000
36.	37.376239	112.46565	2082	46,140
37.	37.376862	112.46515	2082	113,140
38.	37.377485	112.46465	2082	46,400
39.	37.378731	112.46366	2082	29,560
40	37.379354	112.46316	2082	3,240
41.	37.375616	112.46515	2082	53,980
42.	37.376239	112.46465	2082	168,020
43.	37.376862	112.46416	2082	60,700
44.	37.374933	112.46465	2082	28,860
45.	37.375616	112.46416	2082	31,240
46.	37.376239	112.46366	2082	43,960
47.	37.374370	112.46416	2082	15,360
48.	37.374933	112.46366	2082	5,840
49.	37.375616	112.46316	2082	1,400
50.	37.376239	112.46266	2082	2,200

* All lights are high pressure sodium lamps.

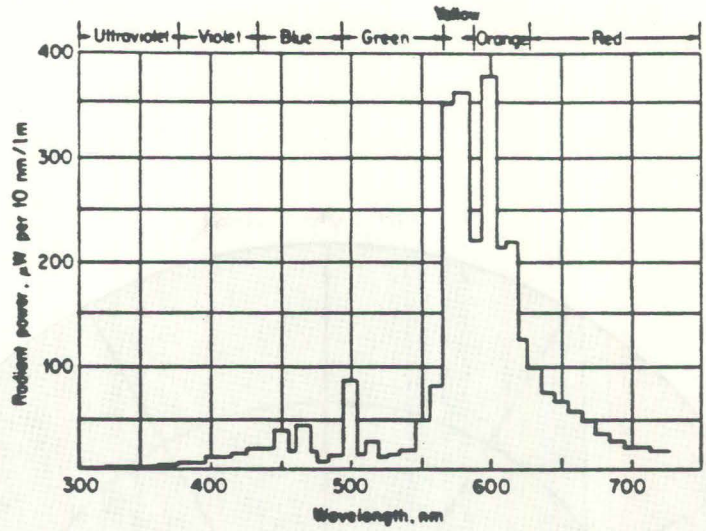


EXHIBIT 3-4a. Spectral output of high pressure sodium lamp. (General Electric Bull. TP-109.)

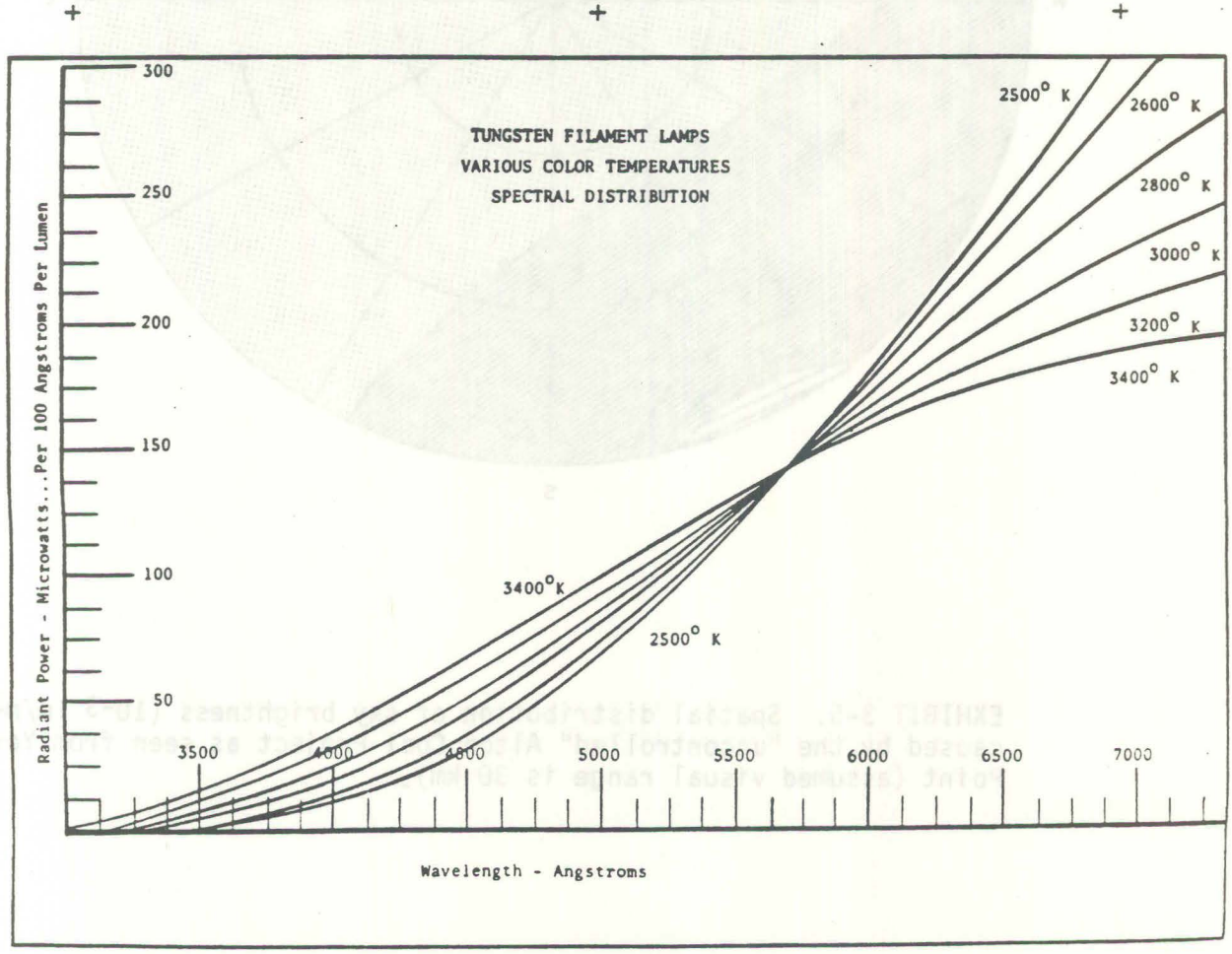


EXHIBIT 3-4b. Spectral output of a halogen lamp.

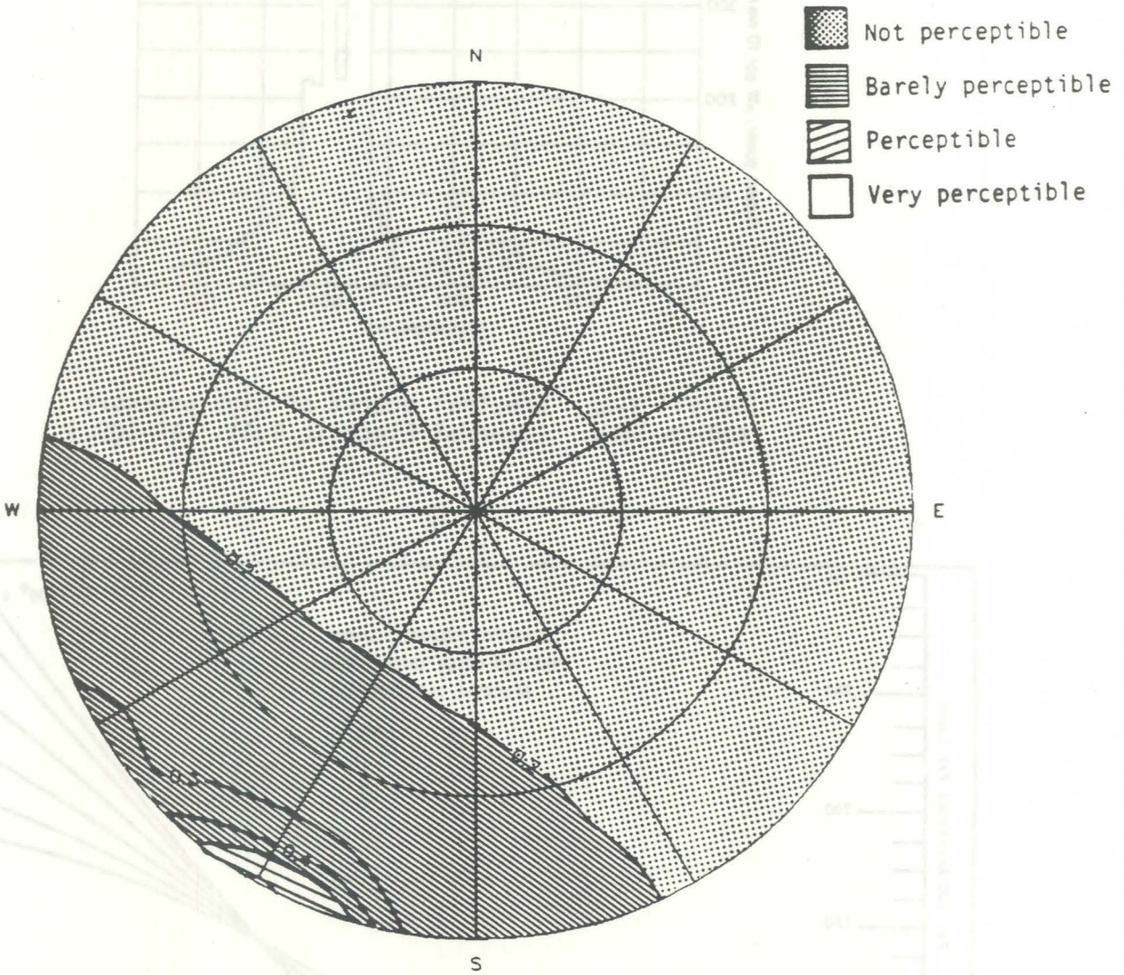


EXHIBIT 3-5. Spatial distribution of sky brightness (10^{-3} lm/m^2/sr) caused by the "uncontrolled" Alton Coal Project as seen from Yovimpa Point (assumed visual range is 30 km).

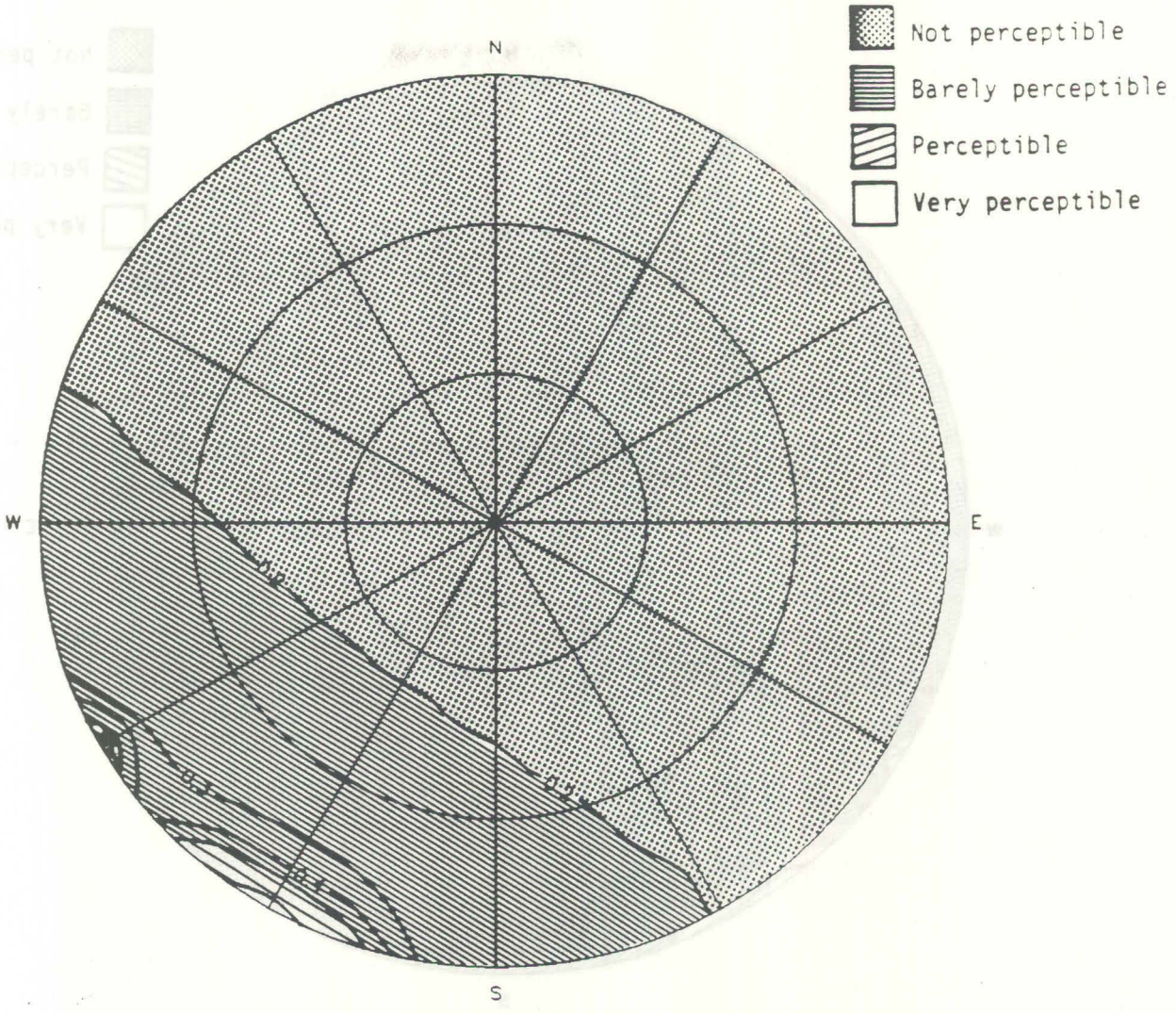


EXHIBIT 3-6. Spatial distribution of sky brightness (10^{-3} lm/m^2/sr) caused by the "uncontrolled" Alton Coal Project from Yovimpa Point (background visual range within each layer is 0-1 km--70 km; 1-3 km--100 km; 3-7 km--400 km; 7-20 km--1000 km).

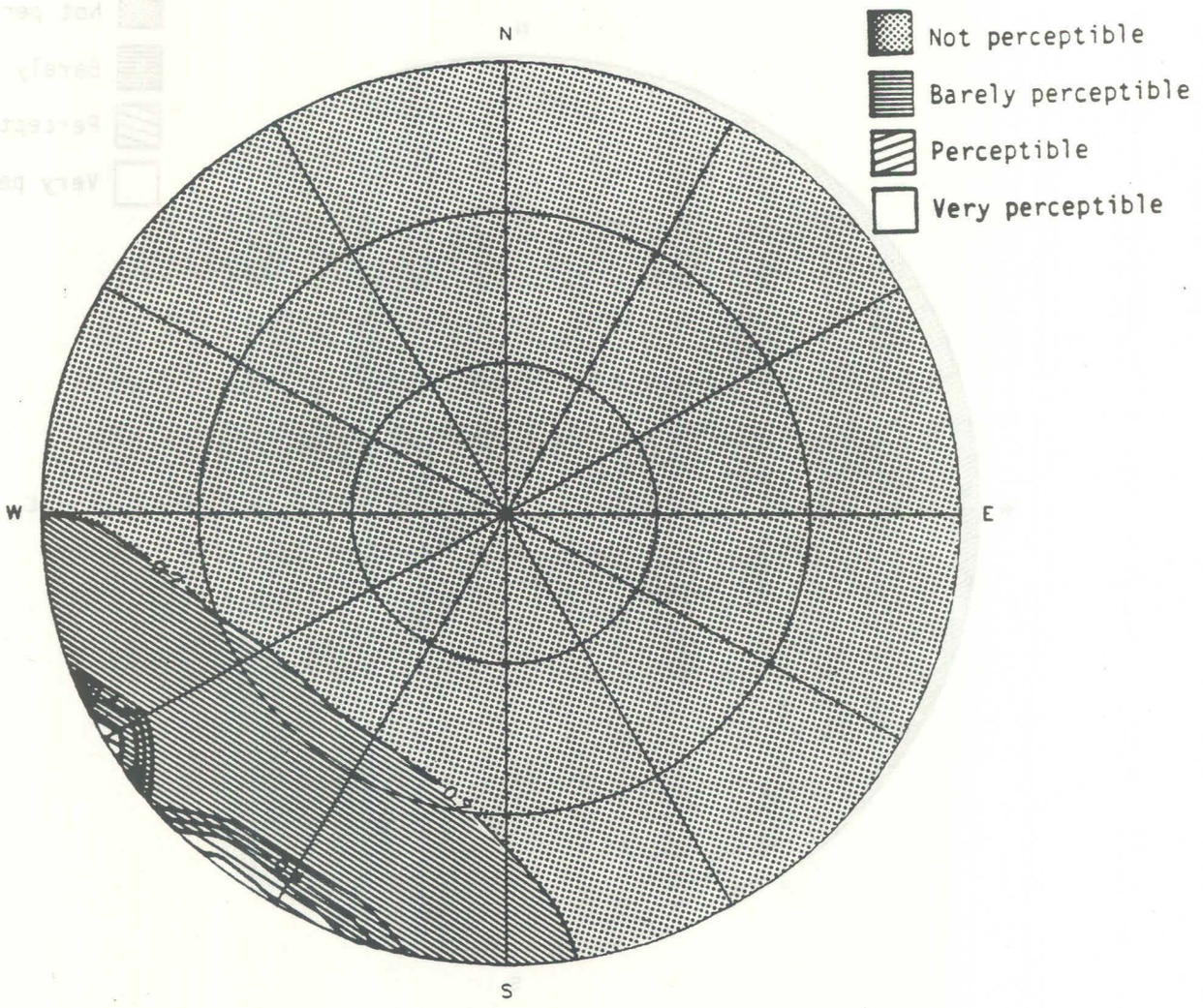


EXHIBIT 3-7. Spatial distribution of sky brightness (10^{-3} lm/m^2/sr) caused by the "uncontrolled" Alton Coal Project as seen from Yovimpa Point (assumed visual range is 391 km).

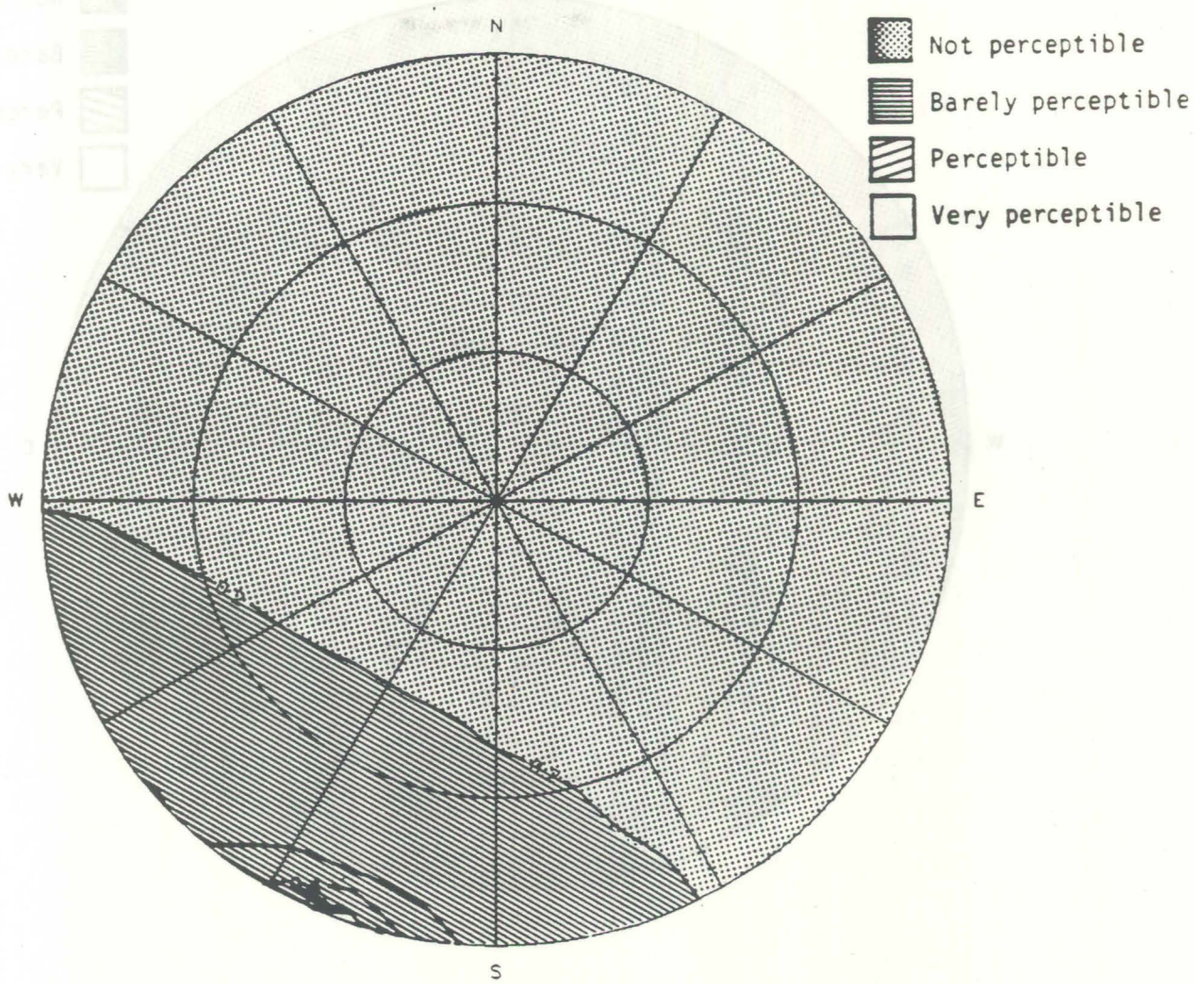


EXHIBIT 3-8. Spatial distribution of sky brightness (10^{-3} lm/m^2/sr) caused by the "uncontrolled" Alton Coal Project as seen from View Point (assumed visual range is 30 km).

87131

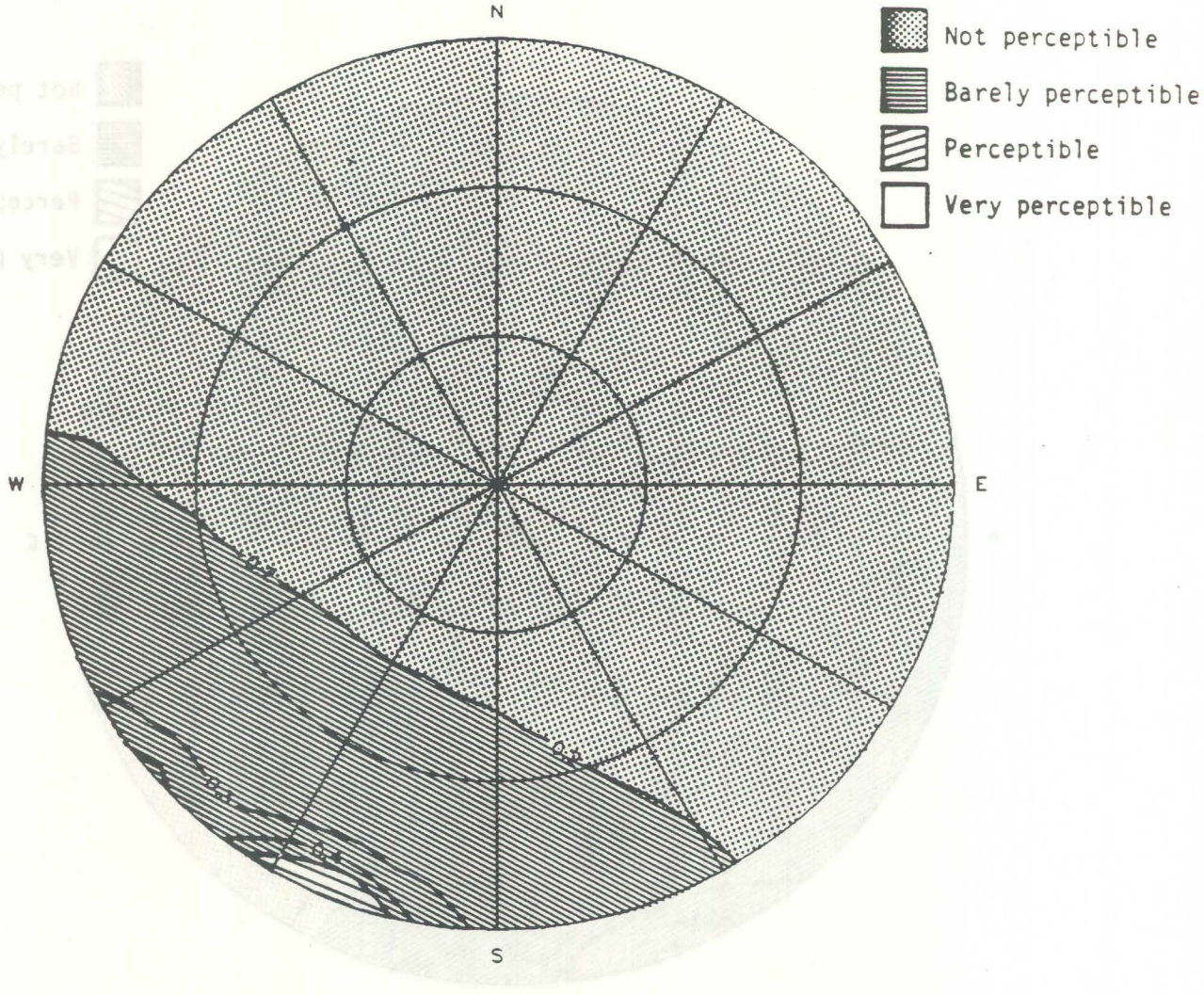


EXHIBIT 3-9. Spatial distribution of sky brightness (10-3 $lm/m^2/sr$) caused by the "uncontrolled" Alton Coal Project as seen from View Point (background visual range within each layer is 0-1 km--70 km; 1-3 km--100 km; 3-7 km--400 km; 7-20 km--1000 km).

87131

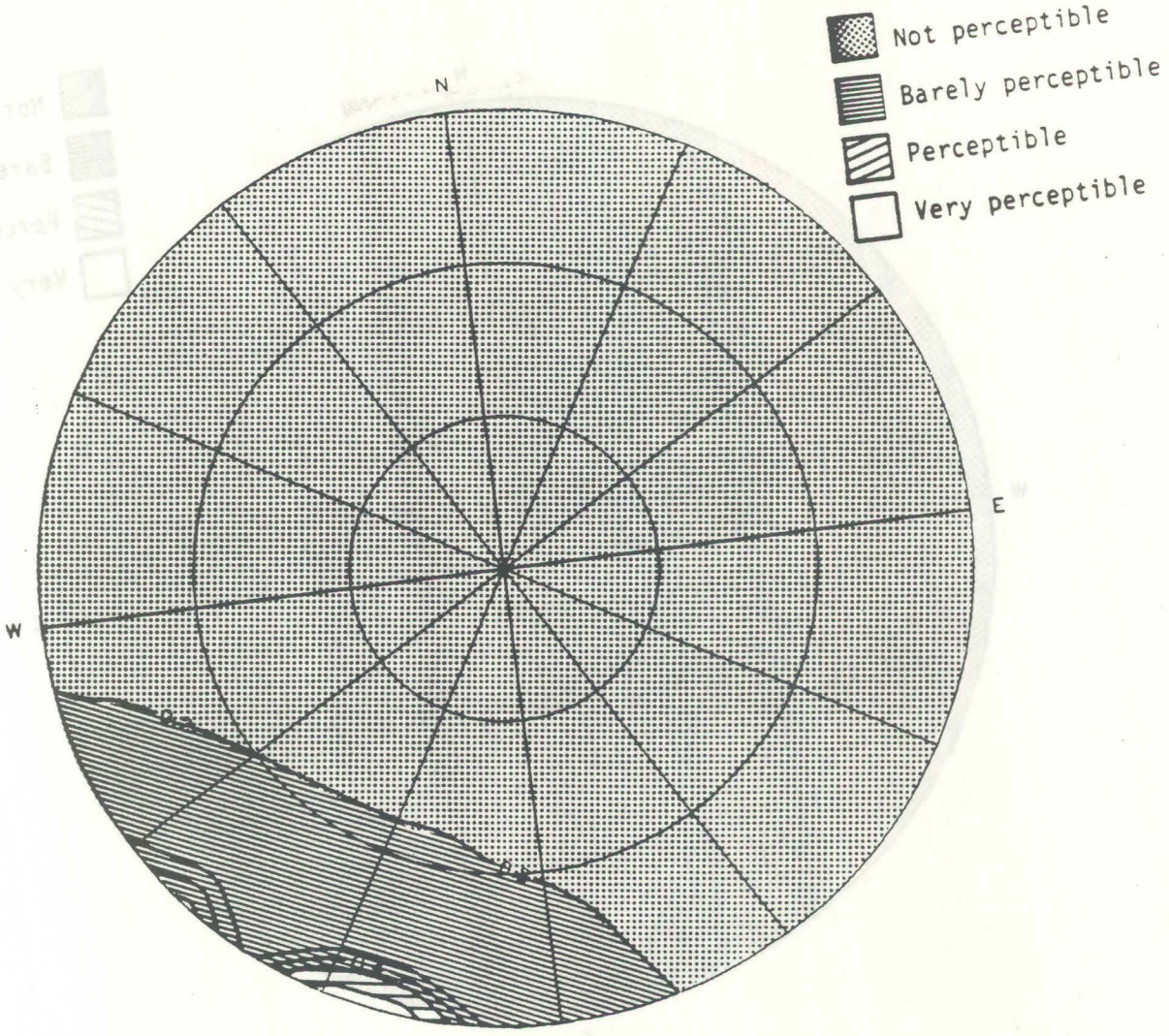


EXHIBIT 3-10. Spatial distribution of sky brightness (10-3 $lm/m^2/sr$) caused by the "uncontrolled" Alton Coal Project as seen from View Point (assumed visual range is 391 km).

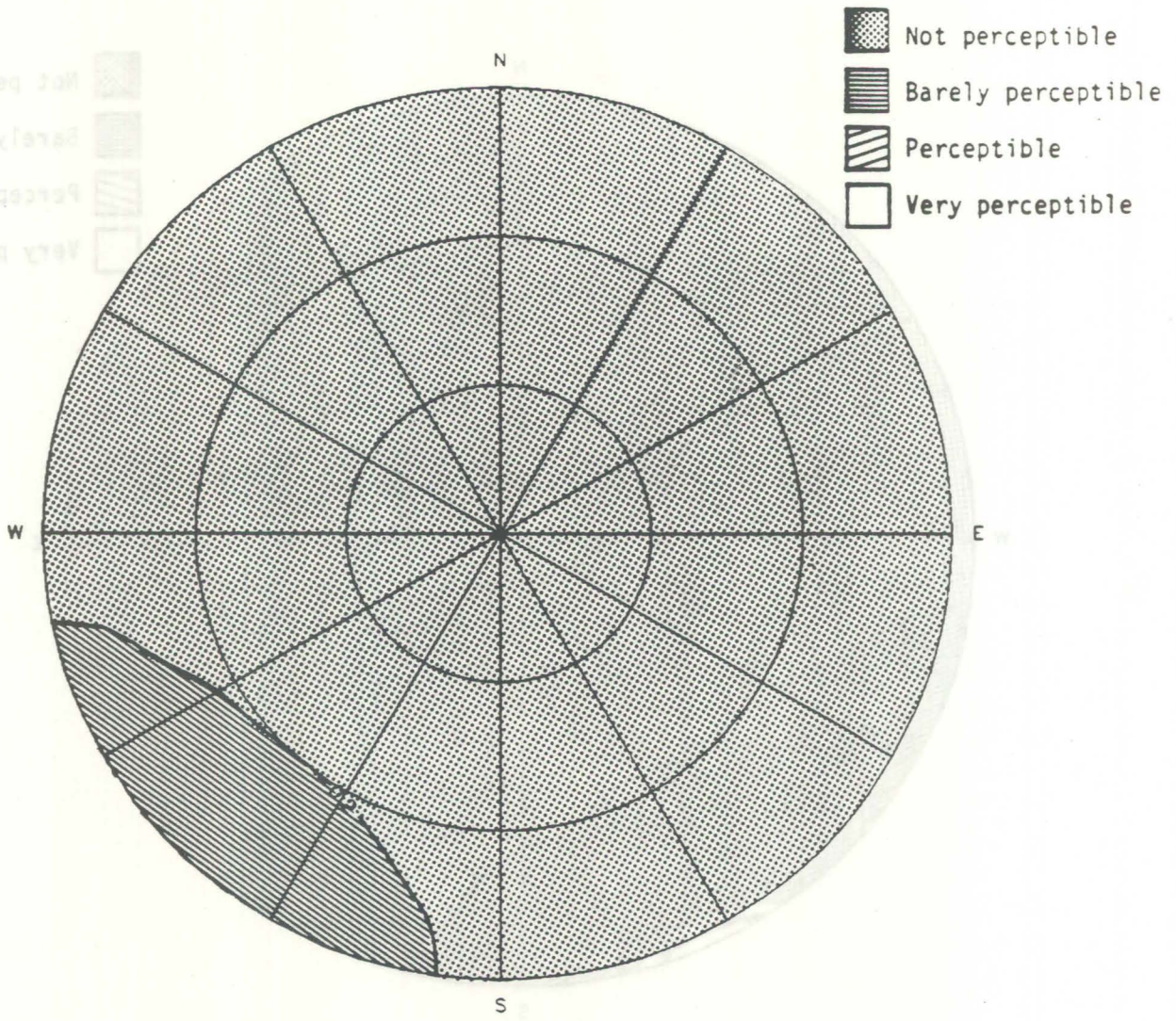


EXHIBIT 3-11. Spatial distribution of sky brightness (10^{-3} $lm/m^2/sr$) caused by the "uncontrolled" Alton Coal Project as seen from Bryce Point (assumed visual range is 30 km).

87131

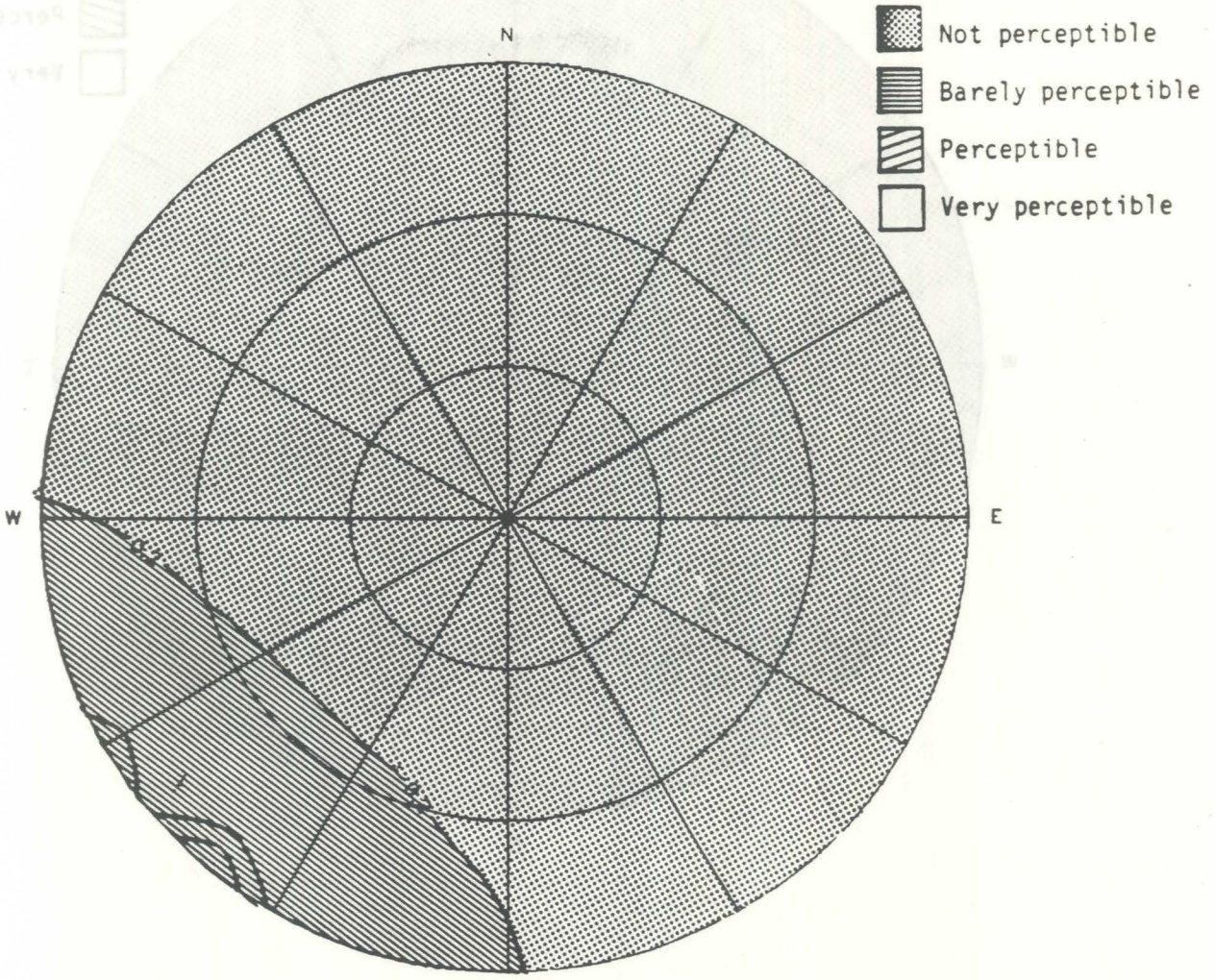


EXHIBIT 3-12. Spatial distribution of sky brightness (10^{-3} $lm/m^2/sr$) caused by the "uncontrolled" Alton Coal Project as seen from Bryce Point (background visual range within each layer is 0-1 km--70 km; 1-3 km--100 km; 3-7 km--400 km; 7-20 km--1000 km).

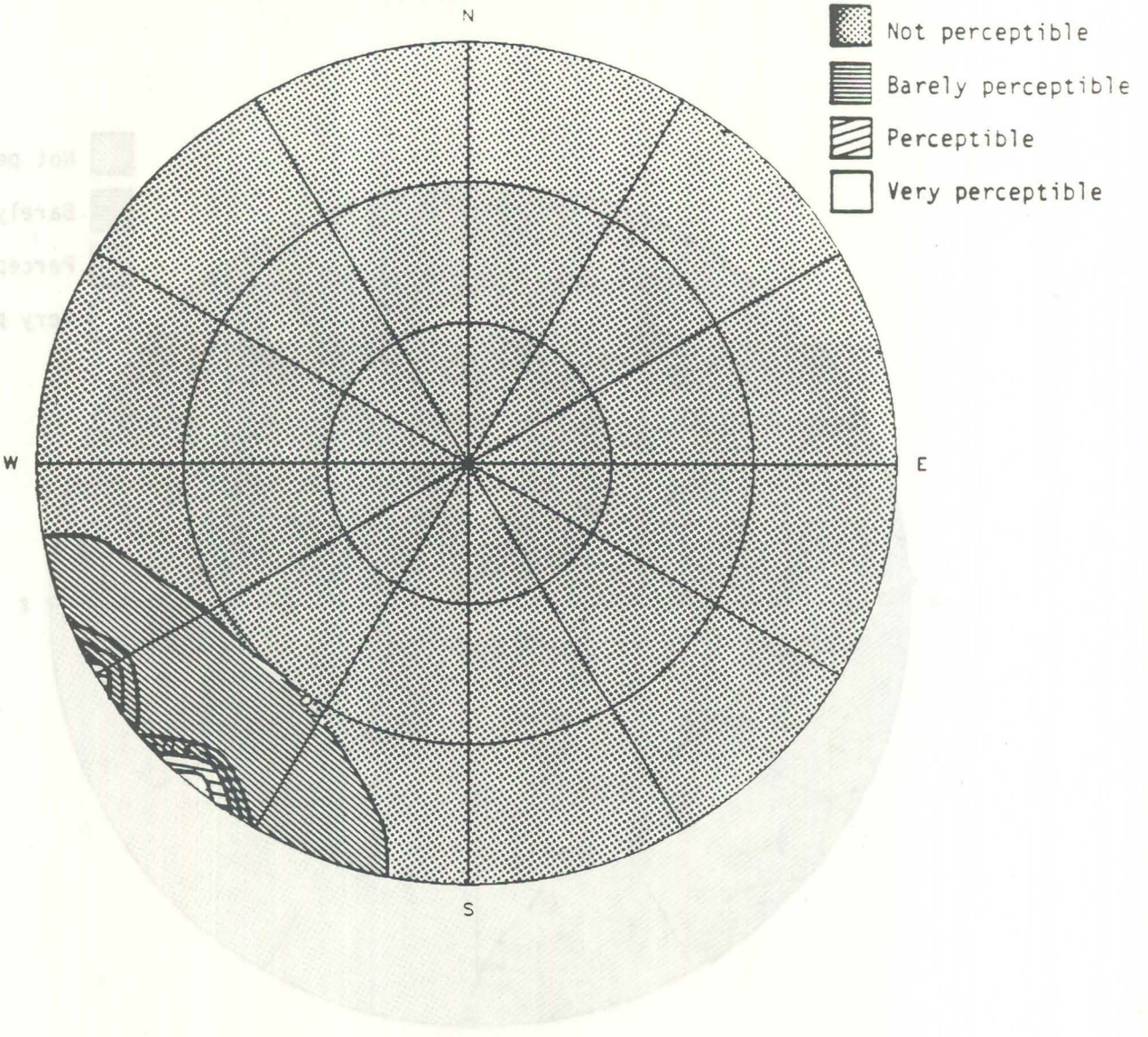


EXHIBIT 3-13. Spatial distribution of sky brightness (10^{-3} lm/m^2/sr) caused by the "uncontrolled" Alton Coal Project as seen from Bryce Point (assumed visual range is 391 km).

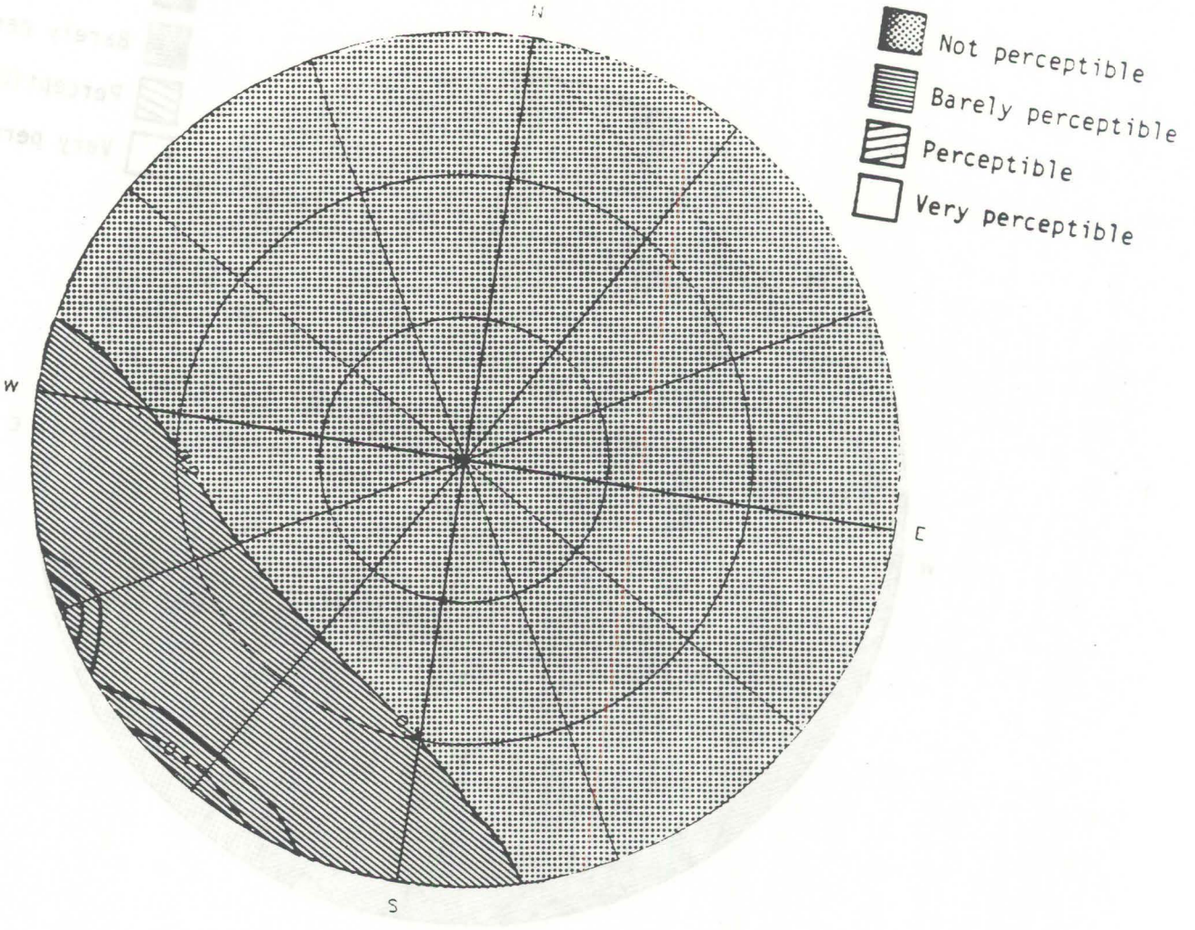


EXHIBIT 3-14. Spatial distribution of sky brightness (10^{-3} lm/m^2/sr) caused by the Alton Coal Project "preliminary design" case as seen from Yovimpa Point (background visual range within each layer is 0-1 km--70 km; 1-3 km--100 km; 3-7 km--400 km; 7-20 km--1000 km).

87131

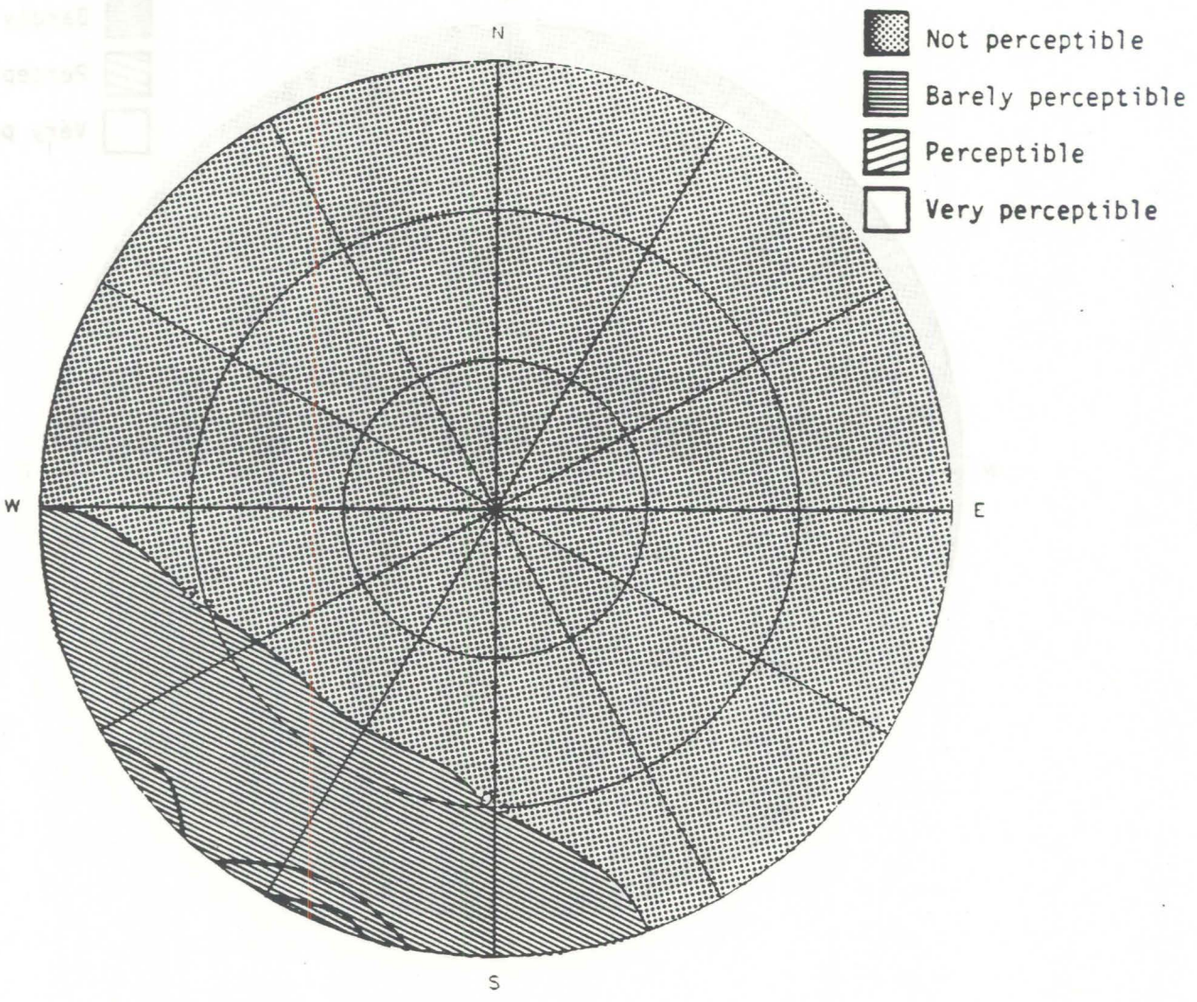


EXHIBIT 3-15. Spatial distribution of sky brightness (10^{-3} lm/m^2/sr) caused by the Alton Coal Project "preliminary design" case as seen from View Point (background visual range within each layer is 0-1 km--70 km; 1-3 km--100 km; 3-7 km--400 km; 7-20 km--1000 km).

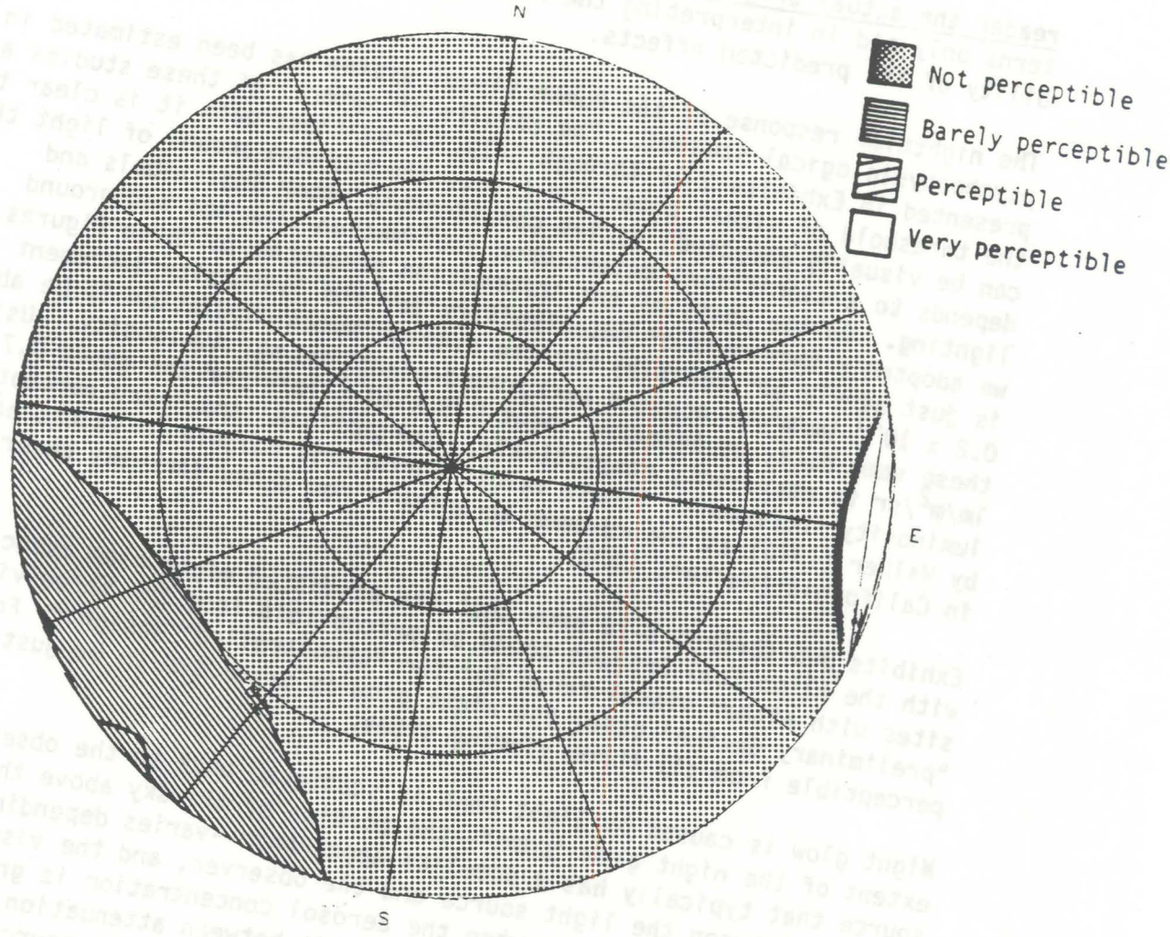


EXHIBIT 3-16. Spatial distribution of sky brightness (10^{-3} $lm/m^2/sr$) caused by the Alton Coal Project "preliminary design" case as seen from Bryce Point (background visual range within each layer is 0-1 km--70 km; 1-3 km--100 km; 3-7 km--400 km; 7-20 km--1000 km).

87131

reader the actual brightness of the sky predicted by the model. The patterns only aid in interpreting the results, and do not represent perceptibility of the predicted effects.

The nighttime response of the human visual system has been estimated in psychophysiological studies. The results of several of these studies are presented in Exhibits 3-17 through 3-19. From these data it is clear that the threshold of visual detection (i.e., the minimum amount of light that can be visually detected) varies considerably among individuals and depends to a significant extent upon acclimation time and background lighting. On the basis of the information presented in these figures, we adopted a threshold of detectability (or the luminosity increment that is just barely perceptible) for the average human population to be about 0.2×10^{-3} $lm/m^2/sr$ above a background nighttime sky luminosity. Using these same data, we selected about 0.5×10^{-3} $lm/m^2/sr$ and about $0.7\ 10^{-3}$ $lm/m^2/sr$ to represent, respectively, "perceptible" and "very perceptible" luminosity increments. These values correspond roughly to values adopted by Walker (1970) as the maximum acceptable for a new dark-sky observatory in California (Walker, 1970).

Exhibits 3-5 through 3-16 show that the predicted night glow associated with the Alton Coal Project could be perceptible from the three viewing sites with either visual range for the "uncontrolled" design." For the "preliminary design" case, the night glow is predicted to be just barely perceptible from all three viewing sites.

Night glow is caused by light that is scattered back to the observer. The extent of the night glow "dome"--the portion of the sky above the light source that typically has a domelike appearance--varies depending on the distance between the light source and the observer, and the visual range (the visual range is lower when the aerosol concentration is greater). Exhibit 3-20 illustrates this relationship between attenuation of the light from the glow dome and the distance from the light source.

When an observer is near a light source (Exhibit 3-20, region 1) in a high aerosol ("dirty") atmosphere, more light is scattered than in a low aerosol ("clean") atmosphere, resulting in the appearance of a brighter glow dome and a higher peak intensity. This characteristic was predicted for the light source located within 5 kilometers of Canyonlands National Park and modeled in the Canyonlands Night Sky Study (1985).

When an observer is located further from the light source, attenuation of the light from the glow dome in the "dirty" atmosphere is greater than attenuation in the "clean" atmosphere (Exhibit 3-20, region 2). In this situation the observer sees a higher peak intensity in the "clean" atmosphere because less attenuation occurs between the glow dome and the

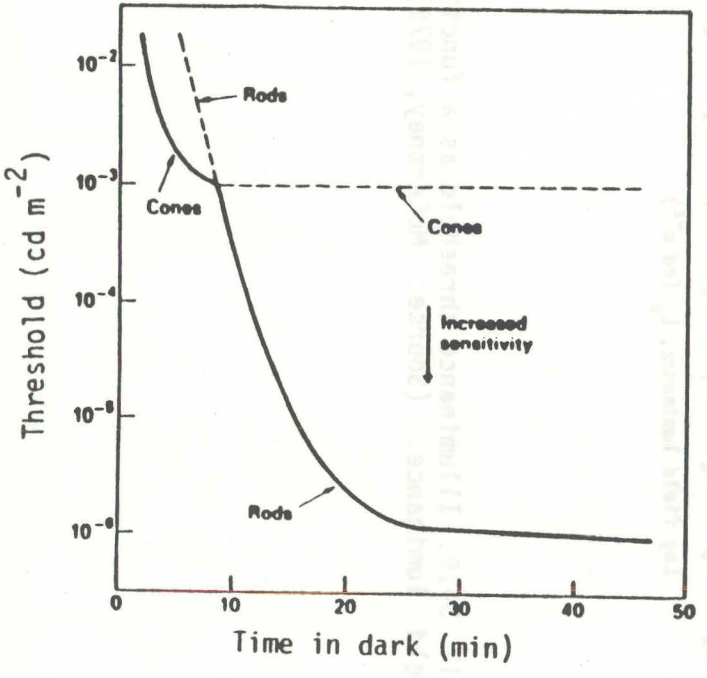


EXHIBIT 3-17. The darkness adaptation function (continuous line) of a light adapted subject. The broken lines are continuations of the separate hypothetical rod and cone functions. (Source: Padgham and Saunders, 1975)

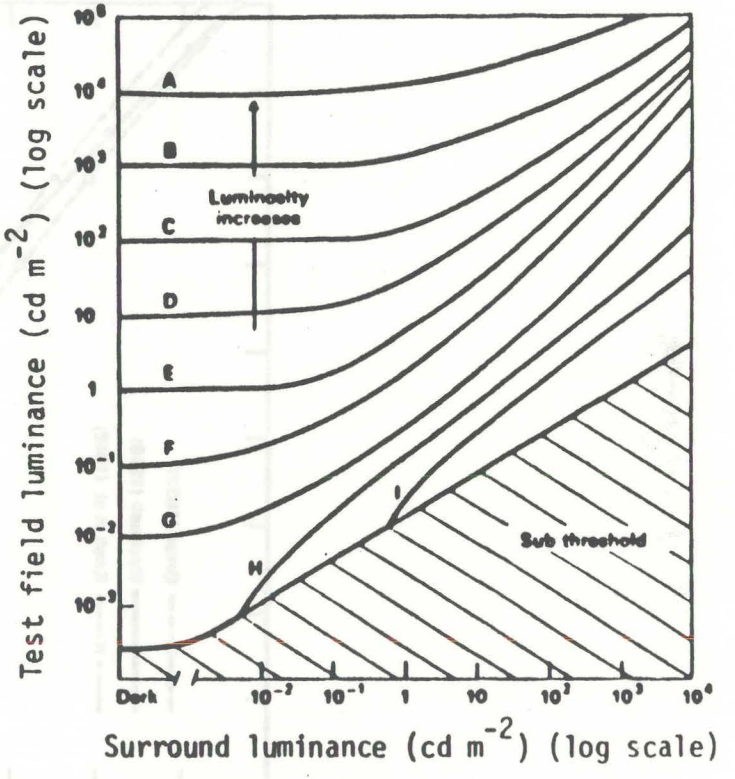


EXHIBIT 3-18. Contours of constant luminosity measured for a range of background luminances. (Source: Padgham and Saunders, 1975)

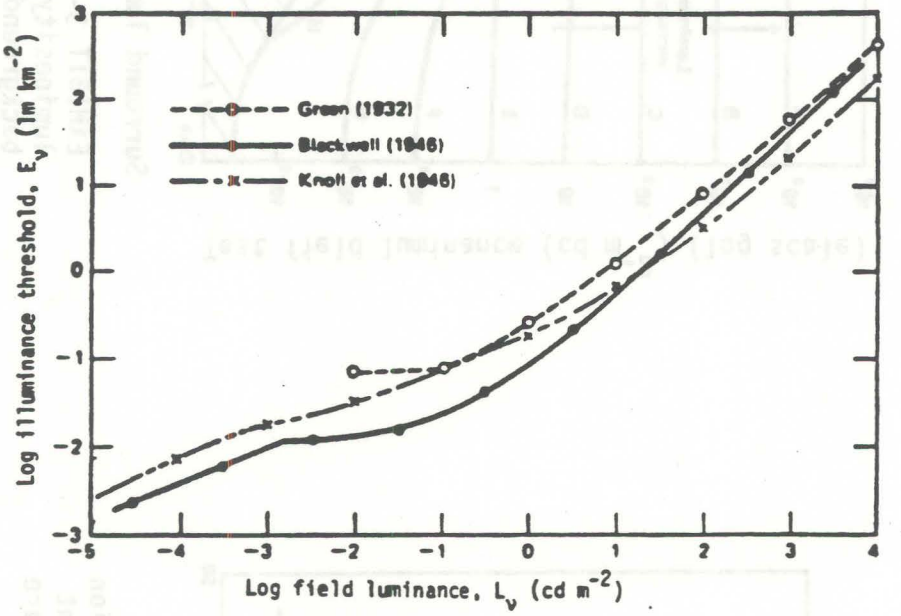


EXHIBIT 3-19. Illuminance threshold as a function of field luminance. (Source: McCartney, 1976)

87131r3
84186

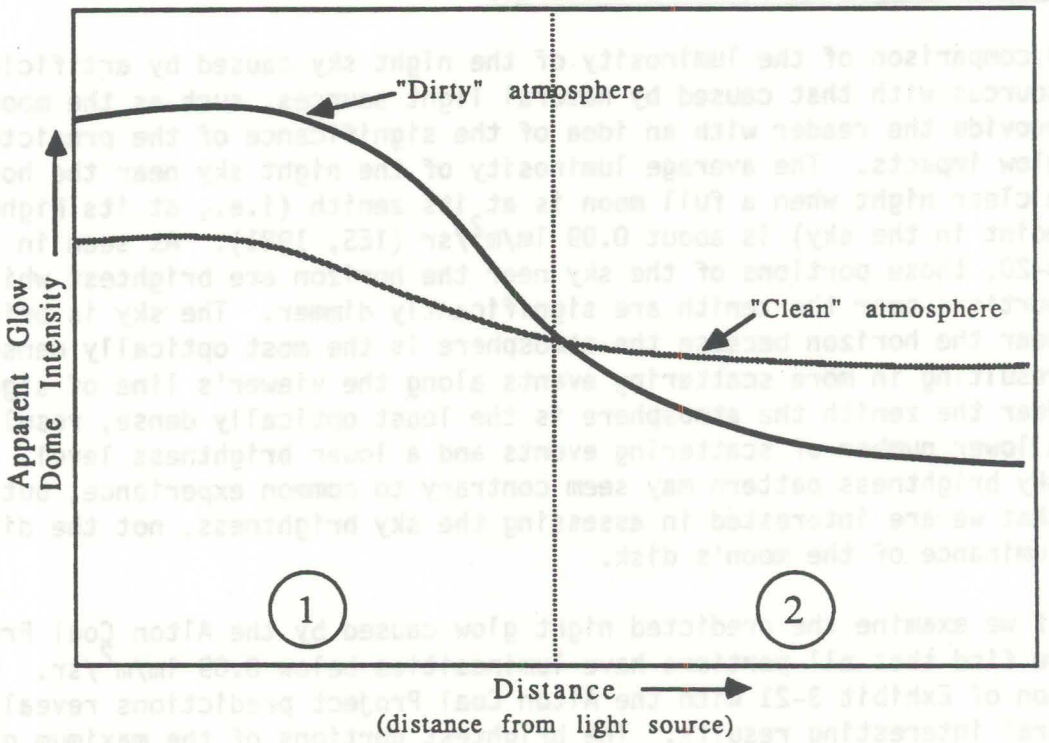


EXHIBIT 3-20. Apparent glow dome intensity as a function of distance from light source.

observer, making the glow appear brighter than in the "dirty" atmosphere. In other words, the glow dome that appears brightest to a close-in observer in the "dirty" case will appear to be dimmest to the distant observer in the same case. This characteristic was observed at all three viewing sites in this study.

Comparison of Night Glow Caused by Artificial and Natural Light Sources

A comparison of the luminosity of the night sky caused by artificial light sources with that caused by natural light sources, such as the moon, may provide the reader with an idea of the significance of the predicted sky-glow impacts. The average luminosity of the night sky near the horizon on a clear night when a full moon is at its zenith (i.e., at its highest point in the sky) is about 0.09 $lm/m^2/sr$ (IES, 1981). As seen in Exhibit 3-20, those portions of the sky near the horizon are brightest while those portions near the zenith are significantly dimmer. The sky is brightest near the horizon because the atmosphere is the most optically dense, resulting in more scattering events along the viewer's line of sight. Near the zenith the atmosphere is the least optically dense, resulting in a lower number of scattering events and a lower brightness level. This sky brightness pattern may seem contrary to common experience, but recall that we are interested in assessing the sky brightness, not the direct luminance of the moon's disk.

If we examine the predicted night glow caused by the Alton Coal Project, we find that all portions have luminosities below 0.09 $lm/m^2/sr$. Comparison of Exhibit 3-21 with the Alton Coal Project predictions reveals several interesting results. The brightest portions of the maximum glow "domes" predictions for the "preliminary design" case (i.e., the portions labeled "barely perceptible") and the "uncontrolled" case are well below the lowest luminosity of the glow from a full moon. The predicted spatial extent of the glow "dome" caused by the Coal Project is much smaller than the spatial extent of the night glow caused by the moon.

In comparison, the Alton Coal Project's light emissions may occur during all nighttime hours, while the full moon is only visible approximately 12.5 percent of all nighttime hours (given cloud-free skies). Similarly, a three-fourths full moon, a half-full moon, and a first-quarter or third-quarter moon are visible only 18.75 percent, 12.5 percent, and 6.25 percent, respectively, of all nighttime hours. The remaining 50 percent of the nighttime hours occur when no moon is visible.

For a further comparison of the amount of night glow caused by artificial light sources, the town of Tropic, Utah was modeled (Exhibits 3-22 and

Very perceptible

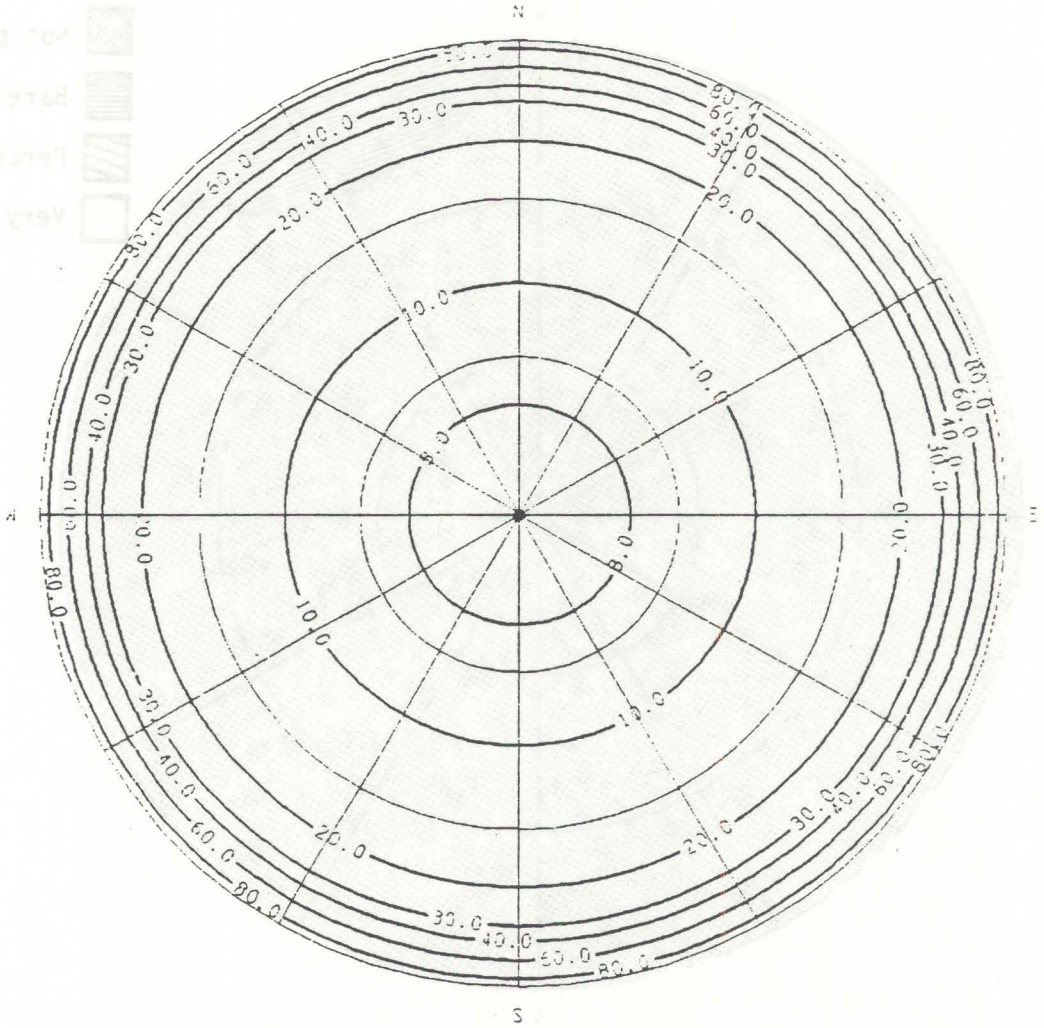


EXHIBIT 3-21. Spatial distribution of sky brightness (10^{-3} lm/m^2/sr) caused by a full moon at the zenith as seen from Bryce Canyon National Park. (Source: Van De Hulst, 1980, and RCA, 1974)

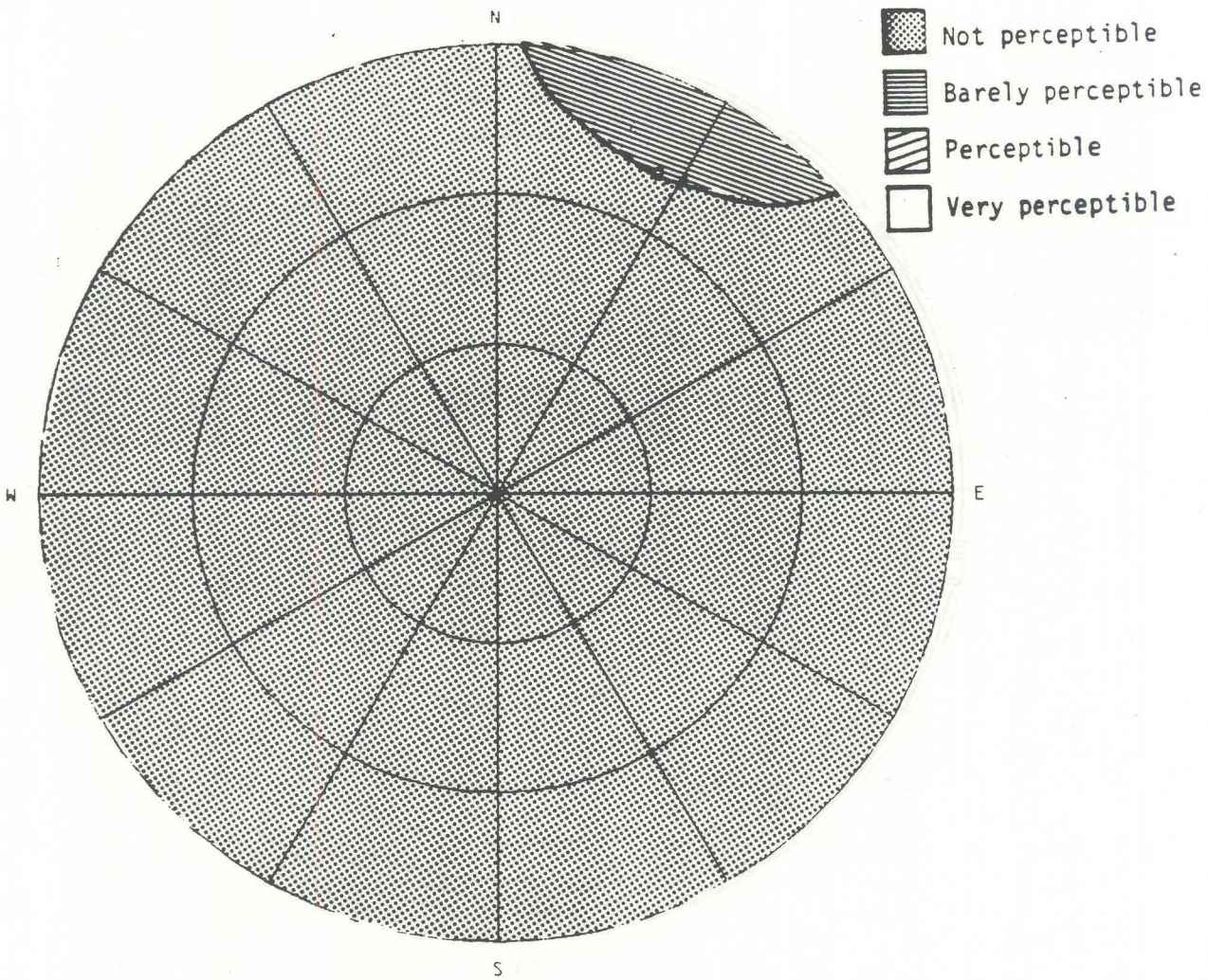


EXHIBIT 3-22. Spatial distribution of sky brightness (10^{-3} lm/m^2/sr) caused by Tropic, Utah as seen from Bryce Point based on street lighting inventory only (background visual range within each layer is 0-1 km--70 km; 1-3 km--100 km; 3-7 km--400 km; 7-20 km--1000 km).

3-23). Tropic is located approximately 6.5 km from Bryce Point and was modeled using two different estimates of the light emission inventory. An estimate of lighting was obtained from Garkane Power Association, which provided an emission inventory of all street lighting for the town. This represents a lower bound since no additional sources of light (such as residential and industrial) were included in the inventory. The second estimate, based on the relationship found by Walker (1977) between population and luminosity, represents an overestimate of the light emissions from Tropic because Walker's relationship was based on larger cities (> 1,000 people), which are more industrialized and contain such nighttime lighting sources as shopping and industrial centers.

Exhibits 3-22 and 3-23 show that a night glow effect due to the town of Tropic is discernible from Bryce Point. However, the amount of sky glow discernible (assuming Walker's estimate of luminosity) by a viewer who noticed just "barely perceptible" effects of increased sky brightness would be less than about 10 percent of the total sky.

Modeling results show that the Alton Coal Project glow dome for the "preliminary design" will be slightly larger than the dome caused by Tropic for the years 21-22 when the mining operations are closest to the park. As viewed from Bryce Point, the areal coverage of the perceptible night glow from the Alton Coal Project will be approximately 1.3 times that for Tropic on the basis of Walker's relationship. Additionally, the dome caused by Tropic is located in the northeast portion of the sky, whereas the dome due to the Alton Coal Project will be in the southwest portion of the sky; as a result, the effects from each source should not be cumulative.

Obscuration of Starlight by Night Glow Caused by the Alton Coal Project

As a result of the perceptible glow "dome" in the night sky, the light from the proposed coal project that is scattered by the atmosphere may at times interfere with the viewing of some stars and the Milky Way (Table 3-5). The faintest star visible to the average human is approximately magnitude six. To ensure that our three background visual range conditions of 30, 70, and 391 km did not obscure the visibility of sixth-magnitude stars, we estimated the limiting magnitude due solely to low visibility. We decided to analyze the 30-km visual range since it obscures the sky the most because of the higher aerosol concentration. The degree to which incoming light is obscured can be roughly estimated through the use of the visual range formula and the assumption that the intensity of incoming light decreases exponentially with source intensity. If we assume that the e-folding distance for the scattering of light is approximately 8 km and that the visual range throughout the layer is 30 km, then

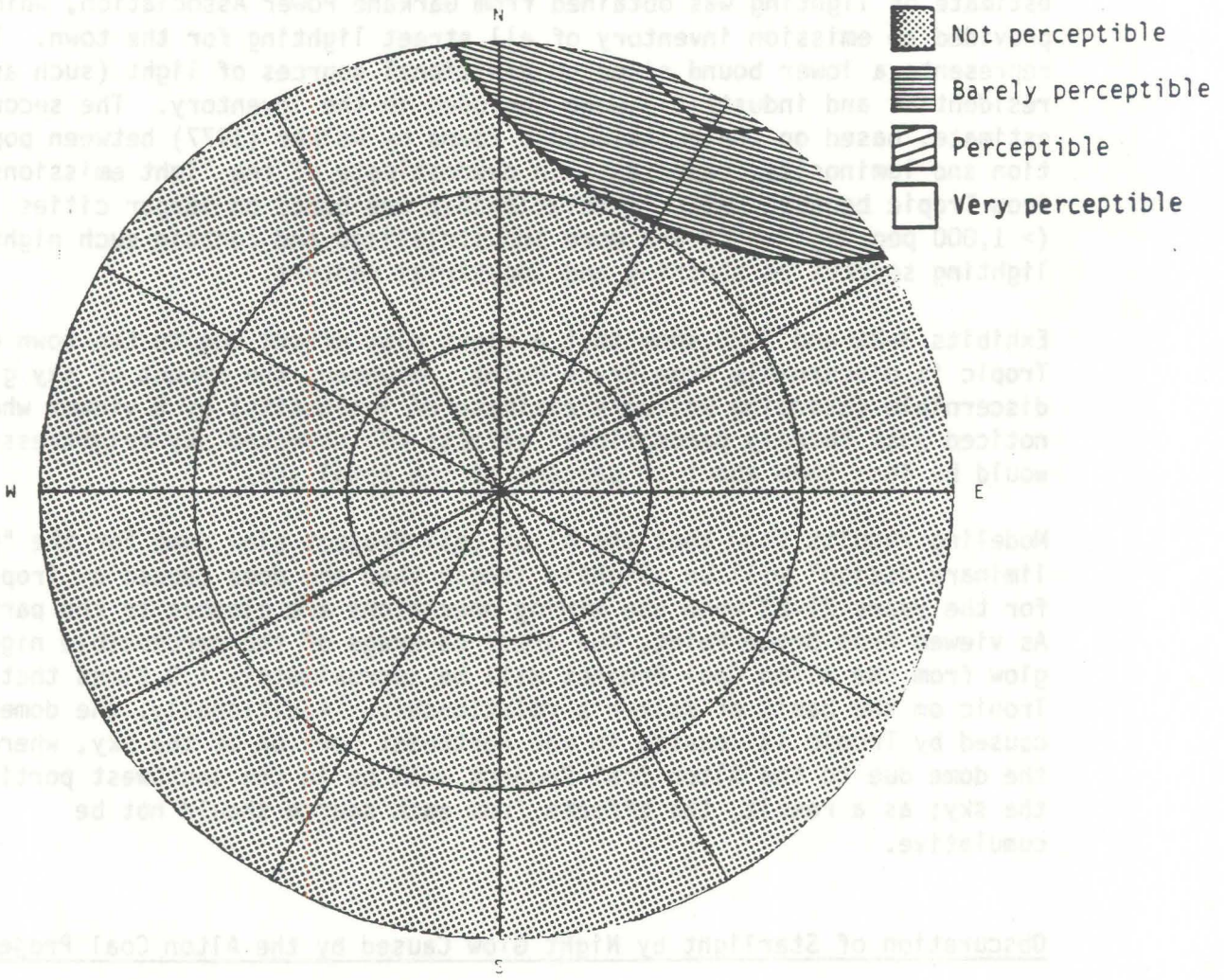


EXHIBIT 3-23. Spatial distribution of sky brightness (10^{-3} lm/m^2/sr) caused by Tropic, Utah as seen from Bryce Point based on Walker's relationship between population and luminosity (background visual range within each layer is 0-1 km--70 km; 1-3 km--100 km; 3-7 km--400 km; 7-20 km--1000 km).

TABLE 3-5. Stellar magnitude* of selected stars and planets (Pasachoff, 1977).

Magnitude	Name
-12.6	Moon
-4.4	Maximum brightness of Venus
-2.8	Maximum brightness of Mars
-1.4	Sirius
-0.7	Canopus
0.0	Vega
0.9	Aldebaran
+2.5	Polaris (North Star)
+3.7	Andromeda Galaxy (M31)
+5.5	Uranus
+7.8	Neptune

* Stellar magnitude numerically increases as perceived brightness decreases.

TABLE 3-6. Number of stars visible by magnitude for the entire celestial sphere (Cambridge University Press, 1985).

Magnitude	Number of Stars
-1	2
0	7
1	13
2	71
3	192
4	625
5	1,963
6	5,606
7	15,565
8	21,225

we could see stars to an approximate limiting magnitude of 6.2. The visual range would have to be about 25 km before the sixth-magnitude stars would no longer be visible.

Altogether there are about 8500 stars in the sky bright enough to be seen with the naked eye under excellent observing conditions. Of these 8500, approximately 5600 are sixth-magnitude stars that are scattered across the entire sky dome (Table 3-6). Thus, sixth-magnitude stars are as likely to be found near the horizon as near the zenith. The Milky Way, which typically extends from one horizon to the other, is usually only visible when sixth-magnitude stars are visible.

Using the formula developed by Weaver (1947) to calculate the limiting magnitudes of stars that can just be seen by the naked eye, we found that if the luminosity were to exceed 0.5×10^{-3} $lm/m^2/sr$, sixth-magnitude stars would no longer be visible. Referring to Exhibits 3-5 through 3-16, it is apparent that in areas labeled perceptible, some of the predicted sky glow exceeds the lumiosity level that would obscure sixth-magnitude stars. Exhibits 3-6, 3-9, and 3-12 represent maximum-effects scenarios for the "uncontrolled" case of the Alton Coal Project. These exhibits show that luminosity levels capable of obscuring sixth-magnitude stars occur at both Yovimpa and View Point and could cover up to 2 percent of the sky. Exhibits 3-14 through 3-16 represent maximum-effects scenarios for the "preliminary design" case of the Alton Coal Project. These exhibits show that luminosity levels capable of obscuring sixth-magnitude stars occur only at Yovimpa Point and account for less than 1 percent of the sky, and that the "preliminary design" case decreases the peak intensity from each viewing point by 33 percent over the "uncontrolled" case. As an approximation, those areas in the plots produced by the Night Sky Glow Model that are labeled "perceptible" and "very perceptible" glow could obscure some sixth-magnitude stars and portions of the Milky Way.

4 SUMMARY AND CONCLUSIONS

This study was performed to estimate the night sky glow that might result from nighttime mining operations of the proposed Alton Coal Project. The study comprised the following work:

Enhancement of an existing mathematical model of atmospheric optics to predict the nighttime sky-glow effects of the proposed Alton Coal Project.

Evaluation of the Night Sky Glow Model's prediction performance to the extent possible with existing data.

Application of the Night Sky Glow Model to the Alton Coal Project viewed from three points within Bryce Canyon National Park and for two lighting scenarios at the Alton Coal Project.

Estimation of the potential for normal perception of the calculated night glow and the potential of the night glow to obscure starlight.

The Night Sky Glow Model was successfully tested with measurements taken at Salinas, California. Although the evaluation of the model's performance was by no means comprehensive, the test results agreed well with the limited amount of night-glow measurements available. A summary of the results of the study is given below.

SUMMARY OF RESULTS

When applied to the light emission of the proposed Alton Coal Project for a mining scenario during years 21 and 22 of the projected 35-year mine, the Night Sky Glow Model predicts sky luminosities that could be perceptible from Yovimpa and View Point and to a lesser degree from Bryce Point. The size and character of the night-glow "dome" depend on the viewing site and its local topographic and natural surroundings, the atmospheric aerosol distribution and characteristics, and the visual range.

For the typical distances between the light source and observer considered in this study, the observer sees a higher peak intensity in a "clean"

atmosphere because less attenuation of light occurs between the glow dome and the observer, making the glow appear brighter than in the "dirty" atmosphere. The extent of the night-glow "dome" was found to be slightly larger in a polluted atmosphere than in a "clean" atmosphere because there are more light-scattering events in the "dirty" atmosphere.

Night glow caused by moonlight was compared to night glow predicted to occur as a result of the Alton Coal Project. It appears that the brightest portion of the glow "domes" due to the proposed coal project under the "preliminary design" and "uncontrolled" case for the years 21-22, when the mining operations are closest to the park, would be well below the lowest luminosity of the sky glow associated with a full moon at its zenith. It also appears that those areas in the Night Sky Glow Model plots that are marked "perceptible" and "very perceptible" could obscure sixth-magnitude stars and the Milky Way.

CONCLUSIONS

The following conclusions can be drawn from this study:

- During years of maximum production in areas approaching the eastern permit area boundary, the proposed Alton Coal Project under "uncontrolled" lighting conditions may cause a perceptible night glow and obscure a portion of the sixth-magnitude stars and Milky Way from both Yovimpa Point and View Point and, to a lesser extent, from Bryce Point. However, for the "preliminary design" condition only Yovimpa Point would have sufficient luminosity levels to obscure sixth-magnitude stars.

- Model results show that the Alton Coal Project may cause a glow dome larger than the currently perceivable dome originating from the city of Tropic. The effects of the glow dome from the Alton Coal Project and the city of Tropic are not expected to be cumulative. However, the Alton Coal Project glow dome could be visible up to 50 percent of the nighttime hours; during the remaining time, light from the moon would overwhelm the light emissions from the Alton Coal Project.

We have performed only limited evaluation of predictions of the model developed and used in this study. More comprehensive evaluation of the model is required before great confidence can be placed in its predictions.

REFERENCES

Blackwell, H. R. 1946. Contrast thresholds of the human eye. J. Opt. Soc. Am., 36:624-643.

Bond, D. S., and F. P. Henderson. 1963. The Conquest of Darkness. Defense Documentation Center, Alexandria, Virginia (AD 346297).

Cambridge University Press. 1985. Sky Catalog 2001. Sky Publishing Corporation.

Driscoll, W. G., and W. Vaughan. 1978. Handbook of Optics. Optical Society of America, Kingsport Press.

Earing, D. G., and J. A. Smith. 1966. "Target Signatures Analysis Center: Data Compilation." Air Force Avionics Laboratory (AD-489-968).

EPA. 1981. "Improved Emission Factors for Fugitive Dust from Western Surface Coal Mining Sources. Vol. II. Emission Factors." Industrial Environmental Research Laboratory, Cincinnati, Ohio.

Garstang, R. H. 1986. Model for artificial night-sky illumination. Publications of the Astronomical Society of the Pacific, 98:364-375.

General Electric Bulletin, TP-109.

Green, H. N. 1932. "The Atmospheric Transmission of Coloured Light." Royal Aircraft Establishment, Farnborough, England (RAE Report E and I.720).

Hering, S. V., J. L. Bowen, J. G. Wengert, and L. W. Richards. 1981. Characterization of the regional haze in the southwestern United States. Atmos. Environ. 10/11:1999-2009.

Johnson, C. D., D. A. Latimer, R. W. Bergstrom, and H. Hogo. 1980. "User's Manual for the Plume Visibility Model (PLUVUE)." U.S. Environmental Protection Agency, Research Triangle Park, North Carolina (EPA-450/4-80-032).

Kaufman, J. E., ed. 1981. IES Lighting Handbook: Application Volume. Illuminating Engineering Society of North America, New York.

Kaufman, J. E., ed. 1981. IES Lighting Handbook: Reference Volume. Illuminating Engineering Society of North America, New York.

Knoll, H. A., R. Tousey, and E. O. Hulburt. 1946. Visual thresholds of steady point sources of light in fields of brightness from dark to light. J. Opt. Soc. Am., 36:480-482.

Krinov, E. L. 1953. Spectral reflectance properties of natural formations. Natl. Res. Counc. Can. Tech. Trans. TT-439, Ottawa (from Russian translation of 1947).

Latimer, D. A., et al. 1978. "The Development of Mathematical Models for the Prediction of Anthropogenic Visibility Impairment." Systems Applications, Inc., San Rafael, California (EF78-63B).

McCartney, E. J. 1976. Optics of the Atmosphere: Scattering by Molecules and Particles. Wiley, New York.

Middleton, W.E.K. 1958. Vision Through the Atmosphere. University of Toronto Press, Toronto, Canada.

Padgham, C. A., and J. E. Saunders. 1975. The Perception of Light and Colour. Academic Press.

Pasachoff, O. M. 1977. Contemporary Astronomy. W. B. Saunders Company, Philadelphia, Pennsylvania.

Penndorf, R. 1956. "Luminous and Spectral Reflectance as Well as Colors of Natural Objects." Air Force Camb. Res. Lab. Geophys. Res. Pap. 44, AFCRL-TR-56-203, February.

RCA. 1974. Electro-Optics Handbook. RCA Corporation, Lancaster, Pennsylvania.

Riegel, K. W. 1973. Light pollution. Science, 179:1285ff.

Roach, F. E., and A. B. Meinel. 1955. J. Air Pollut. Control Assoc., 122:554.

Van De Hulst, H. C. 1980. Multiple Light Scattering Tables, Formulas, and Applications, Volumes 1 and 2. Academic Press, New York.

Walker, M. F. 1970. Pub. of the Astr. Soc. Pacific, 82:672.

Walker, M. F. 1973. Pub. of the Astr. Soc. Pacific, 85:508.

Walker, M. F. 1977. "The Effects of Urban Lighting on the Brightness of the Night Sky." Lick Observatory Bulletin No. 760, University of California.

Weaver, H. F. 1947. Pub. of the Astr. Soc. Pacific, 59:232.

Yocke, M., H. Hogo, and D. Henderson. 1985. A mathematical model for predicting night-sky glow. Pub. of the Astr. Soc. Pacific, 98:889-893.

Appendix A

TECHNICAL DESCRIPTION OF THE NIGHT SKY GLOW MODEL

Appendix A

TECHNICAL DESCRIPTION OF THE NIGHT SKY GLOW MODEL

The Night Sky Glow model is a computer model that solves the radiative transfer equation in the atmosphere using an iterative procedure. The model is capable of having from 1 to 5 vertical layers, each of which may have a unique aerosol distribution. The depth of the atmosphere extends to 200 km in all directions from the observer's point of view. The model corrects for the earth's curvature and obeys Lambert's law of reflection for incident surface lighting. According to Lambert's law, a fraction of the total radiant energy flux incident on the surface is reflected isotropically, independent of the distribution of the incident energy.

The model treats illumination from a single or a clustered set of light sources located at known distance and azimuthal angle from the observer. The observer is assumed to be standing at the center of the model domain and looking up into the sky hemisphere (Exhibit A-1). At any given point in the atmosphere along the observer's sight path, the change in spectral light intensity or spectral radiance $I(\lambda)$ as a function of distance (neglecting multiple scattering) can be calculated as follows:

$$\frac{dI(\lambda)}{dr} = -b_{ext}(\lambda)I(\lambda) + \frac{P(\lambda,\Theta)}{4\pi} b_{scat}(\lambda)F_s(\lambda) \quad , \qquad \text{(A-1)}$$

where

r = the distance (km) along the sight path from the point (β,δ to the observer

$p(\lambda,\Theta)$ = the scattering distribution or phase function for scattering angle Θ (sr^{-1})

F_s = the flux (lm/μm) from the source

b_{scat} = the scattering coefficient, which is the sum of the Rayleight scattering (due to air molecules), b_R, and the scattering due to particles, b_{sp}: (km^{-1})

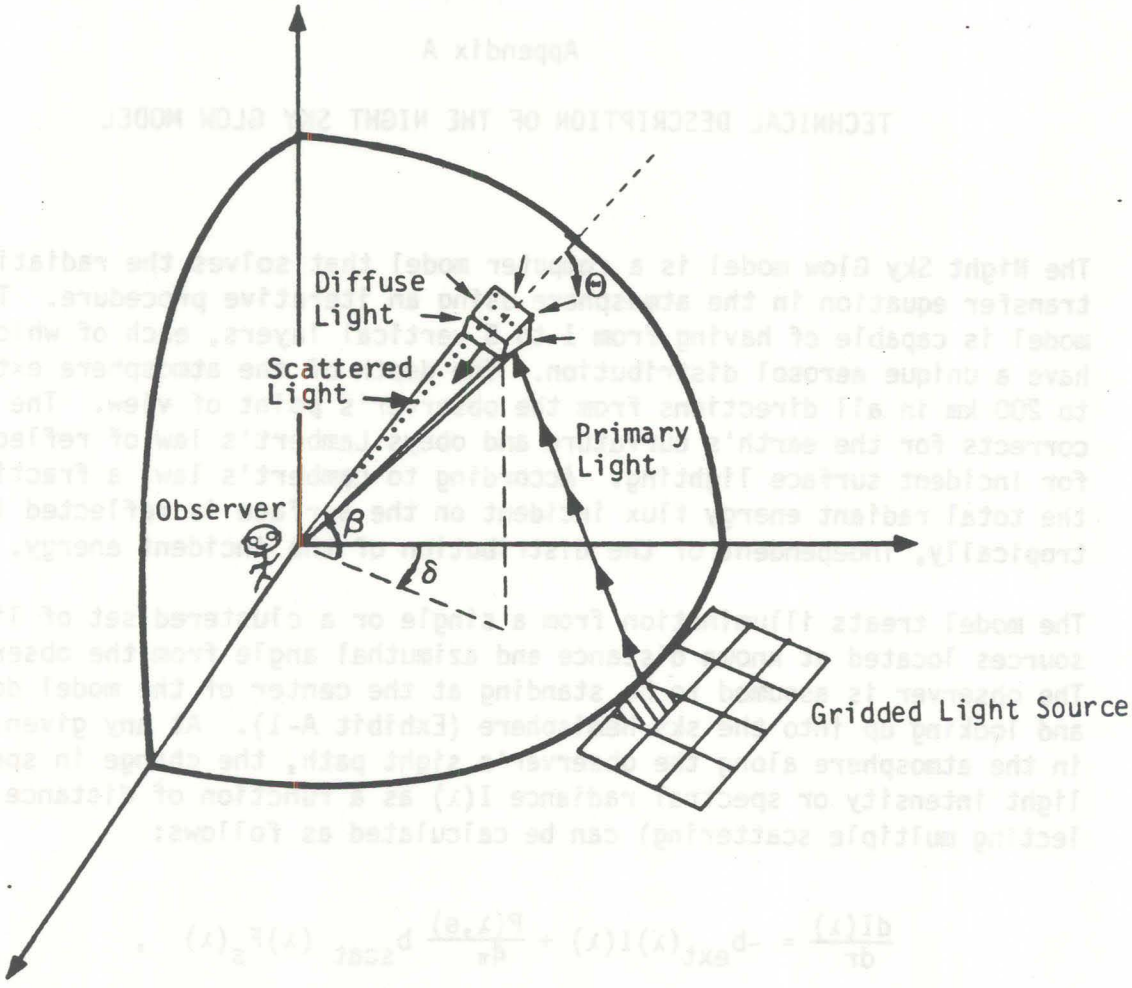


EXHIBIT A-1. Schematic diagram of numerical sky glow modeling framework.

$$b_{scat}(\lambda) = b_R(\lambda) + b_{sp}(\lambda) \quad , \tag{A-2}$$

where

b_{ext} = the sum of the scattering coefficient, b_{scat}, and absorption coefficient, b_{abs}: (km^{-1}), and

$$b_{ext}(\lambda) = b_{scat}(\lambda) + b_{abs}(\lambda) \quad , \tag{A-3}$$

where

Θ = scattering angle (radians)
β = zenith angle (radians)
δ = azimuth angle (radians).

On the right side of Equation A-1, the first term represents light absorbed or scattered out of the line of sight; the second term represents light scattered into the line of sight. The values of b_{scat} and b_{abs} can be evaluated if the aerosol and NO_2 concentrations and such characteristics as the refractive index and the size distribution of the aerosol are known. Except in the cleanest atmospheres, b_{scat} is dominated by b_{sp}; also, unless soot is present, b_{abs} is dominated by the absorption coefficient due to NO_2. Scattering and absorption are wavelength-dependent, and effects are greatest at the blue end (λ = 0.4 μm) of the visible spectrum ($0.36 < \lambda < 0.75$ μm). The Rayleigh scattering coefficient b_R is proportional to λ^{-n}; the scattering coefficient caused by particles is generally proportional to λ^{-n}, where $0 < n < 4$. Also, NO_2 absorption is greatest at the blue end. This wavelength dependence causes the discoloration of the atmosphere.

Equation A-1 can be rewritten as follows:

$$I(\lambda)_{r+\Delta r} = \frac{P(\lambda,\Theta)}{4\pi} b_{scat}(\lambda) F_s(\lambda)\Delta r - \bar{b}_{ext}(\lambda) I_r(\lambda)\Delta r + I_r \quad , \tag{A-4}$$

where Δr represents an elemental distance. Thus the total light incident on the observer can be estimated through an iterative procedure. For example, at a given wavelength λ, the light intensity at each elemental distance of 1 km beginning 50 km away from the observer can be calculated as follows:

$$r = 50 \text{ km}, \quad I_{49}(\lambda) = \frac{P(\lambda,\Theta_{50})}{4\pi} b_{scat}(\lambda) F_{S_{50}}(\lambda)$$

$$r = 49 \text{ km}, \quad I_{48}(\lambda) = \frac{P(\lambda,\Theta_{49})}{4\pi} b_{scat}(\lambda) F_{S_{49}}(\lambda) - b_{ext}(\lambda) I_{49}(\lambda) + I_{49}(\lambda)$$

$$r = 48 \text{ km}, \quad I_{47}(\lambda) = \frac{P(\lambda,\Theta)_{48})}{4\pi} b_{scat}(\lambda) F_{S_{48}}(\lambda) - b_{ext}(\lambda) I_{48}(\lambda) + I_{48}(\lambda)$$

.
.
.

$$r = 1 \text{ km}, \quad I_o(\lambda) = \frac{P(\lambda,\Theta_1)}{4\pi} b_{scat}(\lambda) F_{S_1}(\lambda) - b_{ext}(\lambda) I_1(\lambda) + I_1(\lambda)$$

The individual intensity values are accumulated into the $I_o(\lambda)$ step. Estimates of the light flux (F_S) from the source are based on the spectral distribution; intensity of the source, which depends upon the amount of light that reaches the scattering point and is attenuated by a $2\pi R^2$ term (where R is the distance from the source to the scattering point) (EXHIBIT A-1); the exponential decrease with distance along the path length R due to absorption and scattering; and the fraction of the radiant energy that is reflected skyward.

Multiple Scattering

Thus far only primary scattering has been considered in the model. To account for multiple scattering, we make a rough approximation of the ratio $R(\lambda)$ defined by $R(\lambda) \equiv (MS(\lambda) + I_o(\lambda))/I_o(\lambda) = 1 + MS(\lambda)/I_o(\lambda)$, where $I_o(\lambda)$ is the amount of light that reaches the ground by primary scattering, and $MS(\lambda)$ is the amount reaching the ground by multiple scattering. That is, we approximate the ratio R = (light reaching ground by either primary or multiple scattering)/(light reaching ground by primary scattering). After the model calculates $I_o(\lambda)$, by integrating the radiative transfer equation, $I_o(\lambda)$ is multiplied by $R(\lambda)$.

$R(\lambda)$ is found by calculating separately, for each ray of light that leaves the source, how much of that ray reaches the ground by primary scattering and how much reaches the ground by multiple scattering. To perform the calculations, the following simplifying assumptions and approximations are made:

The amount of light that scatters more than twice is negligible. The approximation could be extended to include the effects of three or more scatters; however, under the circumstances considered here (in particular, when the atmosphere is relatively clean and b_{scat} is small), one does not expect those effects to be significant.

The amount of light that "bounces" back to the ground, i.e., that scatters to the ground, is reflected back into the atmosphere, scatters back to the ground, etc., is negligible. The approximation could be extended to include the effects of bouncing, but these effects are small.

The atmosphere does not absorb radiation. The approximation could be extended to include the effects of absorption, but again, these effects are small.

The source consists of a collection of point sources, each of which emits photons isotropically (this assumption is present throughout the entire night-glow model).

The final, and key, assumption involves the scattering phase functions, $P(\lambda,\theta)$. From equations or graphs of these phase functions, one can estimate, for a given wavelength, the fraction $\alpha(\lambda)$ of the light that scatters into a forward direction (see Exhibit A-2) (Brunberger et al., 1968). The figure, which illustrates the general behavior of the phase functions for both Mie and Rayleigh scattering, shows that, as wavelength decreases, forward scattering of the light becomes more pronounced--in particular, α increases. The range of α is approximately 0.5 to 0.8 for the wavelengths of interest in this study. Thus if a photon of light is scattered, after emission from the source into the night sky, it tends to continue in a direction that takes it out of the atmosphere rather than back to the ground. Furthermore, there is a tendency for photons of light to scatter into roughly the same direction as they were going before the scattering occurred--"skyward" if they were already travelling skyward, and "groundward" if they were already travelling groundward. This tendency is formalized and exaggerated in the final assumption that is made in the approximation used to calculate $R(\lambda)$:

When a photon of wavelength λ is scattered, there is a probability $\alpha(\lambda)$ that the scattered photon will keep going in the same direction (i.e., the scattering angle will be 0), and a probability $(1 - \alpha)$ that the photon will reverse direction. (While this exaggeration would not be appropriate in looking for effects that are sensitive to angle, it is used here in a calculation in which the only concerns about a photon emitted into the night sky are whether it returns to the ground, and whether the return is by multiple or primary scattering.)

To calculate the approximation for $R(\lambda)$, we first calculate an approximation for $R(\lambda,\beta)$, where β is the zenith angle. $R(\lambda,\beta)$ is then averaged over angle, to give $R(\lambda)$. Calculation of $R(\lambda,\beta)$ begins by the consideration of any ray (any collection of photons, all of the same wavelength and

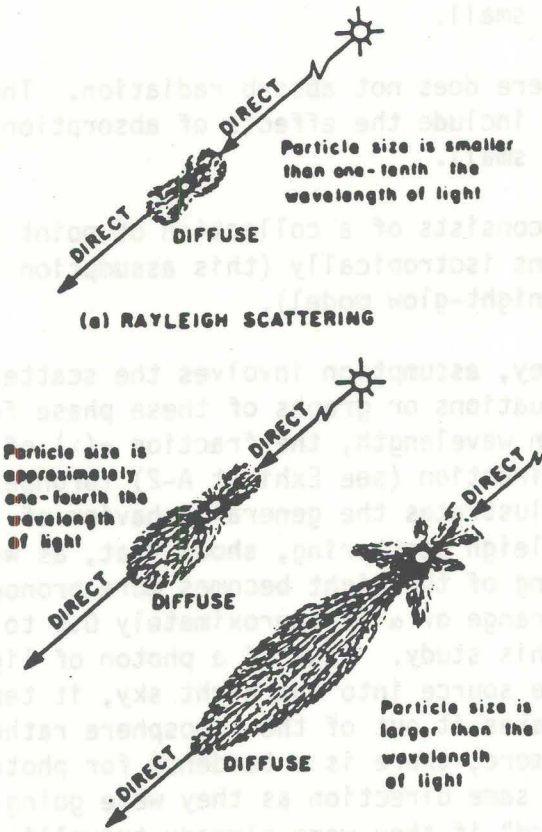


EXHIBIT A-2. Scattering of electromagnetic radiation. (a) Rayleigh scattering. (b) Mie scattering. Adapted with permission from H. Brunberger, R. S. Stein, and R. Powell, Light Scattering: Science and Technology, p. 38 (1968).

all travelling in the same direction) that leaves the source. The intensity of the ray is $I(\lambda,\beta)$. By assumption, all of the photons in this ray remain on the straight line determined by r, either escaping the atmosphere (after 0, 1, or 2 scatters), or arriving at the surface (after 1 or 2 scatters).

The ray is viewed as a collection of distinct components, some of which reach the ground, and others of which escape the atmosphere. These different components are illustrated in Exhibit A-3. Those reaching the ground are called I_d, I_{dd}, and I_{ud} (d = down, and u = up):

> I_d is the component of the ray that arrives at the surface after one scatter, i.e., I_d is the collection of photons in the ray which, after one scatter, reverse their initial direction and reach the ground without further scattering;
>
> I_{dd} is the component of the ray that arrives at the surface after two scatters, both downward; and
>
> I_{ud} is the component of the ray that arrives at the surface after two scatters, the first upward and the second downward.

Components of I that leave the atmosphere (e.g., I_u, the collection of photons in the ray that leave the atmosphere after an upward scatter) are not of interest here, and we ignore them, as well as the components involving three or more scatters.

Under the current set of assumptions, the ratio $R(\lambda,\beta)$ is given by

$$R(\lambda,\beta) = (I_d + I_{dd} + I_{ud})/I_d. \qquad \text{(A-5)}$$

Each of the quantities I_d, I_{dd}, and I_{ud} can be found by directly integrating the radiative transfer equation.

The results are

$$I_d = \frac{1}{2}\,\alpha\, I(1 - e^{-2\tau\infty}) \qquad \text{(A-6)}$$

$$I_{ud} = \frac{1}{2}\,\alpha(1 - \alpha)I[\frac{1}{2} - e^{-2\tau\infty}(\tau\infty + \frac{1}{2})] \qquad \text{(A-7)}$$

and

$$I_{dd} = \frac{1}{2}\,\alpha(1 - \alpha)I[\frac{1}{2} - e^{-2\tau\infty}(\tau\infty + \frac{1}{2})] = I_{ud} \qquad \text{(A-8)}$$

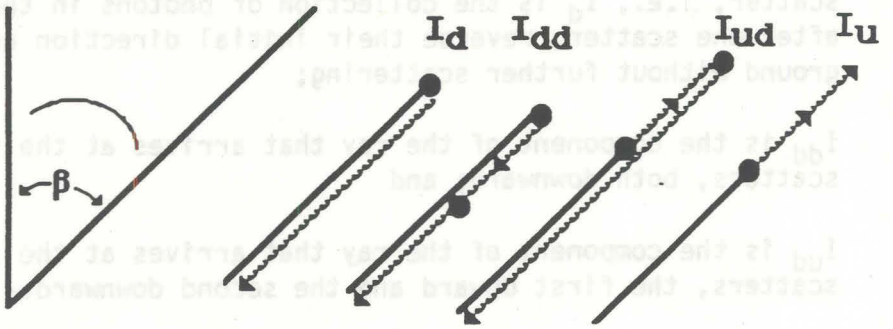


EXHIBIT A-3. **The ray I may be viewed as the sum of different components, of which I_d, I_{dd}, and I_{ud} are used in the calculation of R (● indicates a scattering; the arrows indicate the direction of the scattering).**

where $\tau_\infty(\lambda,\beta)$ is the optical depth through the atmosphere in the direction β at wavelength λ. The vertical value of $\tau_\infty(\lambda,\beta)$, i.e., $\tau_\infty(\lambda,0)$, is called $\tau_z(\lambda)$; in the current model (or in any model in which the atmosphere is horizontally stratified), $\tau_z(\lambda)$ and $\tau_\infty(\lambda,\beta)$ are related by

$$\tau_\infty(\lambda,\beta) = \tau_z(\lambda)/\cos(\beta). \qquad \text{(A-9)}$$

Substituting the expressions for I_d, I_{dd}, and I_{ud} into Equation (A-5) gives

$$R = 1 + 2I_{ud}/I_d =$$
$$1 + 2\alpha(\lambda)[\tfrac{1}{2} - e^{-2\tau_\infty}(\tau_\infty + \tfrac{1}{2})]/(1 - e - 2\tau_\infty) \quad . \qquad \text{(A-10)}$$

Equation (A-10) shows R as a function of λ and τ_∞. Since τ_∞ is a function of β (by Equation A-9), R also may be viewed as a function of λ and β, i.e., $R = R(\lambda,\beta)$.

$R(\lambda,\beta)$ is now averaged over all angles, to give an expression $R(\lambda)$, which depends only on wavelength. The result is

$$R(\lambda) = 1 + \alpha - 2\alpha\tau_z \int_{\tau_z}^{\infty} \frac{1}{e^{2\tau_\infty} - 1} \frac{1}{\tau_\infty} d\tau_\infty \quad . \qquad \text{(A-11)}$$

The integral is calculated numerically. As would be expected, $R(\lambda)$ approaches 1, as τ_z approaches 0.

Thus for each $I_0(\lambda)$ calculated from Equation A-4 for primary scattering, we can calculate the total diffuse term by applying this factor for multiple scattering.

The light intensities at each 0.01 μm wavelength interval are summed over the visible spectrum to arrive at the total radiance reaching the observer from the source.

To exercise the model within reasonable cost, assumptions are made to reduce computational efforts. Calculations are made at azimuthal angles from 0 to 360° and at zenith angles from 0 to 90° every 10° increment. However, this procedure can be altered by the user if a more refined solution is desired.

Calculation of Scattering and Absorption Properties

In general, a particle's ability to scatter and absorb radiation at a particular frequency is a function of size, composition, shape, and relative humidity. To alter the size distribution of both primary and secondary particles, it is necessary to compute the effect of particle size on the wavelength dependence of the extinction coefficient and the scattering distribution function.

For a sphere of uniform refractive index, it is possible to obtain a closed-form solution to Maxwell's equations. This solution, known as the Mie equations, enables calculation of the scattering and absorption of light at a particular wavelength for a particle given its size and refractive index. Computer programs for this computation are readily available (Dave, 1970; Hansen and Travis, 1974). For these calculations, the IBM computer program DAMIE (Dave, 1970) was incorporated into the Night Sky Glow Model.

The difficulty encountered in using these calculations for particle scattering in the atmosphere is that most of the particles are not spheres, and they are of mixed composition. Concern over the applicability of these calculations to particles in the real atmosphere has prompted much discussion. The salient points of this controversy are as follows:

> The Mie equations are essentially the only way of computing the effect of particle size and index of refraction on scattering and absorption.
>
> Regardless of the degree of non-sphericity and mixed composition, the particles can be considered to have an effective radius and an effective index of refraction. These effective values are determined by comparing calculations with observed scattering and absorption (Bergstrom and Peterson, 1977).

To describe a particle's interaction with light, one must know its scattering coefficient, absorption coefficient, and scattering distribution. The scattering coefficient, b_{scat}, is a measure of the particle's ability to intercept light and to redirect it. The absorption coefficient, b_{abs}, is a measure of the particle's ability to absorb light. The description of the probability of the redirection of the scattered light into a particular θ is called the scattering distribution function (or phase function).

The scattering coefficient for a single particle is defined as:

$$b_{scat} = \pi r^2 Q_{scat}(\lambda, r, \tilde{n}) \quad , \tag{A-12}$$

where

r = the radius of the particle
Q_{scat} = the scattering efficiency factor computed from the Mie equations
λ = the wavelength
$\tilde{n}$ = the index of refraction.

The absorption coefficient is similarly defined as:

$$b_{abs} = \pi r^2 Q_{abs}(\lambda, r, \tilde{n}) \quad , \tag{A-13}$$

where Q_{abs} is the absorption efficiency factor. The sum of the scattering and absorption coefficients is called the extinction coefficient, b_{ext}.

Where there are many particles of different sizes in a particular volume element, the total scattering and extinction coefficient is simply the integral over size:

$$\begin{aligned} b_{ext} &= \int_0^\infty \pi r^2 (Q_{scat} + Q_{abs}) n(r)\, dr \\ &= \int_0^\infty Q_{ext}\, s(r)\, dr \quad , \end{aligned} \tag{A-14}$$

where $n(r)$ is the number distribution (number of particles per radius interval) and $s(r)$ is the surface area distribution equal to $\pi r^2 n(r)$. The scattering distribution function $p(\theta)$ is written:

$$p(\theta) = \frac{\lambda^2}{b_{scat}} \int_0^r \frac{1}{2} i(\theta) + i_{\perp}(\theta)\, n(r)\, dr \quad , \tag{A-15}$$

where i and $i_{\perp}$ are the intensity of parallel and perpendicularly polarized scattering radiation, respectively (computed from the Mie equations). EXHIBIT A-4 shows phase functions for various particle size distributions.

The scattering and extinction coefficients are usually expressed per unit mass, M (aerosol density, $\mu g/m^3$). The quantity for a single particle is thus:

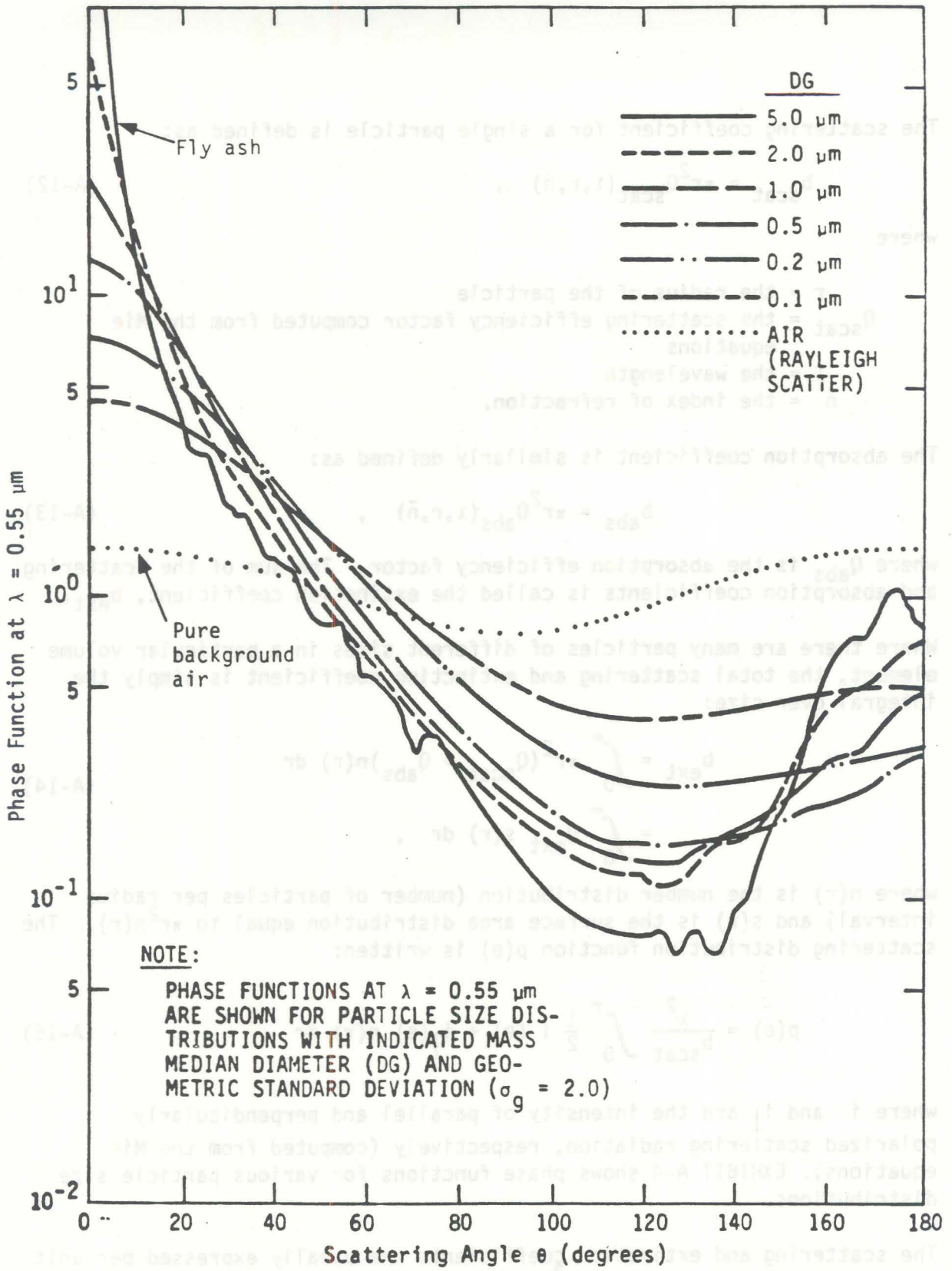


EXHIBIT A-4. Phase functions for various particle size distributions.

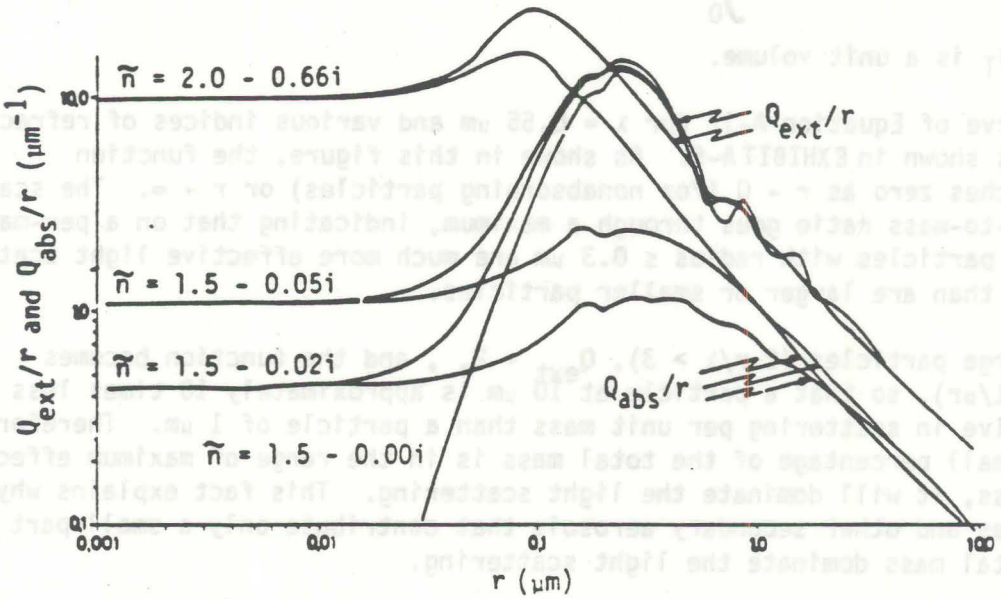


EXHIBIT A-5. Extinction and absorption per unit mass as a function of particle radius for four different refractive indices at a solar wavelength of 0.55 μm. (Source: Bergstrom, 1973)

$$\frac{b_{ext}}{M} = \frac{Q_{ext}(2\pi r/\lambda,\ \tilde{n})}{(4/3)\ \rho r} \quad , \tag{A-16}$$

and for many particles,

$$\frac{b_{ext}}{M} = \frac{\int_0^\infty \pi r^2 Q_{ext}\ n(r)\ dr}{(4/3)\rho \int_0^\infty \pi r^3 n(r)\ dr} = \frac{\int_0^\infty Q_{ext}\ s(r)\ dr}{\rho V_T} \quad , \tag{A-17}$$

where V_T is a unit volume.

The curve of Equation A-17 for λ = 0.55 μm and various indices of refraction is shown in EXHIBIT A-5. As shown in this figure, the function approaches zero as $r \to 0$ (for nonabsorbing particles) or $r \to \infty$. The scattering-to-mass ratio goes through a maximum, indicating that on a per-mass basis, particles with radius ≤ 0.3 μm are much more effective light scatterers than are larger or smaller particles.

For large particles ($2\pi r/\lambda > 3$), $Q_{ext} \to 2$, , and the function becomes $(3/2)(1/\rho r)$, so that a particle at 10 μm is approximately 10 times less effective in scattering per unit mass than a particle of 1 μm. Therefore, if a small percentage of the total mass is in the range of maximum effectiveness, it will dominate the light scattering. This fact explains why sulfates and other secondary aerosols that contribute only a small part of the total mass dominate the light scattering.

REFERENCES

Bergstrom, R. W. 1973. Extinction and absorption coefficients of the atmospheric aerosol as a function of particle size. Beitrage zur Physik der Atmosphare, 46:223-234.

Bergstrom, R. W., and J. T. Peterson. 1977. Comparison of predicted and observed solar radiation in an urban area. J. Appl. Meteorol., 16:1107-1116.

Brunberger, H., R. S. Stein, and R. Powell. 1968. Light Scattering: Science and Technology, p. 38.

Dave, J. V. 1970. "Subroutines for Computing the Parameters of the Electromagnetic Radiation Scattered by a Sphere." IBM System 360 Program 3600-17.4.002.

Hanson, J. E., and L. D. Travis. 1974. Light scattering in planetary atmospherics. Space Science Reviews, 16:527-610.

Appendix B

NIGHT SKY GLOW MODEL LISTING AND SAMPLE INPUT

B.1 SKYBAC

SKYBAC - Sample Input
SKYBAC - Source Code

```
lowback.sav
2
80.          10.          30.          0.          0.002       .04
2774.
.125         3.
1.6          2.2
1.8          2.0
1.           1.           1.           0.          0.
1.5          0.           1.5          0.
0.           0.
```

```
      PROGRAM SKYBACK
*     *** Prepares background radiative properties for the
*         skyglow program
*
*         Prepared by Systems Application, Inc.
*                     101 Lucas Valley Road
*                     San Rafael, CA 94903
*
*         Most of the code is extracted from the PLUVUE program
*
*         Reference: C. Seigneur, et al (1983) "User's Manual for
*                    Plume Visibility Model (PLUVUE II)." Systems
*                    Applications, Inc. SYSAPP-83/221
*
*         Coded by G.W. Lundberg/SAI  June 1987
*
*     ------------------------------------------------------------
*
*     *** for input filename
      character*30 fname
*
*     *** common blocks used by INRAD
      REAL LAMB
      COMMON/BCKGND/ ELEV,RVAMB,ACCAMB,AMBNO2,RH,ROVA,ROVC,ROVS,ROVP,
     1SIGA,SIGC,SIGS,SIGP,HPBL,IREAD,CORAMB,AMBNO3,AMBSO4,INTYP
     2,DENA,DENC,DENP,DENS,ROVCAR,SIGCAR,DENCAR,AMBCAR
      COMMON/MIESCT/ROG,SIGMA,NLAMB,LAMB(20),JX,IT,TT(200),DUM(20),
     1PDUM(20,50),DUMA(20),DUMG(20)
      COMMON/RADPRP/BTASO4(39),BTACOR(39),BTAPRM(39),BTAAER(39),
     1PAER(39,36),PPRIM(39,36),PSO4(39,36),PCOR(39,36),BTABAC(39)
     2,PCAR(39,36),ABSCAR(39),BTACAR(39),ABSSO4(39),ABSCOR(39),
     3 ABSPRM(39),GSO4(39),GCOR(39),GPRM(39),GCAR(39),GAER(39)
     4,GBAC(39),PBAC(39,36)
      COMMON / OPTDEP / TAUOIZ(39),TATHIZ(39),TATOHZ(39),XI(39),
     1X2(39),TAUTDI(39),TAUTOD(39),XHDI(39),XHOD(39)
      COMMON/ MISC/ ABSNO2(39),SOLAR(39),RAD,FORPIN,OMZ(39),OMH(39)
     1,NTHETA,RFR,RFI
      COMMON/INDREF/RFRSO4,RFISO4,RFRCOR,RFICOR,RFRPRM,RFIPRM
     1,RFRCAR,RFICAR
*
*     ------------------------------------------------------------
*
*     *** set hpbl for inrad
      hpbl = 2.0
*
*     *** check for filename on command line
      call getarg (2,fname)
      if (fname .eq. ' ') then
         call dialog
      else
         open (8,file=fname,status='old')
      endif
*
*     *** read output filename and open
      read (8,'(a)') fname
      open (7,file=fname,form='unformatted')
```

```
*       *** get input for this background
        read (8,*) intyp
        read (8,*) rh,coramb,ambso4,ambno3,ambno2,o3amb
        if (intyp .eq. 2) then
           rvamb = ambso4
        endif

*       *** get mean source elevation
        read (8,*) elev

*       *** convert relative humidity to a fraction
        rh = rh/100.0

        read (8,*) rova,rovc
        read (8,*) siga,sigc
        read (8,*) dena,denc
        read (8,*) rovcar,sigcar,dencar,fractc,ambcar
        read (8,*) rfrso4,rfiso4,rfrcor,rficor
        read (8,*) rfrcar,rficar

*       *** let user know whats happening
        print *, '...working--this will take a minute or two'

*       *** inrad does all the work
        call inrad (dummy)

*       *** save for albedo
        write (7) ambno2,pbac,btabac

        print *, '...radiative properties calculated--saved in '//fname
        stop '...all done'
        end

        SUBROUTINE INRAD(ZENITH)
C
C   CALCULATE OPTICAL PROPERTIES OF BACKGROUND ATMOSPHERE AND FOUR
C   AEROSOL MODES
C
        REAL LAMB
        COMMON/BCKGND/ ELEV,RVAMB,ACCAMB,AMBNO2,RH,ROVA,ROVC,ROVS,ROVP,
       1SIGA,SIGC,SIGS,SIGP,HPBL,IREAD,CORAMB,AMBNO3,AMBSO4,INTYP
       2,DENA,DENC,DENP,DENS,ROVCAR,SIGCAR,DENCAR,AMBCAR
        COMMON/MIESCT/ROG,SIGMA,NLAMB,LAMB(20),JX,IT,TT(200),DUM(20),
       1PDUM(20,50),DUMA(20),DUMG(20)
        COMMON/RADPRP/BTASO4(39),BTACOR(39),BTAPRM(39),BTAAER(39),
       1PAER(39,36),PPRIM(39,36),PSO4(39,36),PCOR(39,36),BTABAC(39)
       2,PCAR(39,36),ABSCAR(39),BTACAR(39),ABSSO4(39),ABSCOR(39),
       3 ABSPRM(39),GSO4(39),GCOR(39),GPRM(39),GCAR(39),GAER(39)
       4,GBAC(39),PBAC(39,36)
        COMMON / OPTDEP / TAUOIZ(39),TAUHIZ(39),TAUOHZ(39),X1(39),
       1X2(39),TAUTDI(39),TAUTOD(39),XHDI(39),XHOD(39)
        COMMON/ MISC/ ABSNO2(39),SOLAR(39),RAD,FORPIN,OMZ(39),OMH(39)
       1,NIHEIA,RFR,RFI
        COMMON/INDREF/RFRSO4,RFISO4,RFRCOR,RFICOR,RFRPRM,RFIPRM
       1,RFRCAR,RFICAR
        COMMON/DIFFI/FLUXUP(39),DIFIDN(39,21,41),DIFIUP(39,21,41)
```

```
      COMMON/DIFRAY/DIFRDN(9,21,41),DIFRUP(9,21,41)
      DIMENSION YMU(21),XAZ(21),
     2SUMT(39),GI(39),PPLM(39,36),SPECBI(39),SPECBU(39)
      DIMENSION DUMP(41),D(2)
      DIMENSION COEF(57),W(57)
      DIMENSION WINK(9),REL(9)
      DIMENSION OSO4(39),OCOR(39),OCAR(39),OAER(39)
      DIMENSION SPECRU(39),SPECRI(39)
      DATA WINK / 0. , 0.03 , 0.05 , 0.1 , 0.18 , 0.3 , 0.5,0.75 , 1. /
      DATA D / 0.,0. /
C     DATA YMU/1.0,0.9,0.8,0.7,0.6,0.5,0.4,0.3,0.2,0.1,0.0/
      DATA YMU/1.0,0.95,0.9,0.85,0.8,0.75,0.7,0.65,0.6,0.55,0.5,
     20.45,0.40,0.35,0.30,0.25,0.20,0.15,0.10,0.05,0.0/
C     DATA XAZ/0.,18.,36.,54.,72.,90.,108.,126.,144.,162.,180./
      DATA XAZ/0.,9.,18.,27.,36.,45.,54.,63.,72.,81.,90.,99.,108.,117.,
     2126.,135.,144.,153.,162.,171.,180./
      IREAD = 0
      TWOPI = 2.*3.141596
      FORPI = 2.*TWOPI
      FORPIN = 1./FORPI
      SQRTPI = SQRT(3.141596)
      SQR2PI = SQRTPI*SQRT(2.)
      HR = 9.8
      HA=3.5
      CONR = SQRT(2.*6356.*HR)
      CONA = SQRT(2.*6356.*HA)
      PARMA = CONA*SQRTPI*0.5
      PARMR = CONR*SQRTPI*0.5
      DX = SQRT(2.*6356.*HPBL)
      DR = DX/CONR
      DA = DX/CONA
C***  COMPUTE THE BACKGROUND RADIATIVE PROPERTIES
C*****
C*****
C*** GENERATE THE BSCAT TO MASS RATIOS AND THE PHASE FUNCTIONS
C*****
C*****
C***  ACCUMULATION MODE
C*****
      ROG = ROVA
      SIGMA = SIGA
      RFR = RFRSO4
      RFI = RFISO4
      DO 5 I = 1,39
    5 DUMP(I) = 0.36 + 0.01*FLOAT(I)
      IF(IREAD.EQ.1) GO TO 210
      CALL BSIZE
C     WRITE(6,6677)
C6677 FORMAT(/,2X,'TEST FOR CALL TO BSIZE',/)
      GO TO 250
  210 READ(5,1100) (   DUM(I),I=1,NLAMB)
      DO 220 I = 1,NLAMB
  220 READ(5,1200) (PDUM(I,J),J=1,NTHETA)
  250 CONTINUE
 1100 FORMAT(9F7.4)
 1200 FORMAT(7E11.4)
      CALL SPLNA (NLAMB,LAMB,DUM,2,D,COEF,W)
```

```
      DO 12 I = 1,39
      X = DUMP(I)
      DO 13 J = 2,NLAMB
   13 IF(X.LE.LAMB(J)) GO TO 14
   14 Q = LAMB(J) - LAMB(J-1)
      Z = (X - LAMB(J-1))/Q
   12 BTASO4(I) =((Z*COEF(3*J-3)+COEF(3*J-4))*Z+COEF(3*J-5))*Z+DUM(J-1)
      DO 10 JT = 1,NTHETA
      DO 15 I = 1,NLAMB
   15 DUM(I) = PDUM(I,JT)
      CALL SPLNA (NLAMB,LAMB,DUM,2,D,COEF,W)
      DO 17 I = 1,39
      X = DUMP(I)
      DO 18 J = 2,NLAMB
   18 IF(X.LE.LAMB(J)) GO TO 19
   19 Q = LAMB(J) - LAMB(J-1)
      Z = (X - LAMB(J-1))/Q
   17 PSO4(I,JT) =((Z*COEF(3*J-3)+COEF(3*J-4))*Z+COEF(3*J-5))*Z+DUM(J-1)
   10 CONTINUE
      DO 50 I=1,NLAMB
   50 DUM(I)=DUMA(I)
      CALL SPLNA(NLAMB,LAMB,DUM,2,D,COEF,W)
      DO 53 I=1,39
         X=DUMP(I)
         DO 52 J=2,NLAMB
   52       IF(X.LE.LAMB(J))GO TO 51
   51    Q=LAMB(J)-LAMB(J-1)
         Z=(X-LAMB(J-1))/Q
   53    ABSSO4(I)=((Z*COEF(3*J-3)+COEF(3*J-4))*Z+COEF(3*J-5))*Z+
     1 DUM(J-1)
      DO 150 I=1,NLAMB
  150 DUM(I)=DUMG(I)
      CALL SPLNA(NLAMB,LAMB,DUM,2,D,COEF,W)
      DO 151 I=1,39
      X=DUMP(I)
      DO 152 J=2,NLAMB
  152 IF(X.LE.LAMB(J)) GO TO 153
  153 Q=LAMB(J)-LAMB(J-1)
      Z=(X-LAMB(J-1))/Q
  151 GSO4(I)=((Z*COEF(3*J-3)+COEF(3*J-4))*Z
     2+COEF(3*J-5))*Z+DUM(J-1)
C*****
C*****
C*****
C***  COARSE PARTICLE MODE
C*****
      ROG = ROVC
      SIGMA = SIGC
      RFR=RFRCOR
      RFI=RFICOR
      IF(IREAD.EQ.1) GO TO 310
      CALL BSIZE
C     WRITE(6,6678)
C6678 FORMAT(/,2X,'TEST2 FOR CALL TO BSIZE',/)
      GO TO 350
  310 READ(5,1100) (    DUM(I),I=1,NLAMB)
      DO 320 I = 1,NLAMB
```

```
  320 READ(5,1200) (PDUM(I,J),J=1,NTHETA)
  350 CONTINUE
      CALL SPLNA (NLAMB,LAMB,DUM,2,D,COEF,W)
      DO 22 I = 1,39
      X = DUMP(I)
      DO 23 J = 2,NLAMB
23    IF(X.LE.LAMB(J)) GO TO 24
   24 Q = LAMB(J) - LAMB(J-1)
      Z = (X - LAMB(J-1))/Q
   22 BTACOR(I) =((Z*COEF(3*J-3)+COEF(3*J-4))*Z+COEF(3*J-5))*Z+DUM(J-1)
      DO 20 JT = 1,NTHETA
      DO 25 I = 1,NLAMB
25    DUM(I) = PDUM(I,JT)
      CALL SPLNA (NLAMB,LAMB,DUM,2,D,COEF,W)
      DO 27 I = 1,39
      X = DUMP(I)
      DO 28 J = 2,NLAMB
28    IF(X.LE.LAMB(J)) GO TO 29
   29 Q = LAMB(J) - LAMB(J-1)
      Z = (X - LAMB(J-1))/Q
   27 PCOR(I,JT) =((Z*COEF(3*J-3)+COEF(3*J-4))*Z+COEF(3*J-5))*Z+DUM(J-1)
   20 CONTINUE
      DO 60 I=1,NLAMB
60    DUM(I)=DUMA(I)
      CALL SPLNA(NLAMB,LAMB,DUM,2,D,COEF,W)
      DO 63 I=1,39
         X=DUMP(I)
         DO 62 J=2,NLAMB
62       IF(X.LE.LAMB(J))GO TO 61
61       Q=LAMB(J)-LAMB(J-1)
         Z=(X-LAMB(J-1))/Q
63    ABSCOR(I)=((Z*COEF(3*J-3)+COEF(3*J-4))*Z+COEF(3*J-5))*Z+DUM(J-1)
      DO 160 I=1,NLAMB
 160  DUM(I)=DUMG(I)
      CALL SPLNA(NLAMB,LAMB,DUM,2,D,COEF,W)
      DO 161 I=1,39
      X=DUMP(I)
      DO 162 J=2,NLAMB
  162 IF(X.LE.LAMB(J)) GO TO 163
  163 Q=LAMB(J)-LAMB(J-1)
      Z=(X-LAMB(J-1))/Q
  161 GCOR(I)=((Z*COEF(3*J-3)+COEF(3*J-4))*Z
     2+COEF(3*J-5))*Z+DUM(J-1)
C
C     COMPUTE THE CARBON AEROSOL PROPERTIES.  FIRST
C     DO THE SCATTERING COEFFICIENT, THEN PHASE FUNCTION FOR
C     CARBON SCATTERING, THEN THE ABSORPTION
C     COEFFICIENT FOR CARBON.
C
      IF (AMBCAR.LE.0.) GO TO 44
      ROG=ROVCAR
      SIGMA=SIGCAR
      RFR = RFRCAR
      RFI = RFICAR
      CALL BSIZE
C     WRITE(6,6680)
C6680 FORMAT(/,2X,'TEST4 FOR CALL TO BSIZE',/)
```

```
      CALL SPLNA(NLAMB,LAMB, DUM, 2,D, COEF,W)
      DO 612 I=1,39
         X=DUMP(I)
         DO 613 J=2,NLAMB
613         IF(X.LE.LAMB(J))GO TO 614
614      Q=LAMB(J)-LAMB(J-1)
         Z=(X-LAMB(J-1))/Q
612      BTACAR(I)=((Z*COEF(3*J-3)+COEF(3*J-4))*Z+COEF(3*J-5))*Z+DUM(J-1
     1   )
      DO 610 JT=1,NTHETA
         DO 615 I=1,NLAMB
615         DUM(I)=PDUM(I,JT)
         CALL SPLNA(NLAMB,LAMB,DUM,2,D,COEF,W)
         DO 617 I=1,39
            X=DUMP(I)
            DO 618 J=2,NLAMB
618            IF(X.LE.LAMB(J))GO TO 619
619         Q=LAMB(J)-LAMB(J-1)
            Z=(X-LAMB(J-1))/Q
617         PCAR(I,JT)=((Z*COEF(3*J-3)+COEF(3*J-4))*Z+COEF(3*J-5))*Z+DUM
     1      (J-1)
610      CONTINUE
C
C     NEXT DO ABSORPTION DUE TO CARBON
C     DUMA= ABS/VIOT, DUMA F(WAVELENGTH ONLY)
C
      CALL SPLNA(NLAMB,LAMB,DUMA,2,D,COEF,W)
      DO 620 I=1,39
         X=DUMP(I)
         DO 625 J=2,NLAMB
625         IF(X.LE.LAMB(J))GO TO 624
624      Q=LAMB(J)-LAMB(J-1)
         Z=(X-LAMB(J-1))/Q
620      ABSCAR(I)=((Z*COEF(3*J-3)+COEF(3*J-4))*Z+COEF(3*J-5))*Z+DUMA(J-
     2   1)
      DO 180 I=1,NLAMB
  180 DUM(I)=DUMG(I)
      CALL SPLNA(NLAMB,LAMB,DUM,2,D,COEF,W)
      DO 181 I=1,39
      X=DUMP(I)
      DO 182 J=2,NLAMB
  182 IF(X.LE.LAMB(J)) GO TO 183
  183 Q=LAMB(J)-LAMB(J-1)
      Z=(X-LAMB(J-1))/Q
  181 GCAR(I)=((Z*COEF(3*J-3)+COEF(3*J-4))*Z
     2+COEF(3*J-5))*Z+DUM(J-1)
C*****
C*** ADJUST FOR THE RELATIVE HUMIDITY
C*****
   44 DO 41 I = 1,9
   41 REL(I) = 0.1*FLOAT(I-1)
      CALL SPLNA(9,REL,WINK,2,D,COEF,W)
      DO 42 I = 2,9
   42 IF(RH.LE.REL(I)) GO TO 43
   43 Z = (RH-REL(I-1))*10.
      FH = ((Z*COEF(3*I-3)+COEF(3*I-4))*Z+COEF(3*I-5))*Z+WINK(I-1)
      FACT =  1. + (0.85*FH)/(1.-RH) /DENA
```

```
      DO 40 I = 1,39
   40 BTASO4(I) = BTASO4(I)*FACT
C*****
C***  DETERMINE THE TYPE OF INPUT AND COMPUTE THE BACKGROUND RADIATIVE
C***  PROPERTIES.  INTYP = 1 MEANS THE NO3,SO4,COARSE MODE LEVEELS ARE
C***  SPECIFIED IN UGM/M3.  INTYPE = 2 MEANS THE VISUAL RANGE AND
C***  THE ACCUMULATION MODE ARE SPECIFIED IN KM-1 AND UGM/M3
C*****
      DENSO4=DENA
      DENNO3=DENA
      DENCOR=DENC
      WAVE = 0.55
      WV2 = (1./WAVE)**2
      WV4 = WV2*WV2
      TAROIZ = 0.008569*WV4*(1. +0.0113*WV2+0.00013*WV4)*EXP(-ELEV/HR)
      RAY = TAROIZ/HR
      IF(INTYP.EQ.2) GO TO 500
      IF(INTYP.NE.1) RETURN
      DO 460 I = 1,39
      X8 = BTASO4(I)*(AMBSO4/DENA + AMBNO3/DENA)
      X9 = BTACOR(I)*CORAMB/DENC
      X10 = BTACAR(I)*AMBCAR/DENCAR
      BTAAER(I) = (X8+X9+X10)*1.E-03
      IF(BTAAER(I).NE.0.) GO TO 458
      X8=0.
      X9=0.
      X10=0.
      GO TO 459
  458 CONTINUE
  459 CONTINUE
      OSO4(I)=(BTASO4(I)-ABSSO4(I))/BTASO4(I)
      OCOR(I)=(BTACOR(I)-ABSCOR(I))/BTACOR(I)
      IF (AMBCAR.GT.0.) OCAR(I)=(BTACAR(I)-ABSCAR(I))/BTACAR(I)
      SIG8=OSO4(I)*X8
      SIG9=OCOR(I)*X9
      SIG10=OCAR(I)*X10
      SIGAR=(X8+X9+X10)*1.E-03
      OAER(I)=SIGAR/BTAAER(I)
      GAER(I) = (GSO4(I)*SIG8+GCOR(I)*SIG9+GCAR(I)*SIG10)*1.E-03
     2 /SIGAR
      DO 460 J = 1,NTHETA
  460 PAER(I,J)=(PSO4(I,J)*SIG8+PCOR(I,J)*SIG9+PCAR(I,J)*SIG10)*1.E-03
     1 /SIGAR
      SIGKOS = RAY + BTAAER(19) + ABSNO2(19)*AMBNO2
      RVAMB = -ALOG(.02)/SIGKOS
      GO TO 600
  500 CONTINUE
C*****
C***  DETERMINE THE MASS OF THE ACCUMULATION MODE
C*****
      SIGKOS = -ALOG(.02)/RVAMB
      SIGINT = BTACOR(19)*CORAMB*1.E-03/DENC + RAY + ABSNO2(19)*AMBNO2
     1 + BTACAR(19)*AMBCAR*1.E-03/DENCAR
      IF(SIGKOS-SIGINT) 100,100,120
  100 AMBSO4 = 0.
      CORAMB = (SIGKOS-RAY-ABSNO2(19)*AMBNO2-AMBCAR*BTACAR(19)
     1 *1.E-03/DENCAR)/(BTACOR(19)*1.E-03/DENC)
```

```
      IF(CORAMB.LT.0.) PRINT 2000
 2000 FORMAT(1H ,44HTROUBLE WITH THE CONCENTRATION SPECIFICATION)
      GO TO 1150
  120 AMBSO4 = (SIGKOS - SIGINT)/(BTASO4(19)*1.E-03/DENA)
 1150 CONTINUE
      DO 1160 I = 1,39
      X8 = BTASO4(I)*(AMBSO4/DENA+AMBNO3/DENA)
      X9 = BTACOR(I)*CORAMB/DENC
      X10 = BTACAR(I)*AMBCAR/DENCAR
      BTAAER(I) =(X8 + X9 + X10)*1.E-03
      OSO4(I)=(BTASO4(I)-ABSSO4(I))/BTASO4(I)
      OCOR(I)=(BTACOR(I)-ABSCOR(I))/BTACOR(I)
C     OCAR(I)=(BTACAR(I)-ABSCAR(I))/BTACAR(I)
      SIG8=OSO4(I)*X8
      SIG9=OCOR(I)*X9
      SIG10=OCAR(I)*X10
      SIGAR=(SIG8+SIG9+SIG10)*1.E-03
      OAER(I)=SIGAR/BTAAER(I)
      DO 2160 J = 1,NTHETA
 2160 PAER(I,J) = (PSO4(I,J)*SIG8+PCOR(I,J)*SIG9+PCAR(I,J)*SIG10)*1.E-03
     1 /SIGAR
      GAER(I) = (GSO4(I)*SIG8+GCOR(I)*SIG9+GCAR(I)*SIG10)*1.E-03
     2 /SIGAR
C     WRITE(6,2345) GAER(I)
 2345 FORMAT(2X,E13.4)
 1160 CONTINUE
      AMBNO3 = 0.
  600 CONTINUE
C*****
C***  COMPUTE THE VERTICAL AND HORIZONTAL OPTICAL DEPTHS
C*****
      DO 200 I = 1,39
      WAVE = 0.36 + FLOAT(I)*0.01
      WV2 = WAVE**(-2)
      WV4 = WV2*WV2
      TAROIZ = 0.008569*WV4*(1. + 0.0113*WV2 + 0.00013*WV4)*EXP(-ELEV/
     1HR)
      TAAOIZ = BTAAER(I)*HA
      TATOIZ(I) = TAROIZ + TAAOIZ
      TARHIZ = TAROIZ*EXP(-HPBL/HR)
      TAROHZ = TAROIZ - TARHIZ
      TAAHIZ = TAAOIZ*EXP(-HPBL/HA)
      TATHIZ(I) = TARHIZ + TAAHIZ
      TATOHZ(I) = TATOIZ(I) - TATHIZ(I)
      BETAOR = TAROIZ/HR
      BTABAC(I) = BTAAER(I) + BETAOR + ABSNO2(I)*AMBNO2
      TAAOHZ=TAAOIZ-TAAHIZ
      X1(I)=TARHIZ/(TAAHIZ*OAER(I)+TARHIZ)
      X2(I)=TAROHZ/(TAAOHZ*OAER(I)+TAROHZ)
C     COMPUTE THE HORIZONTAL PATH DEPTH
      TAUROI = BETAOR*PARMR
      TAUAOI = BTAAER(I)*PARMA
      TAUROD = BETAOR*ERF(DR)*PARMR
      TAUAOD = BTAAER(I)*ERF(DA)*PARMA
      TAUROI = TAUROI - TAUROD
      TAUAOI = TAUAOI - TAUAOD
      TAUTOD(I) = TAUROD + TAUAOD
```

```
      TAUTDI(I) = TAURDI + TAUADI
      XHDI(I) = TAURDI/(TAURDI + TAUADI*OAER(I))
      XHOD(I) = TAUROD/(TAUROD + TAUAOD*OAER(I))
      GBAC(I) = GAER(I)*TAAOIZ/TATOIZ(I)
      DO 510 J=1,NTHETA
      PRAY=0.75*(1.+COS(RAD*TT(J))**2)
      PBAC(I,J)=(PAER(I,J)*TAAOIZ+PRAY*TAROIZ)/TATOIZ(I)
  510 CONTINUE
C     WRITE(6,2346)GBAC(I)
 2346 FORMAT(2X,E13.4)
C
C     ****** DIAGNOSTIC PRINT OUT *********
C
C     IF (I .NE. 19) GO TO 300
C     WRITE(6,260)
260   FORMAT(1H ,5X,'TAROIZ, TAAOIZ, TATOIZ(19), TARHIZ, TAROHZ, TAAHIZ,
     1 TATHIZ(19), TATOHZ(19), BETAOR, BTABAC')
C     WRITE(6,261)TAROIZ,TAAOIZ,TATOIZ(19),TARHIZ,TAROHZ,TAAHIZ,
C    1 TATHIZ(19),TATOHZ(19),BETAOR,BTABAC(19)
261   FORMAT(1H ,5X,10(E9.3,1X))
C     WRITE(6,262)
262   FORMAT(1H ,5X,'TAAOHZ, X1(19), X2(19), OAER(19), TAUROI, TAUAOI, T
     1AUROD, TAUAOD, TAURDI, TAUADI')
C     WRITE(6,261)TAAOHZ,X1(19),X2(19),OAER(19),TAUROI,TAUAOI,TAUROD,
C    1 TAUAOD,TAURDI,TAUADI
C     WRITE(6,263)
263   FORMAT(1H ,5X,'TAUTOD(19), TAUTDI(19), XHDI(19), XHOD(19)')
C     WRITE(6,261)TAUTOD(19),XHDI(19),XHOD(19)
C 300 CONTINUE
C
C     ************************************
C
C***  ADJUST THE OPTICAL DEPTH FOR NO2
      TAAOHZ = TAAOIZ - TAAHIZ
      TATOIZ(I) = TAROIZ + TAAOIZ + ABSNO2(I)*AMBNO2*HPBL
      TATOHZ(I) = TATOIZ(I) - TATHIZ(I)
      TAUTOD(I) = TAUROD + TAUAOD + ABSNO2(I)*AMBNO2*DX
      OMZ(I) = (TAROHZ + TAAOHZ*OAER(I))/TATOHZ(I)
            IF(OMZ(I).GT.0.999) OMZ(I) = 0.999
      OMH(I) = (TAUROD + TAUAOD*OAER(I))/TAUTOD(I)
C*****
C***  CHANGE THE SCATTERING COEFICIENTS FROM BSCAT/VOL TO BSCAT/MASS
C***
      BTASO4(I) = BTASO4(I)*1.E-03/DENSO4
      BTACOR(I) = BTACOR(I)*1.E-03/DENC
C
C     CHANGE COEFFICIENTS FOR CARBON FROM BSCAT/VOL TO BSCAT/MASS.
C     CHANGE ABSORPTION COEFFICIENT FOR CARBON TO ABS/MASS.
C     CHANGE ABSORPTION COEFFICIENTS FOR SULFATE, COARSE
C     MODE AEROSOL, AND PRIMARY PARTICULATE FROM ABS/VOL
C     TO ABS/MASS.
C
      BTACAR(I)=BTACAR(I)*1.E-03/DENCAR
      ABSCAR(I)=ABSCAR(I)*1.E-03/DENCAR
      ABSSO4(I)=ABSSO4(I)*1.E-03/DENSO4
      ABSCOR(I)=ABSCOR(I)*1.E-03/DENC
C
```

```
C     ****************** DIAGNOSTIC PRINT OUT ****************
C
C       IF(I.NE.19)GO TO 355
C      WRITE(6,264)
264    FORMAT(1H ,5X,'TAAOHZ, TATOIZ(19), TATOHZ(19), TAUTOD(19), OMZ(19)
     1, OMH(19), BTASO4(19), BTAPRM(19), BTACOR(19), BTACAR(19)')
C      WRITE(6,261)TAAOHZ,TATOIZ(19),TATOHZ(19),TAUTOD(19),OMZ(19),
C     1 OMH(19),BTASO4(19),BTAPRM(19),BTACOR(19),BTACAR(19)
C      WRITE(6,265)
265    FORMAT(1H ,5X,'ABSCAR(19), ABSSO4(19), ABSCOR(19), ABSPRM(19)')
C      WRITE(6,261)ABSCAR(19),ABSSO4(19),ABSCOR(19),ABSPRM(19)
C355   CONTINUE
C
C    *********************************************
C
   200 CONTINUE
C      WRITE(6,958)
   958 FORMAT(/,3X,'TEST BEFORE CALL BACCLI AND RAYREI',/)
       PI=3.14159
       RAD=PI/180.
C
C      COMPUTE DOWNWARD AND UPWARD INTENSITIES
C
C      UO=COS(ZENITH*RAD)
C      DO 55 J=1,21
C      U=YMU(J)
C      BETA=ASIN(U)/RAD
C      DO 55 K=1,21
C      DD=XAZ(K)
C      THETA=ACOS(U*UO*COS(DD)+SQRT(1.-U**2)*SQRT(1.-UO**2))/RAD
C      CALL BACCLI(U,UO,DD,SPECBI,SPECBU)
C      CALL RAYREI(U,UO,DD,SPECRI,SPECRU)
C      DO 55 I=1,9
C      DIFIUP(I,J,K)=SPECBU(I)
C      DIFION(I,J,K)=SPECBI(I)
C      DIFRUP(I,J,K)=SPECRU(I)
C      DIFRON(I,J,K)=SPECRI(I)
C      WRITE(6,6)U,DD,I,DIFIDN(I,J,K),DIFIUP(I,J,K)
C    6 FORMAT(/,2(2X,E13.4),I5,2(2X,E13.4))
C   55 CONTINUE
       RETURN
       END
       SUBROUTINE BSIZE
C
C    CALCULATE OPTICAL PROPERTIES OF A GIVEN LOG-NORMAL AEROSOL SIZE
C    DISTRIBUTION BASED ON MIE SCATTERING THEORY
C
       COMMON/MIESCT/RVM,SIGMA,NLAMB,LAMB(20),JX,IT,TT(200),DUM(20),
      1PDUM(20,50),DUMA(20),DUMG(20)
       COMMON / RAIN / ITEST,IASD
       COMMON/ MISC/ ABSNO2(39),SOLAR(39),RAD,FORPIN,OMZ(39),OMH(39)
      1,NTHETA,RFR,RFI
       REAL LAMB
       REAL RFR,RFI,QEXT,QSCAT,QRPRD,ELTRMX(4,36,2),
      1 PIF(3,36),TAU(3,36),CSTHT(36),SI2THT(36)
       DIMENSION TTI(36)
       COMPLEX ACAP(7000)
```

```
      DIMENSION S1(36),S2(36),PHASE(36)
      DIMENSION XNT(200),ST(200),VT(200),R(200),DR(200)
C
      DIMENSION AL(31),ALALFA(154),ALPHA(154),QE(154),
     2STMTX(154,36)
     1,QS(154),QG(154),STMT(154,36)
      DIMENSION DOM(20,30),DOMA(20,30),DOMG(20,30),PDOM(9,22,8)
     2,RTMTS(200),STMTS(200)
C     ***************** DIAGNOSTIC PRINT OUT ************
C
C     WRITE(6,1005)RVM,SIGMA,NLAMB,JX,IT
C     WRITE(6,1010)NTHETA,RFR,RFI
1005  FORMAT(1H ,5X,'RVM = ',F6.3,1X,'SIGMA = ',F6.3,1X,'NLAMB = ',
     1 I3,1X,'JX = ',I3,1X,'IT = ',I3)
1010  FORMAT(1H ,5X,'NTHETA = ',I3,1X,'RFR = ',F6.3,1X,'RFI = ',F6.3)
C
C ********** DIAGNOSTIC PRINT OUT *********************
C
      NT=NTHETA
      JX=NTHETA
      IT=36
      LL=7000
      DO 570 J=1,NTHETA
      IF(TT(J).LE.90.) GO TO 560
      TT1(J)=180.-TT(J)
      GO TO 570
 560  CONTINUE
      TT1(J)=TT(J)
 570  CONTINUE
      IF(ITEST.LT.1) GO TO 82
      IF(RFR.EQ.RFRT) GO TO 81
  82  DO 10 I=1,112
      ALPHA(I)=EXP(-4.8+0.1*I)
      ALP=ALPHA(I)
      ALALFA(I)=ALOG(ALPHA(I))
      CALL DAMIE(ALP,RFR,RFI,TT1,JX,QEXT,QSCAT,QRPRD,ELTRMX,PIE,TAU,
     2CSTHT,SI2THT,ACAP,IT,LL)
      QE(I)=QEXT
      QS(I)=QSCAT
      QG(I)=QRPRD
      DO 9 J=1,NTHETA
      IF(TT(J).NE.TT1(J)) GO TO 91
      STMTX(I,J)=0.5*(ELTRMX(1,J,1)+ELTRMX(2,J,1))
      GO TO 9
  91  CONTINUE
      JJ=J
      STMTX(I,JJ)=0.5*(ELTRMX(1,J,2)+ELTRMX(2,J,2))
   9  CONTINUE
  10  CONTINUE
  81  PI = 3.14159267
      IF(IASD.GT.0) GO TO 1
C
C INTEGRATION FOR A LOGNORMAL
C AEROSOL SIZE DISTRIBUTION
C
      TWOPI = 2.*3.14159267
       FTPIN = 3./(4.*PI)
```

```
      PIN = .75
   50 NPOINT = 15
      K = NPOINT
      ITWKP1 = 2*K + 1
      KP1 = K + 1
      KP2 = K + 2
      ALSIGM = ALOG(SIGMA)
      ALSGM2 = ALSIGM**2
      SIGM2 = ALSGM2
      SQRT2 = SQRT(2.)
      RSM = EXP(ALOG(RVM)-ALSGM2)
      RNM = EXP(ALOG(RVM)-3.*ALSGM2)
      TA = 2.*ALSGM2
      CN = 1./(SQRT(TWOPI)*ALSIGM)
      CS = PI*CN*RNM**2*EXP(TA)
      CV = (4./3.)*PI*CN*RNM**3*EXP(4.5*ALSGM2)
      F1 = ALOG(30.*SQRT2*ALSIGM)
      F1 = F1/15.
      F1 = EXP(-F1)
      AA = ALOG(1./F1)
      F2 = 1./F1
      V1 = 1.
      V2 = 1.
      DO 20 I = 1,K
      V1 = V1*F1
      R(I) = RSM*V1
      ST(I) = ALGN(ALSGM2,RSM,R(I))*CS
      VT(I) = ALGN(ALSGM2,RVM,R(I))*CV
      XNT(I) = ALGN(ALSGM2,RNM,R(I))*CN
   20 DR(I) = AA
      R(KP1) = RSM
      ST(KP1) = ALGN(SIGM2, RSM,RSM)*CS
      VT(KP1) = ALGN(SIGM2,RVM,RSM)*CV
      XNT(KP1) = ALGN(SIGM2,RNM,RSM)*CN
      DR(KP1) = AA
      DO 21 I = KP2,ITWKP1
      V2 = V2*F2
      R(I) = RSM*V2
      ST(I) = ALGN(SIGM2,RSM,R(I))*CS
      VT(I) = ALGN(SIGM2,RVM,R(I))*CV
      DR(I) = AA
   21 XNT(I) = ALGN(SIGM2,RNM,R(I))*CN
C     DO THE INTEGRATION OVER THE DISTRIBUTIONS
      XNTOT = 0.
      STOT = 0.
      VTOT = 0.
      DO 30 I = 1,ITWKP1
      VTOT = VTOT + VT(I)*DR(I)
      STOT = STOT + ST(I)*DR(I)
      XNTOT = XNTOT + XNT(I)*DR(I)
   30 CONTINUE
 1000 FORMAT(1H ,10X,10F10.4)
  500 CONTINUE
      DO 40 IL = 1,NLAMB
      XLAM = LAMB(IL)
      WAVE = TWOPI/XLAM
      EXT = 0.
```

```
      SCAT = 0.
      ABS = 0.
      AVCOS = 0.
      DO 31 J = 1,NT
   31 PHASE(J)=0.
      DO 60 I = 1,ITWKP1
   60 AL(I)= ALOG(WAVE*R(I))
      DO 62 I=1,ITWKP1
      DO 61 J=3,110
   61 IF(AL(I).LE.ALALFA(J)) GO TO 63
   63 Q=ALALFA(J)-ALALFA(J-1)
      IF(AL(I).GE.ALALFA(110)) GO TO 160
      Z=(AL(I)-ALALFA(J-1))/Q
      QST=QS(J-1)+0.25*Z*((5.*QS(J)-3.0*QS(J-1)-QS(J-2)-QS(J+1))
     2+(QS(J-2)-QS(J-1)-QS(J)+QS(J+1))*Z)
      QEX=QE(J-1)+0.25*Z*((5.*QE(J)-3.0*QE(J-1)-QE(J-2)-QE(J+1))
     2+(QE(J-2)-QE(J-1)-QE(J)+QE(J+1))*Z)
      QGP=QG(J-1)+0.25*Z*((5.*QG(J)-3.0*QG(J-1)-QG(J-2)-QG(J+1))
     2+(QG(J-2)-QG(J-1)-QG(J)+QG(J+1))*Z)
      GO TO 161
  160 QEX=QE(110)
      QST=QS(110)
      QGP=QG(110)
  161 CONTINUE
      EXT=QEX*ST(I)*DR(I)+EXT
      SCAT=QST*ST(I)*DR(I)+SCAT
      ABS=(QEX-QST)*ST(I)*DR(I)+ABS
      AVCOS=AVCOS+QGP*ST(I)*DR(I)
C     WRITE(6,357)I,J,EXT,SCAT,ABS,AVCOS
  357 FORMAT(2(2X,I4),4(2X,E13.4))
   62 CONTINUE
      DO 64 K=1,NTHETA
      DO 65 I=1,ITWKP1
      DO 66 J=3,110
   66 IF(AL(I).LE.ALALFA(J)) GO TO 67
   67 Q=ALALFA(J)-ALALFA(J-1)
      IF(AL(I).GE.ALALFA(110))GO TO 162
      Z=(AL(I)-ALALFA(J-1))/Q
      STMT(I,K)=STMTX(J-1,K)+0.25*Z*((5.*STMTX(J,K)-3.*STMTX(J-1,K)-
     2STMTX(J-2,K)-STMTX(J+1,K))+(STMTX(J-2,K)-STMTX(J-1,K)-STMTX(J,K)
     3+STMTX(J+1,K))*Z)
      GO TO 163
  162 STMT(I,K)=STMTX(110,K)
  163 CONTINUE
      PHASE(K)=STMT(I,K)*XNT(I)*DR(I) + PHASE(K)
   65 CONTINUE
   64 CONTINUE
C       PRINT OUT THE RESULTS
      RWB = XLAM**2/(PI*SCAT)
      DUM(IL) = EXT/VTOT
      DUMA(IL) = ABS/VTOT
      DUMG(IL) = AVCOS/SCAT
      DO 36 I = 1,NT
   36 PDUM(IL,I)=PHASE(I)*RWB
   40 CONTINUE
      ITEST=ITEST + 1
      RERT=RFR
```

```
      GO TO 24
    1 IF(IASD.GT.1) GO TO 2
C
C INTEGRATION FOR A SECTIONAL
C AEROSOL SIZE DISTRIBUTION
C
      NSEC=11
      GO TO 3
    2 NSEC=22
    3 DX=4./(FLOAT(NSEC)+1.)
      R(1)=0.005
      AL(1)=ALOG(WAVE*R(1))
      DO 4 I=1,NSEC
      R(I+1)=R(I)*10.**DX
    4 AL(I+1)=ALOG(WAVE*R(I+1))
      DXJ=DX/6.
      DO 11 IL=1,NLAMB
      DO 5 I=1,NSEC
      EXT=0.
      SCAT=0.
      AVCOS=0.
      LSR=1
      DO 6 J=1,7
      JJ=6*I-6+J
      DO 7 K=2,150
    7 IF(AL(JJ).LE.ALALFA(K)) GO TO 8
    8 Q=ALALFA(K)-ALALFA(K-1)
      Z=(AL(JJ)-ALALFA(K-1))/Q
      RA=R(JJ)*10.**DXJ
      QEXS=Z*(QE(K)-QE(K-1))+QE(K-1)
      QSTS=Z*(QS(K)-QS(K-1))+QS(K-1)
      QGPS=Z*(QG(K)-QG(K-1))+QG(K-1)
      REX=3./4.*QEXS/RA
      RST=3./4.*QSTS/RA
      RGP=3./4.*QGPS/RA
      IF(LSR.GT.1) GO TO 23
      EXT=REX+EXT
      SCAT=RST+SCAT
      AVCOS=RGP+AVCOS
      LSR=4
   23 IF(LSR.GT.2) GO TO 22
      EXT=2.*REX+EXT
      SCAT=2.*RST+SCAT
      AVCOS=2.*RGP+AVCOS
      LSR=2
      GO TO 6
   22 EXT=4.*REX+EXT
      SCAT=4.*RST+SCAT
      AVCOS=4.*RGP+AVCOS
      LSR=2
      IF(J.EQ.6) LSR=1
    6 CONTINUE
      DOM(IL,I)=EXT/3.*DXJ
      DOMA(IL,I)=(EXT-SCAT)/3.*DXJ
      SCAT=SCAT/3.*DXJ
      DOMG(IL,I)=AVCOS/3.*DXJ/SCAT
      DO 12 J=1,NT
```

```
   12 PHASE(J)=0.
      DO 13 KK=1,NT
      LSR=1
      DO 14 J=1,7
      JJJ=6*I-6+J
      DO 15 K=2,150
   15 IF(AL(JJ).LE.ALALFA(K)) GO TO 16
   16 Q=ALALFA(K)-ALALFA(K-1)
      Z=(AL(JJ)-ALALFA(K-1))/Q
      RA=R(JJ)*10.**DXJ
      STMTS(KK)=Z*(STMTX(K,KK)-STMTX(K-1,KK))+STMTX(K-1,KK)
      RTMTS(KK)=STMTS(KK)*3./4./RA**3
      IF(LSR.GT.1) GO TO 17
      PHASE(KK)=PHASE(KK)+RTMTS(KK)
      LSR=4
      GO TO 14
   17 IF(LSR.GT.2) GO TO 19
      PHASE(KK)=PHASE(KK)+2.*RTMTS(KK)
      LSR=2
      GO TO 14
   19 PHASE(KK)=PHASE(KK)+4.*RTMTS(KK)
      IF(J.EQ.6) LSR=1
   14 CONTINUE
      PDOM(IL,1,KK)=PHASE(KK)/3.*DXJ*LAMB(IL)**2/(PI*SCAT)
   13 CONTINUE
    5 CONTINUE
   11 CONTINUE
   24 RETURN
      END
      SUBROUTINE DAMIE (X,RFR,RFI,THETD,JX,QEXT,QSCAT,CTBRQS,ELTRMX,
     1 PI,TAU,CSTHT,SI2THT,ACAP,IT,LL)
C       LARGE VERSION
C       SUBROUTINE FOR COMPUTING THE PARAMETERS OF THE ELECTROMAGNETIC
C       RADIATION SCATTERED BY A SPHERE. THIS SUBROUTINE CARRIES OUT ALL
C       COMPUTATIONS IN DOUBLE PRECISION ARITHMETIC.
C       THIS SUBROUTINE COMPUTES THE CAPITAL A FUNCTION BY MAKING USE OF
C       DOWNWARD RECURRENCE RELATIONSHIP.
C       X! SIZE PARAMETER OF THE SPHERE,( 2 * PI * RADIUS OF THE SPHERE)
C       WAVELENGTH OF THE INCIDENT RADIATION).
C       RF! REFRACTIVE INDEX OF THE MATERIAL OF THE SPHERE.  COMPLEX
C       QUANTITY..FORM! (RFR - I * RFI )
C       THETD(J)! ANGLE IN DEGREES BETWEEN THE DIRECTIONS OF THE INCIDENT
C       AND THE SCATTERED RADIATION.  THETD(J) IS< OR= 90.0
C       IF THETD(J) SHOULD HAPPEN TO BE GREATER THAN 90.0, ENTER WITH
C       SUPPLEMENTARY VALUE
CSEE COMMENTS BELOW ON ELTRMX.
C       JX! TOTAL NUMBER OF THETD FOR WHICH THE COMPUTATIONS ARE
C       REQUIRED.  JX SHOULD NOT EXCEED IT UNLESS THE DIMENSIONS
C       STATEMENTS ARE APPROPRIATEDLY MODIFIED.
C       MAIN PROGRAM SHOULD ALSO HAVE REAL*8 THETD(IT ),ELTRMX(4,IT ,2).
C       THE DEFINITIONS FOR THE FOLLOWING SYMBOLS CAN BE FOUND IN        LIGHT
        REAL    X,RX,RFR,RFI,QEXT,QSCAT,T(5),TA(4),TB(2),TC(2)
        REAL    TD(2),TC(2),CTBRQS
        REAL    ELTRMX(4,IT ,2),PI(3,IT ),TAU(3,IT ),CSTHT(IT ),SI2THT(IT)
     1 ,THETD(IT)
        COMPLEX    RF,RRF,RRFX,WMI,FNA,FNB,TC1,TC2,WFN(2)
        COMPLEX    FNAP,FNBP,ACAP(1)
```

```
C       IN THE ORIGINAL PROGRAM THE DIMENSION OF ACAP WAS 7000.
C       FOR CONSERVING SPACE THIS SHOULD BE NOT MUCH HIGHER THAN
C       THE VALUE, N=1.1*(NREAL**2 + NIMAG**2)**.5 * X + 1
C       TA(1)! REAL PART OF WFN(1).. TA(2)! IMAGINARY PART OF WFN(1)..
C       TA(3)! REAL PART OF WFN(2)..TA(4)! IMAGINARY PART OF WFN(2).
C       TB(1)! REAL PART OF FNA.. TB(2)! IMAGINARTY PART OF FNA..
C       TC(1)! REAL PART OF FNB.. TC(2)! IMAGINARY PART OF FNB..
C       TD(1)! REAL PART OF FNAP..TD(2) IMAGINARY PART OF FNAP.
C       TE(1)! REAL PART OF FNBP.. TE(2)! IMAGINARY PART OF FNBP.
C      FNAP ? FNBP ARE THE PRECEDING VALUES OF FNA ? FNB RESPECTIVELY.
C**** PRIME VERSION WORKS ONLY IN SINGLE PRECISION WITH THE
C      COMPLEX ARITHMETIC.
       EQUIVALENCE (WFN(1),TA(1)),(FNA,TB(1)),(FNB,TC(1))
       EQUIVALENCE(FNAP,TD(1)),(FNBP,TE(1))
      DATA PII /3.1415926535897932/
C
C      FORMAT STATEMENTS FOLLOW
 5      FORMAT(10X,' THE VALUE OF THE SCATTERING ANGLE IS GREATER THAN
     1 90.0 DEGREES. IT IS ',E15.4)
 6      FORMAT(//10X, 'PLEASE READ COMMENTS.' //)
 7      FORMAT(//10X,'THE VALUE OF THE ARGUMENT JX IS GREATER THAN IT ')
 8      FORMAT(//10X,'THE UPPER LIMIT FOR ACAP IS NOT ENOUGH. SUGGEST GET
     1 DETAILED OUPUT AND MODIFY SUBROUTINE'//)
C
C      EXECUTABLE STATEMENTS FOLLOW
       IF(JX.LE. IT) GO TO 20
       WRITE(6,7)
       WRITE(6,6)
*      CALL EXIT
 20    RF =  CMPLX(RFR,-RFI)
       RRF = 1.0E0/RF
       RX = 1.0F0/X
       RRFX = RRF * RX
       T(1) = (X**2)*(RFR**2 + RFI**2)
       T(1) =  SQRT(T(1))
       NMX1 = 1.10E0 * T(1)
C      WRITE(6,199) X,RFR,RFI,LL,NMX1
C 199 FORMAT(1H ,'X=',E14.6,2X,'RFR=',E14.6,2X,'RFI=',E14.6,2X,'LL=',I10
C     1,2X,*NMX1                                *,I10)
       IF( NMX1 .LE. LL-1 ) GO TO 21
       WRITE(6,8)
       STOP
 21    NMX2 = T(1)
       IF( NMX1 .GT. 150) GO TO 22
       NMX1 = 150
       NMX2 = 135
 22    ACAP(NMX1 + 1 ) = (0.0E0,0.0E0)
       DO 23 N = 1,NMX1
       NN = NMX1 - N + 1
       ACAP(NN)=FLOAT(NN+1)*RRFX-1.0E0/(FLOAT(NN+1)*RRFX+ACAP(NN+1))
 23    CONTINUE
       DO 30 J = 1,JX
       IF ( THETD(J) .LT. 0.0E0 ) THETD(J) =  ABS(THETD(J))
       IF ( THETD(J) .GT. 0.0E0 ) GO TO 24
       CSTHT(J) = 1.0E0
       SI2THT(J) = 0.0E0
       GO TO 30
```

```
 24     IF ( THETD(J) .GE. 90.0E0) GO TO 25
        T(1) = ( PII * THETD(J))/180.0E0
        CSTHT(J) =  COS(T(1))
        SI2THT(J) = 1.0E0 - CSTHT(J)**2
        GO TO 30
 25     IF ( THETD(J) .GT. 90.0E0) GO TO 28
        CSTHT(J) = 0.0E0
        SI2THT(J) = 1.0E0
        GO TO 30
 28     WRITE(6,5) THETD(J)
        WRITE(6,6)
*       CALL EXIT
 30     CONTINUE
        DO 35 J = 1,JX
        PI(1,J) = 0.0E0
        PI(2,J) = 1.0E0
        TAU(1,J) = 0.0E0
        TAU(2,J) = CSTHT(J)
 35     CONTINUE
        T(1) =  COS(X)
        T(2) =  SIN(X)
        WM1 =  CMPLX( T(1),-T(2))
        WFN(1) =  CMPLX(T(2),T(1))
        WFN(2) = RX * WFN(1) - WM1
        TC1 = ACAP(1) * RRF + RX
        TC2 = ACAP(1) * RF + RX
        FNA = (TC1*TA(3) - TA(1))/(TC1*WFN(2) - WFN(1))
        FNB = ( TC2*TA(3) - TA(1))/(TC2  * WFN(2) - WFN(1))
        FNAP = FNA
        FNBP = FNB
        T(1) = 1.50E0
C       FROM HERE TO THE STATMENT NUMBER 90, ELTRMX(I,J,K) HAS
C       FOLLOWING MEANING!
C       ELTRMX(1,J,K)! REAL PART OF THE FIRST COMPLEX AMPLITUDE.
C       ELTRMX(2,J,K)! IMAGINARY PART OF THE FIRST COMPLEX AMPLITUDE.
C       ELTRMX(3,J,K)! REAL PART OF THE SECOND COMPLEX AMPLITUDE.
C       ELTRMX(4,J,K)! IMAGINARY PART OF THE SECOND COMPLEX AMPLITUDE.
C       K = 1 ! FOR THETD(J) AND K = 2 ! FOR 180.0 - THETD(J)
C       DEFINITION OF THE COMPLEX AMPLITUDE! VAN DE HULST,P.125.
        TB(1) = T(1) * TB(1)
        TB(2) = T(1) * TB(2)
        TC(1) = T(1) * TC(1)
        TC(2) = T(1) * TC(2)
        DO 60 J = 1,JX
        ELTRMX(1,J,1) = TB(1) * PI(2,J) + TC(1) * TAU(2,J)
        ELTRMX(2,J,1) = TB(2) * PI(2,J) + TC(2) * TAU(2,J)
        ELTRMX(3,J,1) = TC(1) * PI(2,J) + TB(1) * TAU(2,J)
        ELTRMX(4,J,1) = TC(2) * PI(2,J) + TB(2) * TAU(2,J)
        ELTRMX(1,J,2) = TB(1) * PI(2,J) - TC(1) * TAU(2,J)
        ELTRMX(2,J,2) = TB(2) * PI(2,J) - TC(2) * TAU(2,J)
        ELTRMX(3,J,2) = TC(1) * PI(2,J) - TB(1) * TAU(2,J)
        ELTRMX(4,J,2) = TC(2) * PI(2,J) - TB(2) * TAU(2,J)
 60     CONTINUE
        QEXT = 2.0E0 * ( TB(1) + TC(1))
C      WRITE(6,999) TB(1),TC(1)
        QSCAT =(TB(1)**2 + TB(2)**2 + TC(1)**2 + TC(2)**2)/0.75E0
        CTBRQS = 0.0E0
```

```
      N = 2
   65 T(1) = 2*N - 1
      T(2) = N - 1
      T(3) = 2 * N + 1
      DO 70 J = 1,JX
      PI(3,J) = (T(1)*PI(2,J)*CSTHT(J)-FLOAT(N)*PI(1,J))/T(2)
      TAU(3,J) = CSTHT(J)*(PI(3,J)-PI(1,J))-T(1)*SI2THT(J)*PI(2,J)+
     1 TAU(1,J)
   70 CONTINUE
      WM1 = WFN(1)
      WFN(1) = WFN(2)
      WFN(2) = T(1)*RX*WFN(1) - WM1
      TC1 = ACAP(N)*RRF + FLOAT(N)*RX
      TC2 = ACAP(N)*RF + FLOAT(N)*RX
      FNA = (TC1*TA(3)-TA(1))/(TC1*WFN(2) - WFN(1))
     TC2 = TC2
     TA(3) = TA(3)
     TA(1) = TA(1)
     TC1 = TC1
     WFN(2) = WFN(2)
     WFN(1) = WFN(1)
      FNB = (TC2*TA(3)-TA(1))/(TC2*WFN(2) - WFN(1))
      T(5) = N
      T(4) = T(1)/(T(5)*T(2))
      T(2) = (T(2)*(T(5) + 1.0E0))/T(5)
      CTBRQS = CTBRQS + T(2)*(TD(1)*TB(1) + TD(2)*TB(2) + TE(1)*TC(1) +
     1 TE(2)*TC(2))  + T(4)*(TD(1)*TE(1) + TD(2)*TE(2))
      QEXT = QEXT + T(3)*(TB(1)+TC(1))
      T(4) = TB(1)**2 + TB(2)**2 + TC(1)**2 + TC(2)**2
      QSCAT = QSCAT + T(3) *T(4)
      T(2) = N*(N+1)
      T(1) = T(3)/T(2)
C     WRITE(6,999) T(1),QEXT
      K = (N/2)*2
      DO 80 J = 1,JX
      ELTRMX(1,J,1)=ELTRMX(1,J,1)+T(1)*(TB(1)*PI(3,J)+TC(1)*TAU(3,J))
      ELTRMX(2,J,1)=ELTRMX(2,J,1)+T(1)*(TB(2)*PI(3,J)+TC(2)*TAU(3,J))
      ELTRMX(3,J,1)=ELTRMX(3,J,1)+T(1)*(TC(1)*PI(3,J)+TB(1)*TAU(3,J))
      ELTRMX(4,J,1)=ELTRMX(4,J,1)+T(1)*(TC(2)*PI(3,J)+TB(2)*TAU(3,J))
      IF ( K .EQ. N) GO TO 75
     ELTRMX(1,J,2)=ELTRMX(1,J,2) +T(1)*(TB(1)*PI(3,J)-TC(1)*TAU(3,J))
      ELTRMX(2,J,2)=ELTRMX(2,J,2)+T(1)*(TB(2)*PI(3,J)-TC(2)*TAU(3,J))
      ELTRMX(3,J,2)=ELTRMX(3,J,2)+T(1)*(TC(1)*PI(3,J)-TB(1)*TAU(3,J))
      ELTRMX(4,J,2)=ELTRMX(4,J,2)+T(1)*(TC(2)*PI(3,J)-TB(2)*TAU(3,J))
      GO TO 80
   75 ELTRMX(1,J,2)=ELTRMX(1,J,2)+T(1)*(-TB(1)*PI(3,J)+TC(1)*TAU(3,J))
      ELTRMX(2,J,2)=ELTRMX(2,J,2)+T(1)*(-TB(2)*PI(3,J)+TC(2)*TAU(3,J))
      ELTRMX(3,J,2)=ELTRMX(3,J,2)+T(1)*(-TC(1)*PI(3,J)+TB(1)*TAU(3,J))
      ELTRMX(4,J,2)=ELTRMX(4,J,2)+T(1)*(-TC(2)*PI(3,J)+TB(2)*TAU(3,J))
   80 CONTINUE
      IF( T(4) .LT.  1.0E-6 ) GO TO 100
      N = N + 1
      DO 90 J = 1,JX
      PI(1,J) = PI(2,J)
      PI(2,J) = PI(3,J)
      TAU(1,J) = TAU(2,J)
      TAU(2,J) = TAU(3,J)
```

```
 90    CONTINUE
       FNAP = FNA
       FNBP = FNB
       IF ( N .LE. NMX2) GO TO 65
       WRITE(6,8)
**     CALL EXIT
 100   DO 120 J = 1,JX
       DO 120 K = 1,2
       DO  115  I= 1,4
       T(I) = ELTRMX(I,J,K)
 115   CONTINUE
       ELTRMX(2,J,K) = T(1)**2 + T(2)**2
       ELTRMX(1,J,K) = T(3)**2 + T(4)**2
       ELTRMX(3,J,K) = T(1)*T(3) + T(2)*T(4)
       ELTRMX(4,J,K) = T(2)*T(3) - T(4)*T(1)
 120   CONTINUE
       T(1) = 2.0E0 * RX**2
       QEXT = QEXT * T(1)
C     WRITE(6,999) T(1),QEXT
C999    FORMAT(1H ,3E20.8)
       QSCAT = QSCAT * T(1)
       CTBRQS = 2.E0 * CTBRQS * T(1)
C      THE DETAIL ABOUT THIS SUBROUTINE CAN BE FOUND IN THE FOLLOWING
C      REPORT!                                  SUBROUTINES FOR COMPUTING THE PARAM
C      ELECTROMAGNETIC RADIATION SCATTERED BY A SPHERE                    J.V. DA
C      I B M SCIENTIFIC CENTER, PALO ALTO , CALIFORNIA.
C      REPORT NO. 320 - 3236 .. MAY 1968 ..
99999  RETURN
       END
      SUBROUTINE SPLNA (N,X,Y,J,D,C,W)
      DIMENSION X(10), Y(10), D(2), C(30), W(30)
C     ------------------------------------------------------------------
C           OVER THE INTERVAL X(I) TO X(I+1), THE INTERPOLATING
C           POLYNOMIAL
C                 Y=Y(I)+A(I)*Z+B(I)*Z**2+E(I)*Z**3
C           WHERE Z=(X-X(I))/(X(I+1)-X(I))
C           IS USED. THE COEFFICIENTS A(I),B(I) AND E(I) ARE COMPUTED
C           BY SPLNA AND STORED IN LOCATIONS C(3*I-2),C(3*I-1) AND
C           C(3*I) RESPECTIVELY.
C           WHILE WORKING IN THE ITH INTERVAL,THE VARIABLE Q WILL
C           REPRESENT Q=X(I+1) - X(I), AND Y(I) WILL REPRESENT
C           Y(I+1)-Y(I)
C     ------------------------------------------------------------------
C
      Q=X(2)-X(1)
      YI=Y(2)-Y(1)
      IF (J.EQ.2) GO TO 5
C     ------------------------------------------------------------------
C           IF THE FIRST DERIVATIVE AT THE END POINTS IS GIVEN,
C           A(1) IS KNOWN, AND THE SECOND EQUATION BECOMES
C           MERELY B(I)+E(1)=YI - Q*D(1).
C     ------------------------------------------------------------------
      C(1)=Q*D(1)
      C(2)=1.0
      W(2)=YI-C(1)
      GO TO 10
C     ------------------------------------------------------------------
```

```
C            IF THE SECOND DERIVATIVE AT THE END POINTS IS GIVEN
C            B(1) IS KNOWN, THE SECOND EQUATION BECOMES
C            A(1)+E(1)=Y1-0.5*Q*Q*D(1). DURING THE SOLUTION OF
C            THE 3N-4 EQUATIONS,A1 WILL BE KEPT IN CELL C(2)
C            INSTEAD OF C(1) TO RETAIN THE TRIDIAGONAL FORM OF THE
C            COEFFICIENT MATRIX.
C     ------------------------------------------------------------------
    5 C(2)=0.0
      W(2)=0.5*Q*Q*D(1)
   10 M=N-2
      IF (M.LE.0) GO TO 20
C     ------------------------------------------------------------------
C            UPPER TRIANGULARIZATION OF THE TRIDIAGONAL SYSTEM OF
C            EQUATIONS FOR THE COEFFICIENT MATRIX FOLLOWS--
C     ------------------------------------------------------------------
      DO 15 I=1,M
      A1=Q
      Q=X(I+2)-X(I+1)
      H=A1/Q
      C(3*I)=-H/(2.0-C(3*I-1))
      W(3*I)=(-Y1-W(3*I-1))/(2.0-C(3*I-1))
      C(3*I+1)=-H*H/(H-C(3*I))
      W(3*I+1)=(Y1-W(3*I))/(H-C(3*I))
      Y1=Y(I+2)-Y(I+1)
      C(3*I+2)=1.0/(1.0-C(3*I+1))
   15 W(3*I+2)=(Y1-W(3*I+1))/(1.0-C(3*I+1))
C     ------------------------------------------------------------------
C            E(N-1) IS DETERMINED DIRECTLY FROM THE LAST EQUATION
C            OBTAINED ABOVE, AND THE FIRST OR SECOND DERIVATIVE
C            VALUE GIVEN AT THE END POINT.
C     ------------------------------------------------------------------
   20 IF (J.EQ.1) GO TO 25
      C(3*N-3)=(Q*Q*D(2)/2.0-W(3*N-4))/(3.0-C(3*N-4))
      GO TO 30
   25 C(3*N-3)=(Q*D(2)-Y1-W(3*N-4))/(2.0-C(3*N-4))
   30 M=3*N-6
      IF (M.LE.0) GO TO 40
C     ------------------------------------------------------------------
C            BACK SOLUTION FOR ALL COEFFICENTS EXCEPT
C            A(1) AND B(1) FOLLOWS--
C     ------------------------------------------------------------------
      DO 35 II=1,M
      I=M-II+3
   35 C(I)=W(I)-C(I)*C(I+1)
   40 IF (J.EQ.1) GO TO 45
C     ------------------------------------------------------------------
C            IF THE SECOND DERIVATIVE IS GIVEN AT THE END POINTS,
C            A(1) CAN NOW BE COMPUTED FROM THE KNOWN VALUES OF
C            B(1) AND E(1). THEN A(1) AND B(1) ARE PUT INTO THEIR
C            PROPER PLACES IN THE C ARRAY.
C     ------------------------------------------------------------------
      C(1)=Y(2)-Y(1)-W(2)-C(3)
      C(2)=W(2)
      RETURN
   45 C(2)=W(2)-C(3)
      RETURN
      END
```

```
      BLOCK DATA
      COMMON/MIESCT/ROG,SIGMA,NLAMB,LAMB(20),JX,IT,TT(200),DUM(20),
     1PDUM(20,50),DUMA(20),DUMG(20)
      COMMON/ MISC/ ABSNO2(39),SOLAR(39),RAD,FORPIN,OMZ(39),OMH(39)
     1,NTHETA,RFR,RFI
      COMMON/COLOR/YCAP,VAL,X,Y,YCAPD,VALD,XD,YD,DELUV,DELAB,
     1XBAR(39),YBAR(39),ZBAR(39),PI,CONT1,CONT2,CONT3,BRATIO
      REAL LAMB
      DATA LAMB / 0.35,0.40,0.45,0.50,0.55,0.60,0.65,0.70,0.75,11*0.0/
      DATA TT /0.,10.,20.,30.,40.,50.,60.,70.,80.,90.,100.,110.,120.,
     1          130.,140.,150.,160.,170.,180.,190.,200.,210.,220.,230.,
     2          240.,250.,260.,270.,280.,290.,300.,310.,320.,330.,340.,
     3          350.,164*0. /
      DATA NLAMB / 9 /
      DATA NTHETA / 19 /
      DATA ABSNO2 /1.58, 1.63,1.67,1.71,1.67, 1.63, 1.54, 1.45,
     1             1.36, 1.17, 1.06, 0.92, 0.80, 0.69, 0.61, 0.54,
     2             0.46, 0.39, 0.31, 0.26, 0.21, 0.18, 0.15, 0.12, 0.1,
     3             0.080, 0.063, 0.053, 0.041, 0.035, 0.029, 0.024,
     4             0.021, 0.017, 0.014, 0.010, 0.0068, 0.0034,0./
      DATA  SOLAR / 1163., 1124., 1121., 1423., 1730., 1740., 1659.,
     1 1801., 1998., 2059., 2040., 2042., 1959., 1941., 1879., 1838.,
     2 1839., 1785., 1731., 1704., 1712., 1716., 1699., 1640., 1635.,
     3 1602., 1570., 1544., 1511., 1466., 1456., 1427., 1402., 1369.,
     4 1344., 1314., 1290.,1260., 1235.   /
      DATA XBAR /  0.0000, 0.0014, 0.0042, 0.0143, 0.0435, 0.1344,
     1 0.2839, 0.3483, 0.3362, 0.2908, 0.1954, 0.0956, 0.0320,
     2 0.0049, 0.0093, 0.0633, 0.1655, 0.2904, 0.4334, 0.5945, 0.7621,
     3 0.9163, 1.0263, 1.0622, 1.0026, 0.8544, 0.6424, 0.4479, 0.2835,
     4 0.1649, 0.0874, 0.0468, 0.0227, 0.0114, 0.0058, 0.0029, 0.0014,
     5 0.0007, 0.0003 /
      DATA YBAR / 0.0000, 0.0000, 0.0001, 0.0004, 0.0012, 0.0040,
     1 0.0116, 0.0230, 0.0380, 0.0600,0.0910, 0.1390, 0.2080, 0.3230,
     2 0.5030, 0.7100, 0.8620, 0.9540, 0.9950, 0.9950, 0.9520, 0.8700,
     3 0.7570,0.6310, 0.5030, 0.3810, 0.2650, 0.1750, 0.1070, 0.0610,
     4 0.0320, 0.0170, 0.0082, 0.0041, 0.0021, 0.0010, 0.0005, 0.0002,
     5 0.0001   /
      DATA ZBAR / 0.0000, 0.0065, 0.0201, 0.0679, 0.2074, 0.6456,
     1 1.3856, 1.7471, 1.7721, 1.6692, 1.2876, 0.8130, 0.4652, 0.2720,
     2 0.1582, 0.0782, 0.0422, 0.0203, 0.0087, 0.0039, 0.0021, 0.0017,
     3 0.0011, 0.0008, 0.0003, 0.0002, 13*0.0000 /
      END
      FUNCTION ERF(XX)
C
C  ERF=2/SQRT(PI)*INTEGRAL OF EXP(-T*T) FROM 0 TO X.
C  USING AN APPROXIMATION DUE TO HASTINGS  GOOD TO SEVEN SI
C  USING AN APPROXIMATION DUE TO HASTINGS. ABSOLUTE ERROR ABOUT 3E-7
C
      DIMENSION A(6)
      DATA A/.0000430638,.0002765672,.0001520143,.0092705272,.0422820123
     1,.0705230784 /
      X=ABS(XX)
      T=A(1)*X
      DO 10 I=2,6
      T=(T+A(I))*X
   10 CONTINUE
      T=1./(T+1.)
```

```
      ERF=1.-T**16
      IF(XX.LT.0.)ERF=-ERF
      RETURN
      END
      FUNCTION ACOS (SIC)
      REAL ACOS, SIC, SINE, PI
      LOGICAL TEST
C
      TEST = ABS(SIC).EQ.0.
      IF(.NOT.TEST) GO TO 10
      ACOS = PI(0.5)
      GO TO 20
   10 AA=ASIN(SIC)
C     IF (SIC.GE.0.) ACOS=PI(.5)-AA
      ACOS=PI(.5)-AA
C     IF (SIC.LT.0.) ACOS=PI(.5)+AA
20    RETURN
      END
      FUNCTION ASIN (X)
      REAL ASIN, PI
      LOGICAL TEST
C
      TEST = ABS(X).EQ.1.E0
C     IF(.NOT.TEST) GO TO 10
      IF (ABS(ABS(X)-1.).GT..0001) GO TO 10
      ASIN = PI(.5)
      GO TO 20
10    Y = SQRT(1.E0-(X*X))
      ASIN = ATAN(X/Y)
20    RETURN
      END
      FUNCTION PI (VALUE)
      REAL VALUE, PI
      PI=3.14159265359E0*VALUE
      RETURN
      END
      FUNCTION ALGN(X,Y,Z)
      TWOX = 2.*X
      U = (ALOG(Y/Z))**2
      ALGN = EXP(-U/TWOX)
      RETURN
      END
```

B.2 ALBEDO

ALBEDO - Source Code
ALBEDO - Sample Input

```
ALTON COAL PROJECT INDUSTRIAL AREA - YOVIMPA POINT 22.4 KM (uncontrolled)
(vertical visual profile 0-1km:70km 1-3km:100km 3-7km:400km 7-20km:1000km)
112.2400  37.4730  2774.0
15.0      15
86
112.46912 37.376862 2082.0  49340.    1   0.15
112.46863 37.377485 2082.0  66820.    1   0.15
112.46813 37.378108 2082.0  23030.    1   0.15
112.46763 37.378731 2082.0  40990.    1   0.15
112.46714 37.379354 2082.0  24860.    1   0.15
112.46863 37.376239 2082.0  42720.    1   0.15
112.46813 37.376862 2082.0  44340.    1   0.15
112.46763 37.377485 2082.0  84120.    1   0.15
112.46714 37.378108 2082.0  32440.    1   0.15
112.46664 37.378731 2082.0  37240.    1   0.15
112.46614 37.379354 2082.0  11800.    1   0.15
112.46565 37.379977 2082.0   4800.    1   0.15
112.46515 37.380600 2082.0  15320.    1   0.15
112.46863 37.374933 2082.0   3240.    1   0.15
112.46813 37.375616 2082.0  39040.    1   0.15
112.46763 37.376239 2082.0  37280.    1   0.15
112.46714 37.376862 2082.0  31440.    1   0.15
112.46664 37.377485 2082.0  74640.    1   0.15
112.46614 37.378108 2082.0  16920.    1   0.15
112.46515 37.379354 2082.0   1400.    1   0.15
112.46465 37.379977 2082.0 111760.    1   0.15
112.46416 37.380600 2082.0  22680.    1   0.15
112.46813 37.374370 2082.0   6480.    1   0.15
112.46763 37.374933 2082.0  59920.    1   0.15
112.46714 37.375616 2082.0  51680.    1   0.15
112.46664 37.376239 2082.0 419760.    1   0.15
112.46614 37.376862 2082.0 538840.    1   0.15
112.46565 37.377485 2082.0  74520.    1   0.15
112.46515 37.378108 2082.0  57560.    1   0.15
112.46465 37.378731 2082.0  69760.    1   0.15
112.46416 37.379354 2082.0 300240.    1   0.15
112.46366 37.379977 2082.0  32400.    1   0.15
112.46714 37.374437 2082.0   9240.    1   0.15
112.46664 37.374933 2082.0   9760.    1   0.15
112.46614 37.375616 2082.0   8000.    1   0.15
112.46565 37.376239 2082.0  46140.    1   0.15
112.46515 37.376862 2082.0 113140.    1   0.15
112.46465 37.374485 2082.0  46400.    1   0.15
112.46366 37.378731 2082.0  29560.    1   0.15
112.46316 37.379354 2082.0   3240.    1   0.15
112.46515 37.375616 2082.0  53980.    1   0.15
112.46465 37.376239 2082.0 168020.    1   0.15
112.46416 37.376862 2082.0  60700.    1   0.15
112.46465 37.374933 2082.0  28860.    1   0.15
112.46416 37.375616 2082.0  31240.    1   0.15
112.46366 37.376239 2082.0  43960.    1   0.15
112.46416 37.374370 2082.0  15360.    1   0.15
112.46366 37.374933 2082.0   5840.    1   0.15
112.46316 37.375616 2082.0   1400.    1   0.15
112.46266 37.376239 2082.0   2200.    1   0.15
112.31520 37.350400 2082.0 712800.    1   0.15
112.31290 37.350400 2082.0  13800.    2   0.15
112.31180 37.350400 2082.0 403000.    1   0.15
112.31180 37.350400 2082.0   9200.    2   0.15
112.31070 37.350500 2082.0 743977.    1   0.15
```

```
112.31507 37.350500 2082.0  13800.    2   0.15
112.31410 37.349500 2082.0  18400.    2   0.15
112.31070 37.349600 2082.0   9200.    2   0.15
112.30960 37.349600 2082.0   9200.    2   0.15
112.31410 37.348600 2082.0  18400.    2   0.15
112.31290 37.347700 2082.0  18400.    2   0.15
112.31180 37.350400 2082.0  13800.    2   0.15
112.31290 37.346800 2082.0 743977.    1   0.15
112.31290 37.346800 2082.0  13800.    2   0.15
112.31170 37.346900 2082.0 743977.    1   0.15
112.31170 37.346900 2082.0  18400.    2   0.15
112.30950 37.346900 2082.0   9200.    2   0.15
112.31510 37.345900 2082.0  18400.    2   0.15
112.38650 37.330900 2012.0 712800.    1   0.15
112.38420 37.330900 2012.0 403000.    1   0.15
112.38420 37.330900 2012.0  23000.    2   0.15
112.38530 37.330000 2012.0   9200.    2   0.15
112.32820 37.384200 2012.0  13800.    2   0.15
112.38310 37.328200 2012.0  13800.    2   0.15
112.38420 37.327300 2012.0 743977.    1   0.15
112.38420 37.327300 2012.0  13800.    2   0.15
112.38300 37.327300 2012.0 743977.    1   0.15
112.38300 37.327300 2012.0   9200.    2   0.15
112.38640 37.326400 2012.0   9200.    2   0.15
112.34960 37.342800 2005.0 712800.    1   0.15
112.34620 37.342800 2005.0  18400.    2   0.15
112.34510 37.342800 2005.0  13800.    2   0.15
112.34390 37.342800 2005.0 1063140.   1   0.15
112.44950 37.386000 2072.0 712800.    1   0.15
112.44950 37.383300 2072.0  13800.    2   0.15
112.44940 37.382400 2072.0 1063140.   1   0.15
4
      1.0070kmbry.sav
      3.00100kmbry.sav
      7.00400kmbry.sav
     20.001000kmbr.sav
yv.out
```

```
      PROGRAM ALBEDO
*     *** Calculates the night glow (albedo) due to multiple
*         artificially illuminated facilities
*
*         A recoding of the original SKYGLOW program written
*         by H Hogo/SAI in November 1984
*
*         Reference: M.A. Yocke, H. Hogo, and G.W. Lundberg (1984)
*                    "Inpacts of a Proposed Nuclear Waste Facility
*                    on the Night Sky in Canyonlands National Park."
*                    Systems Applications, Inc. SYSAPP-84/204
*
*         Modifications and enhancements made by:
*               Ed Carr and Gary Lundberg
*               Systems Applications, Inc.
*               San Rafael, CA 94903
*               August 1987
*
*         Modifications and additions in this version:
*             1.  locations now given in longitude/latitude
*             2.  correction for earth curvature
*             3.  variable sized hemisphere and integration rho step size
*             4.  from 1 to 5 vertical levels
*             5.  variable sized grid spacing  (not true)
*             6.  variable type lighting characteristics for each grid sq
*             7.  variable forward/backward scattering coefficient
*             8.  variable reflectance (surface coverage type) for each
*                 grid sq
*             9.  ambient no2 read from background files
*            10.  fancy input feature
*
*     ------------------------------------------------------
*
*     *** constants for converting radians to degrees
      real*4 pi
      parameter (pi=3.1415926,rtd=180.0/pi,dtr=pi/180.)
*
*     *** a tiny positive number
      real*4 tiny
      parameter (tiny=1.0e-30)
*
*     *** scattering function multiplier
      real*4 forpi
      parameter (forpi=1.0/(4.0*pi))
*
*     *** azumith and zenith step size (10 degrees)
      real*4 rad10
      parameter(rad10 = pi/18.0)
*
*     *** scale height or e-folding distance of extinction coefficient
      real*4 sclht
      parameter(sclht=1.1)
*
*     *** background glow (60 nanolamberts = 1.9e-4 lummens/m2/steradian)
      parameter (bkgnd = 1.90e-4)
```

```
*     *** for input, output, background file names
      character*30 filin,filot,filbac

*     *** for title
      character*80 itit1,itit2

*     *** for source locations: x,y,z and distance and
*         distance squared from observer
      real*4 xs(200),ys(200),zs(200),ds2(200),ds(200)

*     *** for unit vector normal to surface of source
      real*4 xt(200),yt(200),zt(200)

*     *** total skyglow--this is final result
      real glow(0:35,0:9)

*     *** top pf height levels  and distance along line of sight paths
*         and ambient NO2 concentration in each layer
      real*4 hgtlvl(0:5),dt(0:5),ambno2(5)

*     *** integrated light intensity at each wavelength
      real*4 tr(39)

*     *** background radiative properties at 39 wavelengths for
*         the scattering function and extinction coefficient
*         at five possible levels
      real*4 pbac(39,0:35,5),btabac(39,5)

*     *** spectral distribution of source light, correction for
*         multiple scattering, scattering coefficients at each
*         of 39 wavelengths and up to 5 levels
      real*4 stemp(39,3),difuse(39,5),bscat(39,5)
      real*4 hlogen(39),mrcury(39),sodium(39)
      equivalence (stemp(1,1),sodium),(stemp(1,2),hlogen),
     &            (stemp(1,3),mrcury)

*     *** illumination , spectral distribution, source type and
*         reflectance for each grid square
      real*4 sf(200),flux(39,200),reflct(200)
      integer*4 istyp(200)

*     *** dimension Romberg array's for integration
      parameter (nn=5)
      dimension romb(nn,nn)

*     *** background extinction and forward scattering coefficient
      real*4 ext(5),coef(5)

*     *** spectral absorption of no2 at 39 wavelengths
      real*4 absno2(39)

*     *** observer location for subroutine trans
      real*4 xobs,yobs,zobs
      common /pool/ xobs,yobs,zobs

*     *** the spectral distributions of three types of source lights
*         for 39 wavelengths--to add an additional type, change
```

```
*        the second dimension of stemp, then add 39 more values
*        to this data statement.

*      *** high pressure sodium vapor light (type 1)
       data sodium/
     &      0.0033898,0.0033898,0.0033898,0.0050847,0.0067797,
     &      0.0067797,0.0067797,0.0067797,0.0101695,0.0101695,
     &      0.0135593,0.0084746,0.0033898,0.0169492,0.0169492,
     &      0.0101695,0.0067797,0.0067797,0.0101695,0.0237288,
     &      0.0949153,0.1254237,0.0779661,0.1288136,0.1016949,
     &      0.0779661,0.0372881,0.0305085,0.0254237,0.0220339,
     &      0.0186441,0.0152542,0.0118644,0.0101695,0.0084746,
     &      0.0084746,0.0067797,0.0084746,0.0101695/

*      *** halogen or tungsten light (type 2)
       data hlogen/
     &      0.0015060,0.0018820,0.0024470,0.0033880,0.0039530,
     &      0.0045170,0.0056470,0.0056470,0.0075290,0.0090340,
     &      0.0107280,0.0120460,0.0135520,0.0152460,0.0163750,
     &      0.0173120,0.0190100,0.0208920,0.0229630,0.0250330,
     &      0.0261620,0.0278560,0.0297387,0.0308680,0.0331260,
     &      0.0348200,0.0365140,0.0385850,0.0399020,0.0421610,
     &      0.0440430,0.0453600,0.0470540,0.0479960,0.0489370,
     &      0.0498780,0.0513830,0.0527010,0.0536420/

*      *** mercury vapor light (type 3)
       data mrcury/
     &      0.0691800,0.0000000,0.0000000,0.0062900,0.0597500,
     &      0.0062900,0.0062900,0.1320800,0.0062900,0.0062900,
     &      0.0062900,0.0062900,0.0031400,0.0062900,0.0062900,
     &      0.0062900,0.0062900,0.1729600,0.0062900,0.0062900,
     &      0.1918200,0.0094300,0.0157200,0.0125800,0.0251600,
     &      0.1195000,0.0188700,0.0031400,0.0094300,0.0031400,
     &      0.0031400,0.0031400,0.0062900,0.0283000,0.0188700,
     &      0.0062900,0.0031400,0.0000000,0.0000000/

*      *** spectral absorption factors for NO2 at 39 wavelengths
       data absno2 /1.58,1.63,1.67,1.71,1.67,1.63,1.54,1.45,
     &              1.36,1.17,1.06,0.92,0.80,0.69,0.61,0.54,
     &              0.46,0.39,0.31,0.26,0.21,0.18,0.15,0.12,0.1,
     &              0.080,0.063,0.053,0.041,0.035,0.029,0.024,
     &              0.021,0.017,0.014,0.010,0.0068,0.0034,0.0/

*      *** initialize total skyglow array
       data glow/360*0.0/

*      *** initialize maximum number of source light types  and lowest
*      level height in kilometers
       data mxstyp/0/
       data hgtlvl(0) /0./

*      *** load values for the forward scattering and extinction coefficient
*          from Middletown, W.E.K.: Vision through the Atmosphere,1952
       data coef/0.50, 0.70, 0.74, 0.77, 0.8/
       data ext /0.011, 0.031, 0.044, 0.125, 0.295/

*      ------------------------------------------------------
```

```
*     *** get command line argument

********* computer/compiler dependent ***************
      call getarg (2,filin)
*************************************************

      if (filin .eq. ' ') then

*         *** no file on command line--go interactive
          call dialog
      else

*         *** filename on command line--open on unit 9
          open (9,file=filin,status='old',iostat=ierr)
          if (ierr .ne. 0) then
              stop '...cannot open input file'
          endif
      endif

*     *** get the input data

*     *** the title (two 80 character strings)
      read (9,'(a)') itit1
      read (9,'(a)') itit2

*     *** get observer location in longitude, latitude and elevation
      read (9,*) xobs,yobs,zobs

*     *** force to east longitude and change z from meters to kilometers
      xobs = -abs (xobs)
      zobs = zobs/1000.0

*     *** hemisphere size number of rho integration steps
      read (9,*) rmx,mxr
      rsiz = rmx/mxr
      mxrm1 = mxr-1

*     *** get number of sources
      read (9,*) ns

      do 10 i=1,ns
*         *** read in a source location in geodetic coordinates and the
*             source emissions in total lumens per grid space, source
*             type category, and reflectance
          read (9,*) x,y,z,sf(i),istyp(i),reflct(i)
          mxstyp = max(istyp(i),mxstyp)
          x = -abs(x)
          z = z/1000.0

*         *** transform source geodetic coordinates to the skyglow
*             spherical polar coordinate system
          call trans (x,y,z,arc,rho,theta,phi)

*         *** and now to the related cartesian system
          xs(i) = rho*sin(phi)*cos(theta)
          ys(i) = rho*sin(phi)*sin(theta)
```

```
          zs(i) = rho*cos(phi)

*         *** and save distance (squared) too
          ds2(i) = rho*rho
          ds(i) = rho

*         *** calculate (and save) unit vectors normal to source surface
          xt(i) = sin(arc)*cos(theta)
          yt(i) = sin(arc)*sin(theta)
          zt(i) = cos(arc)
   10 continue

*     *** read in the number of layers
      read (9,*) nlys

*     *** get the top height (km) and the name of prepared
*         background radiative properties file
      do 15 i=1,nlys

         read (9,'(f10.0,a)') hgtlvl(i), filbac
         open (7,file=filbac,status='old')

*        *** read in radiative background for this level
         read (7,'(f12.0)') ambno2(i)
         do 16 iaz=0,35
            read (7,'(10f12.0)') (pbac(iwv,iaz,i),iwv=1,39)
   16    continue
         read (7,'(10f12.0)') (btabac(iwv,i),iwv=1,39)
         close (7)
   15 continue

*     *** get the output file name and open
      read (9,'(a)') filot
      open (8,file=filot)

*     ----------------------------------------------------------------

*     *** set up some arrays (functions of wavelength)--
*         spectral distribution of the source lights,
*         the ratio of muliple scattering to primary scattering,
*         the scattering coefficient

      do 30 i=1,39
         do 20 j=1,ns
            flux(i,j) = stemp(i,istyp(j))*sf(j) * reflct(j)
   20    continue
         do 25 j=1,nlys

*           *** do until appropriate forward scattering coefficient is
*               found
            do 21 k=1,5
               if (btabac(i,j) .le. ext(k)) then
                  if (k .eq. 1) then
                     bckcf = coef(k)
                  else
                     bckcf = ((coef(k) - coef(k-1))/(ext(k)-ext(k-1)))*
     &                       (btabac(i,j)-ext(k-1)) + coef(k-1)
```

```
              endif
              go to 22
            elseif (k .eq. 5) then
              bckcf = coef(k)
            endif
 21        continue
 22        continue

           tauz = btabac(i,j)*sclht*(1.0 - exp(-hgtlvl(j)/sclht))

           bottom = tauz
           top    = tauz + 4.

*          *** The integral is sensitive to small values of tauz
*              thus we approximate the integral for values less
*              than 0.1 with the first two terms of a Taylor
*              series expansion of the denominator

           if (tauz .lt. 0.1) then
             bottom = 0.1
             call rombrg (bottom,top,nn,romb)
             eps = (1+tauz)/tauz
             romb(nn,nn) = 0.5*(-8.6021 + eps -log(eps)) +
     &                     romb(nn,nn)
           else
             call rombrg (bottom,top,nn,romb)
           endif

           difuse(i,j) = 1.0 * bckcf -2.*bckcf*tauz*romb(nn,nn)
           bscat(i,j) = btabac(i,j) - absno2(i)  *ambno2(j)
 25     continue
 30  continue

*       *** set zenith loop to 9 iterations for first pass
        mxb = 9

*       *** azumith loop: 0 to 350 in 10 deg steps
        do 90 ia= 0,35
           alpha = ia*rad10
           cosa = cos(alpha)
           sina = sin(alpha)

*          *** zenith loop: 0 (or 10) to 90 in 10 deg steps
*              actually the 0 deg zenith is only calculated once
           do 80 ib=0,mxb
              beta = (9-ib)*rad10
              cosb = cos(beta)
              sinb = sin(beta)

*              *** zero summing term for all sources
               wsum = 0.0

*              *** source loop
               do 70 is=1,ns

*                 *** scalarize this source location
                  sx = xs(is)
```

```
      sy = ys(is)
      sz = zs(is)

*     *** radial loop: rmx to rsiz in rsiz steps
      do 50 ir=0,mxrml
         r = rmx - ir*rsiz

*        *** point (alpha,beta,r) minus source
         dx = r*sinb*cosa - sx
         dy = r*sinb*sina - sy
         dz = r*cosb - sz

*        *** calculate distance from source to (alpha,beta,r)
         rst2 = dx*dx + dy*dy + dz*dz
         rst = sqrt(rst2)

*        *** calculate scattering angle (theta) via the cosine law
         pyth = ((r*r + rst2 -ds2(is))/(2.0*r*rst))
         if (pyth .gt. 0.999999) pyth = 1.0
         theta = rtd * (pi - acos (pyth))

*        *** get the low index into pbac for interpolation
         low = 0.1*theta
         lowp1 = low+1

*        *** and the fraction for interpolation of pbac
         frac = 0.1*(theta-10.0*low)

*        *** calculate the cosine of the angle between the line
*           from point to source with the normal to source
*           surface (xt,yt,zt is the normal unit vector)
         alt  = (dx*xt(is) + dy*yt(is) + dz*zt(is))

*        *** determine which layer to use for scattering
*           event
         do 35 i=1,nlys
            if (alt .le. hgtlvl(i)) then
               nht = i
               go to 37
            elseif (i .eq. nlys) then
               nht = i
            endif
   35    continue
   37    continue

*        *** loop over the wavelengths
         do 40 il=1,39

*           *** interpolate scattering function (pbac) at this
*               angle and wavelength
            pn = pbac(il,low,nht) +
     &           frac*(pbac(il,lowp1,nht) -
     &           pbac(il,low,nht))

*           determine extinction coefficient for this wave-
*           length first determine path length through each
*           layer and then uppermost level for this geometry
```

```
                    dt(0) = 0.
                    do 39 i=1,nlys
                      if(theta.lt. 1.0e-8 .or. theta .gt. 179.999)
     &                  then
                        dt(i) = 1.0e+8
                      else
                        dt(i)=(hgtlvl(i)*ds(is))/
     &                       (r*sin(dtr*(theta)))
                      endif

*                     *** do until test fails
                      if ((dt(i)+tiny).lt.r) then
                        go to 39
                      else
                        bext=0.
                        avbsct=0.
                        avdif =0.
                        do 38 n=1,i
                          prct = (dt(n)-dt(n-1))/r
                          if(n.eq.i) prct = (r - dt(n-1))/r
                          bext=prct*btabac(il,n) + bext
                          avbsct=prct*bscat(il,n) + avbsct
                          avdif=prct*difuse(il,n) + avdif
  38                    continue
                        go to 395
                      endif
  39                  continue
  395 B-35            continue

*                     *** determine source intensity at this wavelength
                      fs = flux(il,is)*exp(-bext*rst)
     &                       / (2.0*pi*rst2)
*                     *** integration steps
                      if (ir .eq. 0) then

*                       *** set the initial light for this ray
                        tr(il) = pn*forpi*avbsct
     &                           *fs*rsiz*1.0e-6
                      else

*                       *** accumulate the light along this ray
                        tr(il) = tr(il) +  pn*forpi*
     &                           avbsct*fs*rsiz*1.0e-6 -
     &                           bext*tr(il)*rsiz
                      endif

  40                continue
  50              continue

*                 *** add this source to the total source sum
*                  with multiple scattering
                  do 60 il=1,39
                    wsum = wsum + tr(il)*avdif + tr(il)
  60              continue

  70            continue
```

```
*             *** add in all the sources at this (alpha,beta)
*                 and the background glow too
              glow(ia,ib) = glow(ia,ib) + wsum + bkgnd

*             *** update the user
              print '(a,i2,a,i1,a,1p,e10.3)',
     &              ' glow(',ia,',',ib,') =',glow(ia,ib)

   80     continue

*         *** reset zenith loop for 8 iterations
          mxb = 8
          glow(ia,9) = glow(0,9)
   90 continue

*     *** save title and glow for user (and skyplot program)
      write (8,'(a/a)') ititl,itit2
      write (8,'(1p,10e9.2)') ((glow(ia,ib),ib=0,9),ia=0,35)

      stop '...all done'
      end

*deck trans ************************************************

      subroutine trans (bln,blt,bht,arc,rho,theta,phi)

*     *** translates source geodetic location to skyglow
*         spherical polar coordinates: rho, theta, phi
*             gw lundberg/sai  july '87

*     *** arguments--
*         bln,blt     east longitude and north latitude of point b
*         bht         elevation of point b in kilometers
*         arc         arc length from a to b in geodetic coordinates
*         rho         distance of b from skyglow origin
*         theta       skyglow azimuth east of south in radians
*         phi         skyglow zenith  (colatitude) in radians

*     *** reference: Geological Survey Bulletin 1532, p34, (5-3a),
*                    p35 (5-4) and p146 (16-1,16-2)

*     ---------------------------------------------------------

      real*4 bln,blt,bht,arc,rho,theta,phi

*     *** coordinates of observer
      real*4 aln,alt,aht
      common /pool/ aln,alt,aht

*     *** degrees to radians constant
      real*4 pi,dtr
      parameter (pi=3.141592654,dtr=pi/180.0)

*     *** mean radius of the earth
      real*4 e
      parameter (e=6371.0)
```

```
*     *** cosine, sine of latitudes and delta longitude
      real*4 calt,salt,cblt,sblt,cdln,sdln

*     *** sine of arclength, projected rho, azimuth, temporary
      real*4 sinarc,prho,azimth,temp

*     ------------------------------------------------------------

*     *** calculate cosines and sines of latitudes
      calt = cos (alt*dtr)
      salt = sin (alt*dtr)

      cblt = cos (blt*dtr)
      sblt = sin (blt*dtr)

*     *** and of delta longitude
      cdln = cos ((bln-aln)*dtr)
      sdln = sin ((bln-aln)*dtr)

*     *** calculate arc length in radians
      sinarc = sqrt (cblt*cblt * sdln*sdln +
     &         (calt*sblt - salt*cblt*cdln)**2)
      arc =  asin (sinarc)

*     *** calculate azimuth east of north
      temp =sdln*cblt/sinarc
      azimth = asin (temp)

*     *** adjust for proper quadrant location
      sign = sblt - salt
      theta = azimth
      if ( sign .lt. 0) then
         theta = pi - azimth
      elseif (temp .lt. 0) then
         theta = 2.0*pi  + azimth
      endif

*     *** calculate projected rho
      prho = (e+bht) * sinarc

*     *** calculate true rho
      rho = sqrt ((aht-bht)**2 + 2.0*(e+bht)*(e+aht)*(1.0-cos (arc)))

*     *** check for numerical rounding (insure values are not > than one)
      if ((prho/rho) .gt. 1.00) prho=rho

*     *** calculate zenith
      phi = 0.5*pi + acos (prho/rho)

      return
      end

*deck rombrg ************************************************************
      subroutine rombrg(a,b,n,r)
```

```
*     *** This routine employs the Romberg algorithm to estimate the
*         integral from a to b for the function f (see below)
*         For further details see Cheny and Kincaid " Numerical
*         Mathematics and Computing" , 1980.
*     ----------------------------------------------------------------
      dimension r(n,n)
*     *** declare a function for the calculation of the average
*         value of the optical depth for the atmosphere
      f(tauinf) = 1.0/((exp(2.0*tauinf)-1.0)*tauinf)
*     ----------------------------------------------------------------

      h=b-a
      r(1,1) = 0.5*h*(f(a) + f(b))
      l = 1

      do 40 i=2,n
         h = 0.5*h
         l = l+1
         sum = 0.0

         do 20 k=1,l-1,2
            sum = sum + f (a+h*float(k))
   20    continue

         r(i,1) = 0.5*r(i-1,1) + h*sum
         m = 1

         do 30 j=2,i
            m = 4*m
            r(i,j) = r(i,j-1) + (r(i,j-1) - r(i-1,j-1))/float(m-1)
   30    continue

   40 continue

      return
      end
```

Appendix C

GLOSSARY

Appendix C

GLOSSARY

Aerosols	A colloidal system in which the dispersed phase (or colloid) is uniformly distributed in a finely divided state composed of either solid or liquid particles through the second substance, called the dispersion medium, usually air. The size of particles constituting the dispersed phase is commonly set to one micron.
Airglow	The quasi-steady radiant emission from the upper atmosphere, due primarily to the photochemical luminescence emission of the molecules O_2 and N_2, the hydroxyl radical, and atomic oxygen.
Angstrom	A unit of length used in the measurement of the wavelength of light. One angstrom is equal to 10^{-8} cm or 10^{-4} microns.
Background Natural Sky Brightness	The luminosity of the sky due to natural sources; it is due to the average faint star background and the van Rhijn layer.
Brightness	The luminous flux emitted by a unit area.
Candle	A unit of luminous intensity (or candle-power) of a light source.
Coarse Particles	Particles whose size range is from 2.5 μm to 15 μm.
Fine Particles	Particles whose size range is less than 2.5 μm.
Foot-Candle	A unit of illuminance or illumination equal to one lumen per square foot. This is the illuminance provided by a light source of one candle at a distance of one foot.

Fugitive Dust	Solid particulate matter that is moving and rapidly varying (i.e., dust that is transient in nature).
Illuminance	The total luminous flux received on a unit area of a given real or imaginary surface, expressed in units such as foot-candle, lux, or phot.
Light Pollution	Any light emitted from man-made sources. Typical sources include street lighting, industrial lighting, automobile headlights, searchlights, billboard lighting, and parking lot lighting.
Lumen	A unit of luminous flux. The lumen is equal to the luminous flux radiated into a unit solid angle (steradian) from a small source having a luminous intensity of one candle.
Luminosity	For a given wavelength of visible radiation, the ratio of the flux that is effectively sensed by the human eye to the flux that is intrinsic in the radiation.
Mie Scattering	Any scattering produced by spherical particles without special regard to comparative size of radiation wavelength and particle diameter.
Milky Way	The hazy band of light that stretches across the night sky.
Multiple Scattering	Any scattering in which radiation is scattered more than once before reaching the sensing element. It is often referred to as secondary scattering.
Numerical Model	A method used to predict the behavior of a physical phenomenon through the mathematical solution of the governing equation.
Primary Scattering	Any scattering process in which radiation is received at a sensing element after having been scattered just once.
Radiation Transfer Equation	A mathematical equation describing the change in light intensity within the atmosphere for a given wavelength as a function of distance (neglecting multiple scattering).

Rayleigh Scattering	Any scattering process produced by spherical particles whose radii are smaller than about one-tenth the wavelength of the scattered radiation.
Scattering Coefficient	A measure of the attenuation due to scattering of radiation as it traverses a medium containing scattering particles.
Steradian	A unit of solid angle. The area cut out by a sphere equal to the square of the radius.
Stellar Magnitude	A system of light intensity classification based on the definition that a difference of 5 magnitudes means a ratio of intensity of exactly 100 times. Thus a star of first magnitude is exactly 100 times brighter than a star of sixth magnitude.
Telephotometer	A photometer that measures the received intensity of a distant light source.
Visible Light	The portion of the electromagnetic spectrum occupied by the wavelengths of visible radiation (0.36 to 0.75 μm).
Visual Range	The distance at which the apparent contrast between a specified type of target and its background becomes equal to the threshold contrast of the observer. The standard visual range is defined by the relationship $V = \frac{3.912}{\beta}$ where V is the visual range and β is the extinction coefficient.
Wavelength	The distance between one crest of the wave to the next or one trough to the next, or between any point on a wave and a similar point on the next wave. The wavelengths of visible light range from 0.36 to 0.75 μm.